Charles University
Faculty of Science

Study programme: Biology
Branch of study: Experimental Plant Biology

Bc. Pavel Krupař

The Role of Lipids and Lipid Metabolizing Enzymes in Plant Autophagy

Úloha lipidů a enzymů metabolizujících lipidy v procesu autofagie u rostlin

Master's thesis

Supervisor: RNDr. Jan Martinec, CSc.

Prague, 2021

Prohlášení:

Prohlašuji, že jsem závěrečnou práci zpracoval samostatně a že jsem uvedl všechny použité informační zdroje a literaturu. Tato práce ani její podstatná část nebyla předložena k získání jiného nebo stejného akademického titulu.

V Praze, 26. dubna 2021

……

Bc. Pavel Krupař

ACKNOWLEDGMENTS

The work was supported by the Ministry of Education, Youth and Sports of the Czech Republic, grant No. LTC17084.

The author wishes to express his sincerest gratitude and warm appreciation to the following persons and institutions, who had contributed in helping him shape this valuable piece of work.

The Great Almighty, the author of knowledge and wisdom, for giving me strength to accomplish this thesis.

RNDr. Jan Martinec, CSc., thesis supervisor, for his valuable guidance and critical feedback.

Mgr. Michal Daněk, PhD., who deserves all of the credit, for his support, understanding and many appreciated suggestions.

Mgr. Kristýna Kroumanová, for her help with phenotype screening.

Ing. Zuzana Kčková, Ph.D., for her help with HPTLC.

RNDr. Barbora Radochová, PhD., for her great help with stereological methods.

Department of Experimental Plant Biology, for giving me ideas, feedback and encouragement.

Mgr. Bc. Marek Přikryl, for dealing with my thesis frustration and filling my life with happiness.

My family and friends, that always shared their support morally, financially and physically.

Company Amrest s.r.o for being my understanding employer and providing delicious refreshment during my studies.

The Army of the Czech Republic, for developing my courage and endurance and for keeping our world safe.

TABLE OF CONTENT

TABLE OF FIGURES

ABSTRACT

Plant autophagy is a crucial evolutionary conserved process for recycling cytoplasmic material under stress conditions or during development. The autophagic pathway is negatively regulated by TOR kinase, a versatile molecule modulating a wide range of cellular processes. In mammals, TOR kinase may be activated by phosphatidic acid, a vital signalling lipid. This thesis aims to prove the possible involvement of phospholipids in plant autophagy. I analysed the rate of primary root inhibition in knock-out mutants coding phospholipases in *A. thaliana* with induced autophagy, measured activity of lipid metabolising enzymes in wild type and *atg10* mutant and observed autophagosome formation in selected mutants. Autophagosomes were labelled by fluorescent protein *in vivo* and by indirect immunolabelling in fixed samples. Using advanced stereological approach, I optimized a method for obtaining an unbiased estimate of autophagosome number in plant root cells.

Key words: plant autophagy, phospholipids, stereology

ABSTRAKT

Autofagie u rostlin je klíčový, evolučně konzervovaný proces umožňující recyklaci cytoplazmatických komponent během stresových podmínek, či vývoje rostliny. Autofagická dráha je negativně regulována TOR kinasou, univerzální molekulou, která řídí široké spektrum buněčných procesů. V savčích buňkách může být TOR kinasa aktivována kyselinou fosfatidovou, důležitým signálním lipidem. Tato diplomová práce si klade za cíl odhalit možnou roli fosfolipidů v procesu autofagie u rostlin. Byla analyzována inhibice růstu primárního kořene rostlin s vyřazenými geny kódující fosfolipasy u *A. thaliana*, měřena aktivita enzymů metabolizujících lipidy v rostlinách divokého typu a s vyřazenou autofagií, a také byla pozorována tvorba autofagozomů u vybraných mutantních rostlin. Autofagozomy byly vizualizovány pomocí fluorescenčního proteinu *in vivo* a nepřímého imunoznačení ve fixovaných preparátech. Za použití pokročilých stereologických postupů byla optimalizována metoda pro získání nevychýleného odhadu počtu autofagozomů v buňkách kořene rostlin.

Klíčová slova: autofagie rostlin, fosfolipidy, stereologie

AIMS OF THE THESIS

- Identify *Arabidopsis thaliana* knock out mutants in lipid metabolizing enzymes with disrupted autophagy.
- Introduce a method for quantification of autophagosome formation.
- Reveal how lipid metabolizing enzymes are involved in the process of autophagy.

1 INTRODUCTION

To survive the unfavourable and dynamically changing environment, plants use several mechanisms to survive. One of these mechanisms is autophagy, a process of recycling undesirable material under stress conditions or during various developmental processes. During autophagy, a double-membrane vesicle called autophagosome delivers the cargo to the vacuole for degradation.

Even though the concept of autophagy emerged in 1960s, a little was known about the basic mechanism of autophagy for decades. In 1990s, Yoshinori Ohsumi used yeast to identify genes essential for autophagy. On 3rd October 2016, Ohsumi received the Nobel Prize in Physiology or Medicine for his discoveries of mechanisms for autophagy (Nobel Media AB, 2016).

Plant autophagy is negatively regulated by evolutionary conserved TOR kinase (Kim *et al.*, 2011; Li and Vierstra, 2012). It was reported in literature, that repression of TOR kinase leads to lipid droplets accumulation in plants and algae (Caldana *et al.*, 2013; Imamura *et al.*, 2015). Lipids and lipid metabolizing enzymes play a major role in plant signalling cascades regulating central cellular processes such as, cytoskeletal rearrangement and membrane trafficking. A further question is whether lipids and lipid metabolizing enzymes participate in regulation of the process of plant autophagy.

Phillips, Suttangkakul and Vierstra (2008) showed, that *Arabidopsis thaliana atg10* mutants are unable to accumulate autophagic bodies inside the vacuole. Therefore, *atg10* plants are hypersensitive to nitrogen and carbon starvation. Here, I compared the length of primary root increment of *A. thaliana atg10* mutants and wild type to various knock-out mutants in plant phospholipases. Moreover, activity of plant lipid metabolising enzymes was measured and compared in *A. thaliana* wild type plants and *atg10* mutants using high performance thin layer chromatography.

To study autophagic activity, the number of autophagosomes present in the plant cell can be estimated. Nevertheless, most studies have relied on counting autophagosomes from 2-dimensional sections. Here, I used live cell imaging and indirect fluorescent immunolabelling to visualise autophagosomes and stereological methods to estimate autophagosome number density in *A. thaliana* wild type and knock-out mutants in lipid metabolizing enzymes.

2 LITERATURE REVIEW

2.1 Lipid Signalling in Plants

Lipids have various functions in plant cells. One of their typical roles is being a membrane component and as such, determining compartmentation of cell. However, they can do much more than being a physical barrier. Plant lipids play a dominant role in signalling by recruiting or tethering parts of signal complexes, controlling the production of lipid mediators, such as phosphatidic acid, but also very often by regulating vesicle budding, thus impacting signalling indirectly. Phosphatidic acid (PA) produced by phospholipase D (PLD) is a crucial signalling molecule of plant lipid signalling. Lipid hydrolysing enzymes play a vital role in various processes, such as cytoskeletal rearrangement, membrane trafficking and degradation, or response to various biotic or abiotic stresses. Pleiades of molecules are involved in plant lipid signalling such as glycerolipids (Wang *et al.*, 2002; Wang, 2002; Meijer and Munnik, 2003), sphingolipids (Sperling and Heinz, 2003; Worrall, 2003), fatty acids (Cheong and Choi, 2003; Farmer, Alméras and Krishnamurthy, 2003), oxylipins (Scherer, 2002; Ryu, 2004), and sterols (Li, 2003; Lindsey, Pullen and Topping, 2003).

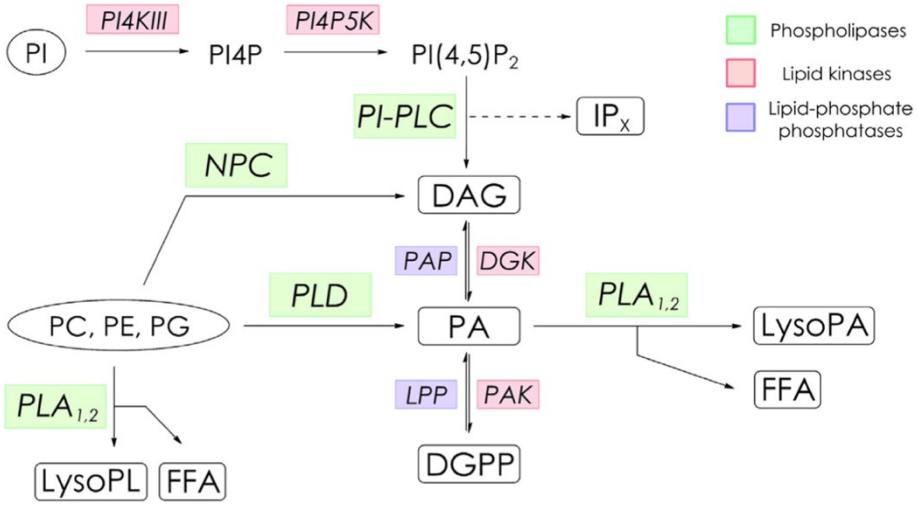

Figure 1 **Metabolism of plant phospholipids.** Phosphatidic acid can be created by activity of PLD or DGK. DAG = diacylglycerol, DGK = diacylglycerolkinase, DGPP = diacylglycerolpyrophos-phate, FFA = free fatty acids, IPx = inositol polyphosphate; LysoPA = lysophosphatidic acid; LysoPL = lysophospholipids; LPP = lipid phosphate phosphatase, NPC = non-specific phospholipase C, PA = phosphatidic acid, PAK = phosphatidic acid kinase, PAP = phosphatidic acid phosphatase, PE = phosphatidylethanolamine, PC = phosphatidylcholine, PG = phosphatidylglycerol, PI = phosphatidylinositol, PI4K = phosphatidylinositol 4-kinase, PI4P5K = phosphatidylinositol-4-phosphate 5-kinase, PI4P = phosphatidylinositol 4-phosphate, PI(4,5)P2 = phosphatidylinositol 4,5-bisphosphate, PI-PLC = phosphatidylinositol-specific phospholipase C, PLA = phospholipase A, PLD = phospholipase D. Reproduced from Ruelland et al., 2014.

2.1.1 Plant Phospholipases

Phospholipases can be found in all living organisms. Based on the nature of their product, they are classified into phospholipases A1, A2, C and D. Some phospholipases are known for preferring specific substrate. Typically, phospholipases C (PLC) can be either phosphoinositide-specific PLCs (PI-PLCs) or non-specific PLC (NPCs).

2.1.1.1 Phospholipases A

Phospholipases A (PLA) are divided into PLA_1s, secretory PLA_2s and patain-like PLAs (pPLAs). Different members of PLA family require various substrates, such as phosphatidylcholine (PC), monogalactosyldiacylglycerol, digalactosyldiacylglycerol and triacylglycerol (TAG; Chen, Greer and Weselake, 2013). By hydrolysis of the membrane phospholipids, PLAs can produce α-linolenic acid, which acts as a precursor of jasmonic acid (JA; Wasternack and Song, 2017). This finding suggests that PLAs are involved in JA signalling and developmental processes depending on JA. Furthermore, PLA1 is linked to vacuole biogenesis and in amyloplast redistribution in the shoot endodermis (Kato *et al.*, 2002; Morita *et al.*, 2002), thus in regulation of shoot gravitropism.

High level of PLA2s is expressed in pollen, flowers, leaf petioles and root pericycle (Bahn *et al.*, 2003).

2.1.1.2 Phospholipases C

Phospholipases C may be classed into three groups based on their preferred substrate and cellular function. NPCs hydrolyse PC and PE (Pokotylo *et al.*, 2013), while PI-PLCs prefer phosphoinositides, such as phosphatidylinositol 4,5-bisphosphate (PIP2; Tasma *et al.*, 2008; Heilmann, 2016). PLCs produce DAG and head group. DAG can be later converted to PA by DAG kinase (DGK; Arisz, Testerink and Munnik, 2009), so the developmental role of PLCs may be also executed via PA.

NPCs are mainly localized to membranous compartments, such as endoplasmic reticulum (NPC1, Krčková *et al.*, 2015) and Golgi apparatus (NPC1, NPC2; Krčková *et al.*, 2015, 2018). Also, NPC2 and NPC6 have been recently found in plastids (Ngo *et al.*, 2018). NPC4 is associated with plasma membrane, while NPC5 is located in cytosol (Nakamura *et al.*, 2005; Gaude *et al.*, 2008; Peters *et al.*, 2014).

PI-PLCs are expressed in whole plant, but mainly in vascular tissues. PI-PLC2 and PI-PLC5 are highly expressed in root tips. Moreover, these two PI-PLCs are together with PI-PLC3 significantly expressed in reproductive organs (Kanehara *et al.*, 2015;

Zhang *et al.*, 2018). Subcellular localization of PI-PLCs (PI-PLC2, PI-PLC3, and PI-PLC9) is mostly to the PM (Zheng *et al.*, 2012a; Kanehara *et al.*, 2015; Di Fino *et al.*, 2017), while PLC3 is localized in the nucleus (Zheng *et al.*, 2012).

Because of their phosphoinositide-hydrolysing activity, PI-PLCs are involved in many developmental processes depending on membrane transport, for instance, root hair or pollen tubes development (Dowd *et al.*, 2006; Helling *et al.*, 2007; Hong *et al.*, 2016). Both *A. thaliana* PI-PLC3 and PI-PLC9 possitively affect thermotolerance, as mutants *plc3* and *plc9* are unable to regulate heat tolerance (Zheng *et al.*, 2012b; Gao *et al.*, 2014). Wheat PI-PLC regulates microtubule formation in plasmolyzed cells in response to hyperosmotic stress. Tubulin polymers were completely disrupted after suppression of PI-PLC by an inhibitor (Komis *et al.*, 2008).

2.1.1.3 Phospholipases D

Phospholipases D (PLD) catalyse the hydrolysis of structural membrane phospholipids, such as phosphatidylcholine (PC), phosphatidylethanolamine (PE) and phosphatidylglycerol (PG). Product of the PLD hydrolysis is phosphatidic acid (PA) and different head groups such as, choline or ethanolamine. In plants, PLDs are encoded by multigenic families, as well as PI-PLCs and NPCs. While mammals have only two PLD genes (Exton, 2002), there are twelve PLD genes in Arabidopsis (Qin and Wang, 2002). Plant PLDs can be subdivided into six classes: α (α1, α2, and α3), β (β1 and β2), γ (γ1, γ2, and γ3), δ, ε, ζ1 and ζ2 (Hong *et al.*, 2016).

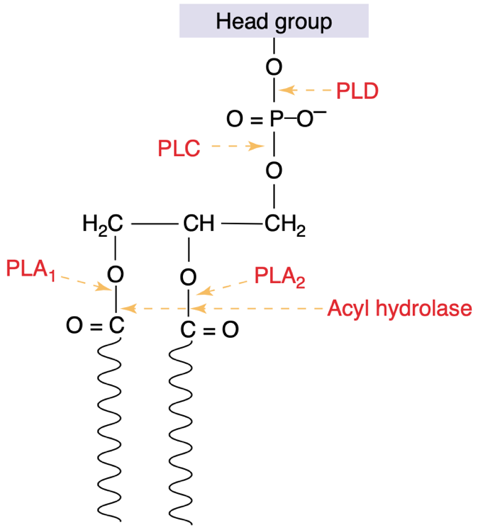

Figure 2 **Phospholipid hydrolysis sites.** Membrane phospholipids can be hydrolyzed by phospholipase D (PLD), phospholipase C (PLC), phospholipase A_1 (PLA_1), phospholipase A_2 (PLA_2) and acyl hydrolases. Reproduced from Wang, 2004

Most of PLDs require Ca^{2+} for their activity (Pappan, Zheng and Wang, 1997). Calcium dependent targeting of PLD to membrane is considered to be a mechanism of PLD activation. However, different classes of PLDs use diverse modes of regulation (Ryu and Wang, 1996). The two major PLD isoforms in Arabidopsis are PLDα1 and PLDδ. Both have strong activity different from other PLDs, as they require different concentrations of Ca^{2+}, phosphatidylinositol 4,5-bisphosphate (PI(4,5)P2) and oleic acid (Wang *et al.*, 2006).

PLDs participate in a typical transphosphatidylation reaction with primary alcohols, producing non-metabolizable phosphatidylalcohol (Rainteau *et al.*, 2012). This reaction is a specific non-physiological function of PLDs and is often used either to inhibit production of PA or to measure the activity of PLDs.

As mentioned above, PLDs produce PA, which is an important signalling molecule. Therefore, many PLD functions in development may be assigned to the production of PA. The function of many crucial signalling and/or structural proteins can modulate PLD activity. For example, components of the G-protein complex (Mishra *et al.*, 2006; Roy Choudhury and Pandey, 2016), sphingosine kinase (Guo *et al.*, 2012), MPK3 (Vadovič *et al.*, 2019) and PLD-regulated protein 1 (Ufer *et al.*, 2017).

PLDβ1 interacts with actin cytoskeleton. This interaction is evolutionary conserved within mammalian and plant cells (Jones, Morgan and Cockcroft, 1999; Kusner *et al.*, 2003). Tobacco NtPLDβ1 stimulates F-actin, while G-actin is inhibited. Moreover, interaction of NtPLDβ1 with actin has function in pollen tube development (Pleskot *et al.*, 2010). Another isoform called PLDδ binds cortical microtubules (Gardiner *et al.*, 2001; Gardiner, 2003; Dhonukshe *et al.*, 2003). PLDs are mainly localized to the PM (PLDγ, PLDε, PLDδ; Fan *et al.*, 1999; Hong *et al.*, 2009; Pinosa *et al.*, 2013), tonoplast (pldζ2; Su *et al.*, 2018), mitochondria, nucleus (PLDγ; Fan *et al.*, 1999) and cytoplasm (PLDα1; Novák et al., 2018).

2.1.2 Diacylglycerol kinase

Diacylglycerol kinases (DGKs) catalyse the phosphorylation of diacylglycerol (DAG) into PA. The genome of *Arabidopsis thaliana* contains 7 *DGK* genes in three phylogenetic clusters (Yang and Klionsky, 2009a), while there are 8 *DGK*s in the rice genome. Enzymes of cluster I are similar to the most basic mammalian DGKε, containing the conserved catalytic DGK domain and two cysteine-rich C1-type domains.

These domains are believed to be responsible for binding DAG. Moreover, cluster I enzymes contain a trans-membrane helix (Vaultier *et al.*, 2008).

A tomato DGK, *Sl*CBDGK seems to possess a calmodulin binding domain (CBD), which allows its Ca^{2+} dependent membrane binding (Snedden and Blumwald, 2000). However, a product of alternative splicing from the same locus creates *Sl*DGK1, where the Ca^{2+} dependent membrane binding and CBD domain absent. *At*DGK5, the *A. thaliana* homolog of *Sl*DGK1 also has two splice variants and one of them may contain the CBD (Yang and Klionsky, 2009a). As a Ca^{2+} dependent membrane localization is common in mammalian cells, the calmodulin-dependent way remains exclusive for plants. This finding suggests their possible physiological function in biotic and abiotic stress signalling pathways, as the Ca^{2+} cytosolic rise involved in these pathways (Arisz *et al.*, 2009).

Activity of plant DGKs was mostly found at the plasma membrane (Kamada and Muto, 1991; Lundberg and Sommarin, 1992; Wissing *et al.*, 1992; Wissing, Riedel and Behrbohm, 1995; Wissing and Wagner, 1992), some of them are associated with cytoskeleton (Tan and Boss, 1992), nucleus (Hendrix, Assefa and Boss, 1989) and also chloroplast (Müller *et al.*, 2000).

2.1.3 Phosphatidic Acid and its Role in Plant Signalling

In plant cells, there are several molecules acting as universal signal messengers. One of them is phosphatidic acid, regulating various cellular processes (Wang *et al.*, 2006; Pleskot *et al.*, 2013). However, PA can be produced via several pathways. The main metabolic route is *de novo* synthesis via sequential acylation of glycerol-3-phosphate and lysoPA (Schmid and Ohlrogge, 2002). Other ways are by hydrolytic cleavage by phospholipase D, subsequent phosphorylation of diacylglycerol (DAG) by diacylglycerol kinase (DGK) and finally, dephosphorylation of diacylglycerol-pyrophosphate (DGPP) by lipid phosphate phosphatase (LPP). Arisz and Munnik (2013) show that PA derived from DGK pathway differs from PLD-produced PA in fatty acid lengths.

More than 30 proteins from numerous physiological pathways have been identified as targets of PA (Zhao, 2015) and many more are being discovered. In spite of many proteins interacting with PA, no PA-binding site was identified in these proteins. A few studies suggested a significant role of positively charged ammino acids in interactions between PA and targeted proteins (Kooijman *et al.*, 2007; Liu, Su and

Wang, 2013). PA binds to various molecules such as, kinases (e.g., mitogen-activated protein kinase 6, MPK6; Yu *et al.*, 2010), enzymes (e.g., glyceraldehyde 3-phosphate dehydrogenase; Kim, Guo and Wang, 2013) and cytoskeleton interacting proteins (e.g., microtubule-associated protein 65-1, MAP65-1; Zhang *et al.*, 2012). Furthermore, Li *et al.*, 2012 have shown that PLD-derived PA binds to actin and promotes actin polymerization. In particular, *Arabidopsis* heterodimeric capping protein (AtCP), which acts as a central regulator of actin filament polymerization by binding to barbed end of actin filaments, binds to PA and is negatively regulated by PA i*n vitro* (Huang *et al.*, 2006).

The location of PA directly affects localization, activity and biological function of PA-targeted proteins. The main pool of PA in plant cells is located in the ER, followed by chloroplasts, cytoplasm and mitochondria (Testerink and Munnik, 2011). PLDs may transfer PA from the ER to chloroplasts in plant tissues (Benning, 2009).

2.2 Autophagy in Plants

Autophagy (from Greek "self-eating") is a process of macromolecule degradation in which cells recycle cytoplasmic material under stress conditions or during development. This process is conserved among all eukaryotes (Bassham, 2007; Yang and Klionsky, 2009b; Mehrpour *et al.*, 2010). In plants, we distinguish microautophagy and macroautophagy. During microautophagy, a small intravacuolar vesicle called autophagic body is formed by invagination of the tonoplast. In macroautophagy, the cellular components for degradation are enclosed by cytoplasmic autophagosome. A specific mechanism called megaphagy takes part in the last step of programmed cell death (PCD) and is also considered to be a form of autophagy (Van Doorn and Papini, 2013). This thesis focuses on plant macroautophagy pathway, hereafter referred as autophagy.

The key feature of autophagy is the formation of double-membrane structures called autophagosomes. When autophagy is induced, an autophagosome is formed around the material which is intended for degradation. This material is delivered to vacuole by the autophagosome. In the vacuole, the outer membrane of the autophagosome fuses with the vacuole and hydrolases inside degrade the cargo and the inner membrane of the autophagosome (Liu and Bassham, 2012).

2.2.1 TOR Kinase as a Key Regulator of Autophagy

The target of rapamycin (TOR) is a serine-threonine protein kinase belonging to the phosphatidylinositol 3-kinase-related protein kinase (PIKK) family. TOR is highly evolutionary conserved and modulates a wide range of cellular processes. Recent studies demonstrate, that TOR has various functions in regulating transcription, translation, bioenergetics, metabolism, stress and immune responses in several cell types, tissues and organs (Ren *et al.*, 2013; Caldana *et al.*, 2013; Xiong *et al.*, 2013; Xiong and Sheen, 2014).Studies with *A. thaliana tor* knock-out mutants confirm that disrupted TOR function leads to embryo lethality (Menand *et al.*, 2002; Ren *et al.*, 2011). Menand *et al.*, (2002) also suggested that TOR is expressed in primary meristem, embryo and endosperm, but not in differentiated cells.

Once TOR kinase is activated by various upstream signals, it controls a countless number of direct or indirect downstream effectors regulating various cellular processes (Fig. 3). Glucose and sucrose synthetised during photosynthesis seem to be one of the most effective nutrient signals activating TOR kinase (Ren *et al.*, 2013; Xiong *et*

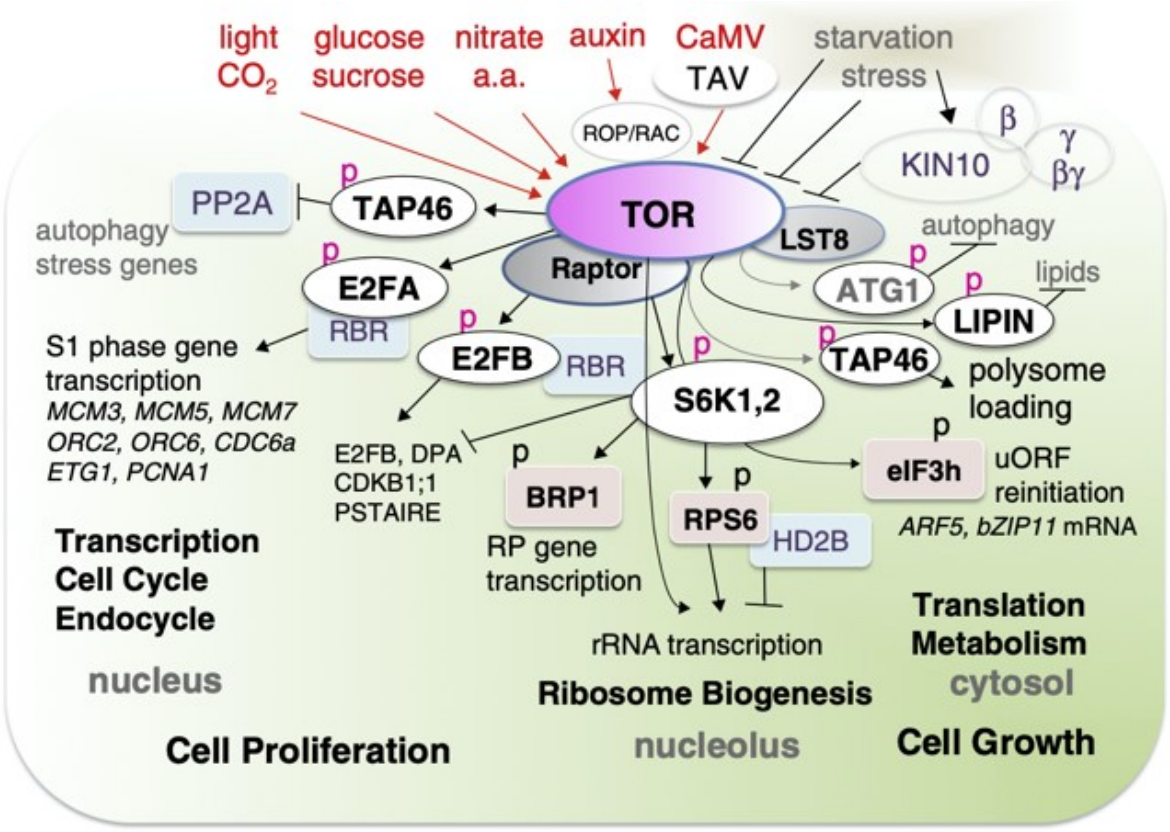

Figure 3 **Plant TOR signalling pathway.** Function of *A. thaliana* TOR kinase is modulated by various upstream regulators. By phosphorylation of S6K1,2, TAP46, E2FA, E2FB, LIPIN and ATG1, TOR kinase regulates transcription, cell cycle, endocycle, rRNA transcription, ribosome biogenesis, translation, metabolism and autophagy. Reproduced from Xiong and Sheen, 2015.

al., 2013). Moreover, TOR may be activated by nitrate and amino acids based on S6K1 phosphorylation (Xiong and Sheen, 2015). Plant TOR kinase likely directly phosphorylates ATG1 to inhibit autophagy (Kim *et al.*, 2011; Li and Vierstra, 2012) and LIPIN to activate lipid synthesis (Peterson *et al.*, 2011). In mammals, active mTOR promotes lipogenesis and adipogenesis and inhibits lipolysis (Ricoult and Manning, 2013).

Regulatory Associated Protein of TOR (RAPTOR) promotes TOR kinase complex stabilisation and substrate recognition. In yeast, RAPTOR binds to substrate which is later phosphorylated by TOR (Hara *et al.*, 2002). In *A. thaliana*, RAPTOR family consists of RAPTOR1/Raptor1B and RAPTOR2/Raptor1A. If RAPTOR1/Raptor1B is disrupted, embryo development and post-embryonic growth is repressed. On the other hand, disruption of RAPTOR2/Raptor1A does not affect plant growth and development (Deprost *et al.*, 2005; Anderson, Veit and Hanson, 2005).

Liu and Bassham, (2010) showed that RNAi *TOR* plants with decreased expression of *TOR* have constitutive autophagy and induced expression of some *ATG* genes even in the absence of stress conditions.

Two independent studies exposed the link between TOR repression and lipid accumulation in plants and algae (Caldana *et al.*, 2013; Imamura *et al.*, 2015). TOR expression repressed by inducible RNA silencing led to enhanced storage of lipids and starch in *Arabidopsis* seedlings (Caldana *et al.*, 2013). Similarly, TOR activity repressed by rapamycin treatment led to TAG accumulation in red alga *Cyanidionschyzon merolae* and green alga *Chlamydomonas reinhardtiii* (Imamura *et al.*, 2015). However, the exact molecular mechanism connecting plant TOR function with lipid metabolism still needs to be elucidated.

2.2.2 Formation of Autophagosomes

Under normal conditions, basal autophagy serves as a housekeeping mechanism to remove damaged and undesirable cytoplasmic material (Sláviková *et al.*, 2005; Inoue *et al.*, 2006; Xiong, Contento and Bassham, 2007a). Once autophagy is induced, a conserved autophagosome formation process occurs. This process involves a few steps: initiation, expansion, maturation and degradation (Liu and Bassham, 2012).

A downstream substrate of TOR in yeast and animals is the ATG1/ATG13 complex. ATG1 serves as a catalytic subunit and activates autophagy in case of nutrient depletion (Díaz-Troya *et al.*, 2008; Mizushima, 2010). In the genome of *A. thaliana*,

ATG1 and *ATG13* are present in multiple copies, which may be redundant. During nutrient depletion, ATG1a is hyperphosphorylated, possibly by SnRK1 (Chen *et al.*, 2017), while ATG13 is hypo-phosphorylated. Mutants in ATG13 are unable to create autophagosomes and are hypersensitive to nutrient starvation (Suttangkakul *et al.*, 2011).

A phagophore is a preautophagosomal structure, containing a characteristic open cup-like double membrane with vastly curved edges. A phagophore arises from an omega-shaped structure located on an ER subdomain called omegasome (Axe *et al.*, 2008). ATG1 and phosphatidylinositol-3-kinase (PI3K) complex are recruited to the omegasome, producing phosphatidylinositol 3-phosphate (PI3P, Fig.4). Similarly, the ATG12-ATG5-ATG16 complex and other downstream regulators are engaged in further conjugation of ATG8 to phosphatidylethanolamine (PE) on the nascent phagophore membrane and its separation from the ER (Lamb, Yoshimori and Tooze, 2013).

Unlike other ATG proteins, ATG9 is a transmembrane protein, which can move rapidly through cytoplasm as a part of various compartments (Yamamoto *et al.*, 2012; Rao *et al.*, 2016; Karanasios *et al.*, 2016). Thus, ATG9 is believed to contribute to delivery of membrane source and other regulators to the phagophore membrane (Fig. 4). For instance, autophagy is completely blocked in yeast *atg9* mutants (Yamamoto *et al.*, 2012). However, Arabidopsis *atg9* mutants show less severe autophagy disruption than other mutants in *ATG* genes (Hanaoka *et al.*, 2002). When the phagophore is formed, it needs to undergo a few steps for expansion, maturation and degradation in the vacuole (Figure 4). In yeast and mammalian cells, cytoskeleton drives the membrane shaping

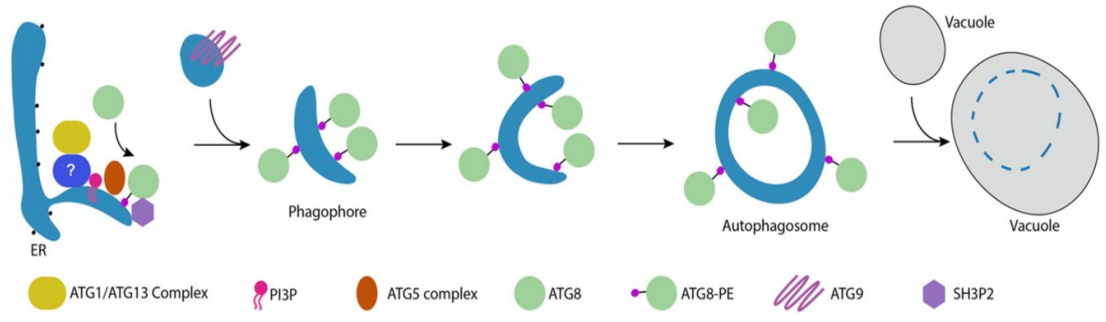

Figure 4: **Formation of autophagosome.** After autophagy induction, a phagophore is created on endoplasmic reticulum. During phagophore formation, ATG1/ATG13 complex recruits downstream regulators to the initiation site. PI3P is present at the phagophore initiation site and ATG8 is anchored to phagophore via conjugation to PE. Moreover, ATG5 and SH3P2 are present on the phagophore, as well. A plant specific protein SH3P2 binds PI3P and is necessary for autophagosome formation and maturation. Vesicles ATG9 are also required for phagophore budding. Reproduced from Soto-Burgos et al., 2018.

during autophagosome formation (Kast and Dominguez, 2017). A few studies provided the evidence of link between plant cytoskeleton and autophagy by demonstrating the colocalization of autophagy markers ATG8 and NBR1 with plant cytoskeletal components (Ketelaar *et al.*, 2004; Zientara-Rytter and Sirko, 2014). Another study showed the role of the exocyst complex in autophagosome transport to the vacuole, as *exo70B1* mutant shows decreased amount of intravacuolar autophagic bodies (Kulich *et al.*, 2013). Moreover, the whole exocyst complex may coordinate the vesicle trafficking with the cytoskeleton (Synek, Sekereš and Žárský, 2014).

2.2.3 Role of Phosphoinositides in Plant Autophagy

Membrane compartments involved in plant autophagy are enriched in PI3P (Fig. 5). By reason of the presence of this signalling lipid, emerging membrane may recruit specific effector proteins based on their specific interaction with PI3P (Noack and Jaillais, 2017). Conversion of phosphatidylinositol (PI) to PI3P is catalysed by class III PI3K vacuolar protein sorting 34 (VPS34). This protein is a part of VPS34 (PI3K) complex together with proteins VPS15, VPS30 and Beclin1/ATG6 (core complex). An alternative way for PI3P production is from $PI(3,5)P_2$ by 5-phosphatases encoded by *SUPRESSOR OF ACTIN* (*SAC*, Fig. 5).

In yeast and mammalian cells, the PI3 kinase complex I is needed for phagophore initiation. The PI3 kinase complex II, where ATG14 is replaced by VPS38 (Fig. 5) regulates vacuolar and endosomal trafficking. Nevertheless, the role of mammalian VPS38 homolog in autophagy is debatable (Levine *et al.*, 2015). A role of plant VSP34

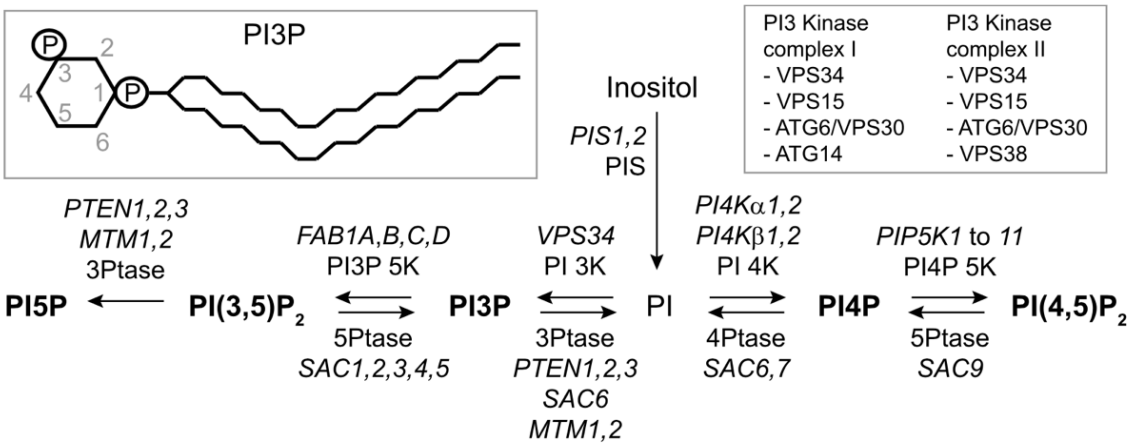

Figure 5 **Phosphoinositide metabolism in plants.** Phosphatidylinositol (PI) is synthetized by PI synthases. PI is phosphorylated by VPS34 PI 3-kinase (PI 3K), or by PI 4-kinase (PI 4K). Both PI3P and PI4P can be phosphorylated by PIP 5-kinases (PIP5K). Reproduced from Chung, 2019.

complexes and their product PI3P in autophagy was discussed after genetic analysis of tobacco and *A. thaliana* ATG6/VP30, a component of VPS34 complexes (Liu *et al.*, 2005; Fujiki, Yoshimoto and Ohsumi, 2007; Qin *et al.*, 2007; Harrison-Lowe and Olsen, 2008; Patel and Dinesh-Kumar, 2008). Fujiki et al. (2007) showed that mutants in *atg6, vps34* and *vsp15* have problems with pollen transmission, which suggests autophagy-independent function of the VPS34 complex. Moreover, studies of inhibition of autophagic trafficking repressed by wortmannin as a PI 3-kinase inhibitor also suggests dual role of plant VPS34 complexes (Zhuang *et al.*, 2013; Shin, Lee and Chung, 2014; Le Bars *et al.*, 2014).

The function of PI3 kinase complex I in autophagy is mediated by PI3P and its effectors. Nevertheless, ATG6 and ATG14 as non-catalytic subunits of the complex contribute to autophagy in independent way of PI3P. For instance, tobacco Beclin1/ATG6 interacts with RNA-dependent RNA polymerase of the turnip mosaic virus, which leads to the degradation of viral enzyme by ATG8-mediated autophagy (Li *et al.*, 2018). This finding suggests that ATG6 homologs may serve as a receptor for selective autophagy. Several studies showed that *A. thaliana vps38* mutants show inhibited autophagic flux during nitrogen starvation (Lee *et al.*, 2018; Liu, Hu and Vierstra, 2018). However, the autophagic flux inhibition is mild compared to autophagy inhibition in *atg7* mutant and no significant difference was observed compared to wild type in nutrient-rich conditions.

An important PI3P-binding protein involved in autophagosome formation at the ER (Zhuang *et al.*, 2013) is SH3 domain-containing protein 2 (SH3P2, Fig. 4). In yeast two-hybrid assay, SH3P2 interacts with itself and ATG8 (Zhuang *et al.*, 2013) In colocalization analysis, SH3P2 showed the colocalization with ATG6 and ATG9 markers and partial colocalization with ATG8 (Zhuang *et al.*, 2013). Immunolabelling of SH3P2-GFP detected the protein at the ER and on the ATG8-positive membrane. Moreover, SH3P2-GFP puncta were detected in the vacuole treated by Concanamycin A (ConcA). This accumulation was inhibited by wortmannin, implying that SH3P2 is a PI3P effector and takes part in plant autophagy (Zhuang *et al.*, 2013).

2.2.4 Regulation of Lipid Metabolism by Autophagy

Lipid droplets (LDs) are conserved eukaryotic organelles present in most cell types and organisms (Walther and Farese, 2012). LDs are composed of triacylglycerol

(TAG) and steryl-ester (SE) formed by enzymatic transfer of acyl chains from fatty acids to DAG and sterols (Pol, Gross and Parton, 2014).

In mammalian hepatocytes, free fatty acids (FFAs) are converted into triacylglycerol (TAG) and stored with cholesterol in lipid droplets (Martin & Parton, 2006). When the cell demands more energy, the TAG hydrolysis is upregulated and FFAs undergo β-oxidation. Autophagy works similarly as an independent process providing energy by breaking cellular components (Komatsu *et al.*, 2005; Mizushima *et al.*, 2008). Singh et al., 2009 showed that lipid droplets and autophagy components associate during nutrient deprivation. Also, when autophagy is inhibited, storage of TAGs in lipid droplets is increased and LD accumulate in different organs.

Plant cells assemble TAG in the ER and store it in form of LDs in the cytosol (Chapman and Ohlrogge, 2012). In Arabidopsis, enzyme responsible for catalysation of the last step of TAG synthesis is phospholipid diacylglycerol acyltransferase1 (PDAT1; Zhang *et al.*, 2009). TAGs are hydrolysed by cytosolic lipases. One of them, SUGAR-DEPENDENT1 (SDP1), is responsible for the initiation of TAG catabolism (Eastmond, 2006). Under extended darkness, TAG level of *sdp1* mutants rapidly increases and then decreases, which suggests activation of alternative pathways for TAG hydrolysis under starvation conditions (Fan, Yu and Xu, 2017).

A recent study of Fan, Yu and Xu (2019) shows that disruption of autophagy blocks membrane lipid turnover, thus TAG synthesis under normal growth conditions. Under starvation conditions, TAG content increases when autophagy is induced, but decreases when autophagy is disabled in *sdp1*. This study suggests that LD degradation happens in a process resembling microautophagy and occurs in autophagic vacuole, a key component in macroautophagy (Eskelinen, 2005).

Moreover, the role of basal autophagy in lipid metabolism is tissue and/or developmental-specific. Autophagy contributes to TAG synthesis insignificantly in young seedlings, rapidly growing leaves and developing seeds. However, the contribution is remarkable in mature and senescing leaves of adult plants (Fan *et al.*, 2019). This difference may be caused by the fact that newly formed organellar membranes in young leaves may not be targeted for autophagy-mediated degradation under normal growth conditions.

Kokabi *et al.*, 2020 show in a very recent study an impact of N and P deprivation on reorganisation of glycerolipids in microalga *Lobosphaera incisa*. This microalga belongs to oleaginous species and accumulates TAG as a form of energy-rich reserve.

The TAG production may be boosted by various stress stimuli, such as light and nutrient availability and N deprivation (Hu *et al.*, 2008). Comparative lipidomic profiling revealed an intensive degradation of chloroplast lipids under N deprivation, while various lyso-PC species increased in their abundance (Kokabi *et al.*, 2020). Autophagy-mediated degradation of chloroplast components can play a crucial role in the supply of amino acids and building blocks for enhanced FA and TAG biosynthesis.

Furthermore, ATGs were upregulated under N starvation. The authors also analysed the expression patterns of *ATG8*, marker of autophagy, *MLDP*, marker of lipid droplets and *DesD5*, as a marker of arachidonic acid (ARA) biosynthesis. Expression of these markers under N deprivation showed relationship between autophagy, LD biogenesis and ARA sequestration in LDs in *L. incisa*. However, a little is known about the function of ATG proteins in *L. incisa.* Despite the proofs of proximity of LDs to the vacuoles (Gorelova *et al.*, 2015; Tsai *et al.*, 2018; Zienkiewicz *et al.*, 2020) the LDs did not form impaired in *Chlamydomonas atg* mutants, which also showed recycling of diverse cytoplasmic components (Kajikawa *et al.*, 2019). Additionally, there are opinions that TOR activation may regulate TAG biosynthesis without activation of the autophagic pathway in algae (Kajikawa and Fukuzawa, 2020).

2.2.5 Visualisation of Autophagosomes in Plant Cells

There is a number of methods for autophagy analysis in plant cells, most of them optimised for *Arabidopsis thaliana*. Many of the non-invasive methods for autophagy analysis track either cargo or receptor proteins. Protein ATG8 is considered to be a perfect marker for autophagic structures during their formation. ATG8 localizes to autophagosomes through their life cycle. Even though ATG8 does not possess a trans-membrane domain, it is stably associated to autophagosome membrane by phosphatidylethanolamine (PE) conjugation (Geng and Klionsky, 2008). Once autophagosome is fused with the vacuole, ATG8 remains on its inner membrane until autophagosome is degraded (Li and Vierstra, 2012).

There are nine genes coding ATG8 in *A. thaliana*, all of them localize to autophagosomes and may be used as autophagosome markers (Yoshimoto *et al.*, 2004; Sláviková *et al.*, 2005; Woo, Park and Dinesh-Kumar, 2014). Visualisation of ATG8 is possible by fusion with fluorescent proteins (FP). While ATG8 is conjugated to PE at its C-terminus, fluorescent protein must be attached to N-terminus. Expression of ATG8

fused with FP may be either transient (Contento, Xiong and Bassham, 2005) or in transgenic plants (Yoshimoto *et al.*, 2004; Thompson *et al.*, 2005; Xiong *et al.*, 2007b).

Besides, there are more proteins coded by autophagy related genes (ATG), that can be used as autophagy markers. For example, ATG1, ATG13 and ATG 11 fused with fluorescent protein localize to punctate structures in the cytoplasm during starvation and are also delivered to the vacuole (Suttangkakul *et al.*, 2011; Li, Chung and Vierstra, 2014). These proteins colocalize to ATG8, therefore may be possibly used as an alternative of ATG8 (Fujiki *et al.*, 2007).

Moreover, other fluorescent markers may be used for autophagy visualisation. Autophagosome lumen is acidified and can accumulate acidotropic dyes, such as Lysotracker Red, quinacrine, Neutral Red and Lucifer Yellow (Moriyasu and Ohsumi, 1996; Yano *et al.*, 2004; Takatsuka *et al.*, 2004; Liu *et al.*, 2005; Inoue *et al.*, 2006; Patel and Dinesh-Kumar, 2008). These dyes weakly stain the central vacuole, but strongly small acidic compartments. They are often used together with cysteine protease inhibitor for intensive accumulation of vesicles. In spite of easier visualisation, using cysteine protease inhibitors leads to different results depending on which inhibitor was used (Bassham, 2015). Unlike previously mentioned dyes, monodansylcadaverine (MDC) does not stain central vacuole, which makes it more selective dye suitable for plant autophagosome staining (Munafó and Colombo, 2001; Contento *et al.*, 2005; Patel and Dinesh-Kumar, 2008).

One of the frequently used approaches to study autophagy efflux in plants is use of ConcA. This inhibitor of vacuolar H^+-ATPase is often used in conjugation with GFP-ATG8 fluorescent marker. ConcA prevents vacuolar acidification and disrupts vesicle trafficking between *trans*-Golgi network and the vacuole (Matsuoka *et al.*, 1997; Dettmer *et al.*, 2006). Due to low pH inside the vacuole, macromolecules degradation is blocked and autophagic bodies accumulate inside the vacuolar lumen (Yoshimoto *et al.*, 2004). Another method working in a similar manner as ConcA is incubation with protease inhibitor blocking vacuolar protein degradation. The most commonly used inhibitor is E-64 and its variants (Moriyasu and Ohsumi, 1996). Inhibitor E-64 causes accumulation of spherical structures in the cytoplasm (autolysosomes) around nucleus, rather than accumulation of autophagosomes inside the vacuole (Moriyasu and Ohsumi, 1996; Yano *et al.*, 2004; Takatsuka *et al.*, 2004). Furthermore, E-64 may have different effects based on used species and experimental conditions (Bassham, 2015).

2.3 Function of Phospholipids in Mammalian Autophagy

Previous studies indicate the important role of phosphatidic acid (PA) in mammalian autophagy; however, little research has been conducted to show how and where exactly PA affects the process of mammalian autophagy (Shatz *et al.*, 2016). In spite of no evidence about PA presence in autophagosome membrane, PA might contribute to the negative curvature of the phagophore. Phospholipase D1 (PLD1), producing PA in mammalian cells, partially colocalize with mammalian autophagy regulator Microtubule-associated protein 1 light chain 3 (LC3) under nutrient deficiency conditions. In addition, inhibition of PLD1 results in impaired mammalian autophagy and decrease of LC3-positive compartments (Dall'Armi *et al.*, 2010)

Fang et al. (2001) identified the role of PA in regulation of mammalian target of rapamycin complex 1 (mTORC1) activity. The negative regulator of mTORC1 activity, protein DEP domain-containing mTOR-interacting protein (DEPTOR), is displaced from mTOR by PLD1-generated PA, which makes PA an activator of mammalian autophagy (Yoon *et al.*, 2015). Another important function of PA is reducing the affinity of Beclin1 towards VPS34 complex (Jang, Choi and Min, 2014). Furthermore, phagophore formation may be affected even by the mitochondrial PLD (mitoPLD) because autophagosomes probably arise at ER-mitochondria contact sites (Hailey *et al.*, 2010; Hamasaki *et al.*, 2013).

Phosphatidylethanolamine (PE) plays a vital role in phagophore expansion in both plants (Section 2.2.2.) and animals. In mammalian cells, the ER-Golgi intermediate compartment (ERGIC) membranes support lipidation of LC3 (Ge *et al.*, 2013). Shatz *et al.* (2016) suggest that strongly curved membranes such as small intracellular vesicles could serve as precursors of autophagosome membranes *in vivo*, as lipidated ATG8 can mediate membrane tethering and fusion *in vitro* (Nakatogawa, Ichimura and Ohsumi, 2007; Weidberg *et al.*, 2011).

3 MATERIAL AND METHODS

3.1 Reagents

Table 1 List of used reagents

Reagent	Manufacturer
Acetic acid	LachNer
Acetone	Merck
Ammonium dihydrogen phosphate ($NH_4H_2PO_4$)	Merck
Bis-tris propane	INC - Biochemicals
BODIPY-phosphatidylcholine	Invitrogen
Boric acid (H_3BO_3)	Lachema
Bovine serum albumin fraction V (BSA)	Merck
Bradford Reagent	Sigma Aldrich
Calcium dichloride ($CaCl_2$)	Calbiochem
Calcofluor white stain	Sigma Aldrich
Calcium nitrate tetrahydrate ($Ca(NO_3)_2 \cdot 4H_2O$)	Lachema
Chloroform	Merck
Cobaltous chloride hexahydrate ($CoCl_2 \cdot 6H_2O$)	Lachema
Copper sulphate pentahydrate ($CuSO_4 \cdot 5H_2O$)	Lachema
Dimethyl sulphoxide (DMSO)	Sigma Aldrich
Dipalmitoylphosphatidylcholine (DPPC)	Sigma Aldrich
Disodium ethylenediaminetetraacetate dihydrate (Na_2EDTA)	Lachema
Ethanol	VWR
Ethylene glycol-bis(β-aminoethyl ether)-N,N,N′,N′-tetraacetic acid (EGTA)	Sigma Aldrich
Ethylenediaminetetraacetic acid (EDTA)	VWR
Goat anti-Rabbit IgG (H+L) Polyclonal Secondary Antibody, DyLight 488 (35552)	Thermo Fisher Scientific
Goat anti-Rabbit Polyclonal Secondary Antibody, Alexa Fluor 555 (A-21428)	Thermo Fisher Scientific
Igepal Ca630	Sigma Aldrich
Iron(II) sulphate heptahydrate (FeSO4 · 7H2O)	LachNer
Iron(III) citrate	Sigma Aldrich
Magnesium sulfate heptahydrate ($MgSO_4 \cdot 7H2O$)	LachNer
Magnesium sulphate ($MgSO_4$)	Merck
Manganese sulphate tetrahydrate ($MnSO_4$. 4H2O)	Sigma Aldrich
Methanol	Merck
2-(4-Morpholino)ethanesulfonic acid (MES)	Sigma Aldrich
Murashige and Skoog Caisson MSP01	Caisson Labs
Murashige and Skoog Caisson MSP21	Caisson Labs
myo-Inositol	Sigma Aldrich
n-Butanol	Lachema

Reagent	Manufacturer
Nicotinic acid	Sigma Aldrich
Paraformaldehyde (PFA)	Sigma Aldrich
Pectolyase Y-23	Duchefa
Pierce Phosphatase Inhibitor Mini Tablets (A32957)	Thermo Fisher Scientific
Piperazine-N,N′-bis(2-ethanesulfonic acid)	Sigma Aldrich
Potassium hydroxide (KOH)	Chemapo
Potassium iodide (KI)	Lachema
Potassium nitrate (KNO_3)	Lachema
Protease Inhibitor Coctail (P9599)	Sigma Aldrich
Pyridoxin	Sigma Aldrich
Rabbit anti-ATG8 Polyclonal Primary Antibody (AS14 2769)	Agrisera
Savo (bleach)	Unilever
Sodium azide (NaN_3)	Sigma Aldrich
Sodium deoxycholate	Sigma Aldrich
Sodium hydroxide (NaOH)	Lachema
Sodium molybdate dihydrate ($Na_2MoO_4 \cdot 2H_2O$)	Sigma Aldrich
Sucrose	Lachner
Thiamine	Sigma Aldrich
TritonX-100	MP Biochemicalsd
Tween 20	Sigma Aldrich
Zinc sulfate heptahydrate ($ZnSO_4 \cdot 7H_2O$)	LachNer

3.2 Equipment

Table 2 List of used equipment

Equipment	Manufacturer
Automatic TLC Sampler	Camag
Centrifuge Eppendorf 5424	Eppendorf
Centrifuge Jouan KR22i	Jouan
Fluorescence scanner FLA-7000	Fuji
Grow box Percival CU-41L4	Percival
Grow box Percival E-36L	Percival
Intavis InsituPro	Intavis Bioanalytical Instruments
Microplate spectrophotometer Micro Quant	Biotech
pH meter: Cyber scan pH 1100	Eutech
Scale H110	Sartorius
Spinning disk microscope Nikon (Eclipse Ti-E, inverted)	Nikon/Yokogawa
Ultracentrifuge Sorvall	Kendro
Ultrasonic cleaner	Tesla

3.3 Plant Material

All *Arabidopsis thaliana* wild type and T-DNA insertion mutant seeds were obtained via Nottingham Arabidopsis Stock Centre (NASC) from Salk Institute Genome Analysis Laboratory (Alonso et al., 2003) and GABI-Kat (Kleinboelting *et al.*, 2012) collections. For phenotype screening, I used 6-day-old *A. thaliana* plants, ecotype Columbia (Col-0) and T-DNA insertion mutants stated below (Table 1). For measuring activity of lipid metabolising enzymes, I used separated roots and leaves of 28-day-old *A. thaliana*, ecotype Col-0 and *atg10* (SALK_084434) T-DNA insertion mutant.

For live cell imaging, I used 6-day-old *A. thaliana*, GFP-ATG8e transgenic lines, described in Le Bars et al. (2014).

For fluorescence immunolabelling, I used 6-day-old *A. thaliana* seedlings, ecotype Col-0 and T-DNA insertion mutant plants *dgk7* (GABI_174H01), *pldα3* (SALK_130690), *pldβ1* (SALK_079133) and *atg10* (SALK_084434).

3.4 Growth Conditions and Autophagy Induction

For phenotype screening, seeds were sterilized in 30% (v/v) bleach (Savo), 0.05% (v/v) Tween-20 for 10 minutes and stratified on half strength MS solid medium (Murashige and Skoog, 1962), 1% (w/v) agar (Sigma), pH = 5.8; for 2 days at 4 °C in the dark. Seedlings were grown vertically for 5 days in Petri dishes sealed with gas-permeable tape 3M Micropore (3M) in a grow box with a 16 h light (22 °C) 8 h dark (20 °C) photoperiod.

Table 3 List of *A. thaliana* mutant plants with knocked-out genes for various lipid-metabolising enzymes and their identifiers used for phenotype analysis.

mutant	identifier	mutant	identifier
pi-plc1	SALK_025769	*pldα1*	SALK_067533
pi-plc2	SALK_101809	*pldα2*	GABI_212E06
pi-plc3	SALK_054406	*pldα4*	SALK_017905
pi-plc4	GABI_832F07	*pldβ2*	SALK_079133
pi-plc5	SALK_144469	*pldγ1*	SALK_066687
pi-plc7	SALK_030333	*pldγ2*	SALK_089965
npc1	SAIL_548_H09	*pldγ3*	SALK_084335
npc2	SALK_018011	*pldδ*	SALK_023247
npc3	SALK_078975	*pldζ2*	SALK_094369
npc4	SALK_046713	*pldζ1ζ2*	SALK_053090,
npc5	SALK_045037	*pldζ1ζ2*	SALK_094369
npc6	SALK_077041	*atg10-1*	SALK_084434

For autophagy induction, 5-day-old seedlings with similar length were transferred to Petri dishes with fresh ½ MS medium (same composition). Each Petri dish was divided into 3 columns, each column containing 4 seedlings of the same genotype. Four Petri dishes of each genotype were grown for alternations of genotypes in columns. All Petri dishes sealed with gas-permeable tape 3M Micropore (3M) were wrapped in aluminium foil and kept in the grow box for 6 days in the dark. After six days of carbon starvation, Petri dishes with seedlings were uncovered and kept in the grow box for seven days in the light for recovery (Tsai *et al.*, 2013).

For measuring activity of phospholipases, seeds were sterilized in 30% (v/v) bleach, 0,05% (v/v) Tween-20 for 10 minutes and stratified in water for 2 days at 4 °C in the dark. Seeds were grown hydroponically in wells (30 x 13,5 mm) filled with Grodan Master slabs (Grodan). Slabs were placed on a growing container filled with 25% (v/v) Hoagland solution (Hoagland, D. R.; Arnon, 1950) and were partly dipped in the solution. The growing container was placed to a grow box with a 10 h light (22 °C) and 14h dark (20 °C) photoperiod for 28 days. After 14 days of cultivation, the Hoagland solution was changed every 7 days to fresh 50 % (v/v) Hoagland solution. Before sample collection, treated plants were kept additional 3 days in the dark (extended dark; Izumi et al., 2013). Samples were taken under green light to avoid morphological changes in plants.

For live cell imaging and fluorescence immunolabelling, seeds were sterilized in 30% (v/v) bleach, 0.05% (v/v) Tween-20 for 10 minutes and stratified on half strength MS solid medium (MS Caisson MSP01) containing 1 % (w/v) sucrose. Seedlings were grown vertically for 6 days in Petri dishes sealed with gas-permeable tape 3M Micropore (3M) in a grow box with a 16 h light (22 °C) 8 h dark (20 °C) photoperiod. Six-day old seedlings of treated plants were moved to half strength MS medium depleted for nitrogen and carbon (MS Caisson MSP21) for two hours. Control 6-day-old seedlings were transferred on fresh half strength MS solid medium containing 1% (w/v) sucrose (Merkulova *et al.*, 2014) for 2 hours.

3.5 Measuring Primary Root Increment

After six days of carbon starvation followed by seven days of recovery, Petri dishes with *Arabidopsis thaliana* wild type and T-DNA insertion mutant plants were scanned and primary root increment of each plant was measured using ImageJ software (Schindelin *et al.*, 2012) with Neurite Tracer plugin (Pool *et al.*, 2008). Values were averaged from 10 to 16 samples and statistically analysed using T-test.

3.6 Isolation of Cytosolic Fraction

Separated leaf and root tissue was frozen in liquid N_2 and stores in the freezer at -80 °C and ground in a chilled mortar and pestle at a ratio of 1g of plant tissue to 5 ml of homogenisation buffer containing 400 mM sucrose, 50 mM HEPES, 100 mM KCl, 100 mM $MgCl_2$. $6H_2O$, 10 mM ascorbic acid, Pierce Phosphatase Inhibitor Mini Tablets (1 tablet per 10 ml), Protease Inhibitor Cocktail (100 µl per 10 ml), pH 7.0. The homogenate was centrifuged at 6000 × g for 10 min at 4 °C. The supernatant was kept and centrifuged at 200000 × g for 60 min. at 4 °C. Supernatant was kept as a cytosolic fraction.

3.7 Protein Quantification in Cytosolic Fraction

To measure protein concentration in cytosolic fraction of root and leaf tissue, I used the Bradford method (Bradford, 1976). Samples of cytosolic fraction were 5x diluted in homogenisation buffer (Section 3.6) and 10 µl of sample was moved to plate for spectrophotometry. To each well, 300 µl of Bradford reagent was added and samples were incubated for 15 min. Absorbance was measured at 595 nm. Bovine serum albumin (BSA) was used as a standard for linear calibration.

3.8 Measuring Activity of Lipid Metabolising Enzymes *in vitro*

Activity of lipid metabolising enzymes was measured by level of their fluorescently labelled products in *Arabidopsis thaliana* leaf and root cytosolic fraction. Fluorescently labelled products were separated by high performance thin layer chromatography (HPTLC) and quantified using fluorescent scanner (Fuji).

First, a reaction mixture of 20 mM $CaCl_2$, 0.4% (v/v) n-butanol and 15 µg of protein in cytosolic fraction was prepared. Then, a substrate containing 0.8 µl of phosphatidylcholine (PC) fluorescently labelled by BODIPY (4,4-difluoro-4-bora-3a,4a-diaza-s-indacene) diluted in ethanol (1mM) and dipalmitoylphosphatidylcholine (DPPC) diluted in ethanol (2.7 mM) was prepared. Ethanol was evaporated at 35 °C and the substrate was resuspended in 25 µl of suspension buffer containing 0.06% sodium deoxycholate in MES (v/v). Substrate was sonicated using ultrasound cleaner for 10 minutes. Reaction started with addition of 25 µl of substrate to reaction mixture at 23 °C, and gently shook at 300 RPM in the dark. After 30 min, reaction was stopped by adding 400 µl of methanol and chloroform mixture 2:1 (v/v). Samples were centrifuged at 400 x g for 15 min. After centrifugation, 100 µl of lower phase was kept

and vacuum evaporated at 35 °C. Sample was resuspended in 50 µl ethanol and using automatic TLC sampler applied on HPTLC silica plate. Fluorescently labelled products were separated by mobile phase containing chloroform, methanol, acetic acid and water (45:45:8:2, v/v/v/v). HPTLC silica plate was scanned by fluorescence scanner (Fuji) at 520 nm and the level of fluorescence of labelled lipids was determined using MultiGauge software (Fujifilm).

3.9 Live Cell Imaging

Seedlings with induced autophagy were mounted to a microscope slide with a drop of half strength MS medium depleted for nitrogen and carbon and covered by a cover slip. Seedlings in control conditions were mounted to a microscope slide with a drop of half strength MS medium. The specimens were mounted in the dark to avoid light stress. Seedlings were observed with Spinning disk microscope Nikon, Eclipse Ti-E, inverted (Nikon) equipped with Plan-Apochromat L 20x/0.75 objective.

3.10 Fluorescent Immunolabelling

Separated roots of seedlings with induced autophagy and in control conditions were placed for fixation in 4% (v/v) paraformaldehyde in microtubule-stabilizing buffer (MTSB; 50 mM PIPES, 5 mM EGTA, 5 mM $MgSO_4$, pH = 6.8) containing 0.1% (v/v) TritonX-100 for 60 min.

For immunostaining, seedlings were moved to incubation baskets of pipetting robot Intavis InsituPro (Intavis Bioanalytical Instruments). Seedlings were stained by a following protocol previously described by Pasternak et al., 2015 (modified);

- Incubation with 0.1% (v/v) TritonX-100 in MTSB buffer for 5x15 min at room temperature.
- Incubation with 0.1% TritonX-100 in water for 5x15 min.
- Incubation with enzymes (0.05% [w/v] pectolyase in MTSB with 0.1% [v/v] TritonX-100) at 37 °C for 30 min.
- Incubation with 0.1% (v/v) TritonX-100 in MTSB for 5x15 min at room temperature.
- Incubation with 10% DMSO (w/v) and 3% (v/v) Igepal Ca630 in MTSB with 0.1% (v/v) TritonX-100 for 2x30 min.
- Incubation with 0.1% (v/v) TritonX-100 in MTSB for 5x15 min.

- Incubation with blocking solution (2% [w/v] BSA Fraction V, 0.1% [v/v] TritonX-100 in MTBS) for 60 min at 37 °C.
- Incubation with rabbit anti-ATG8 polyclonal primary antibody (Agrisera), dilution 1:500 (v/v) in blocking solution for 4 h at 37 °C.
- Incubation with MTSB buffer with 0.1% (v/v) TritonX-100 for 8x15 min at room temperature.
- Incubation with goat anti-rabbit polyclonal secondary antibody, DyLight 488 (Thermo Fischer Scientific) or goat anti-rabbit polyclonal secondary antibody, Alexa Fluor 555 for fluorophore colocalization, dilution 1:1000 (v/v) in blocking solution for 3h at 37 °C.
- Incubation with 0.1% (v/v) TritonX-100 in MTSB buffer for 5x15 min and in water for 5x15 min at room temperature.

After immunostaining, seedlings were incubated with 0.002% (v/v) calcofluor white stain for 20 min and moved to 50% (v/v) glycerol with 0.02% (w/v) sodium azide. Fluorescence signal was observed with Spinning disk microscope Nikon, Eclipse Ti-E, inverted (Nikon/Yokogawa) equipped with Plan-Apochromat LS 40x/1.25 water immersion objective.

3.11 Stereological Methods

Number of autophagosomes was counted using the disector counting technique (Sterio, 1984). A disector was created with ImageJ software (Schindelin *et al.*, 2012) using plugin Disector (Janáček, 2012). The disector X,Y dimension was 150 x 150 µm with the depth of 7.5 µm. The disector consisted of a reference section (first section, Fig. 7) and a look-up section (last section). Only particles present in the disector volume and not

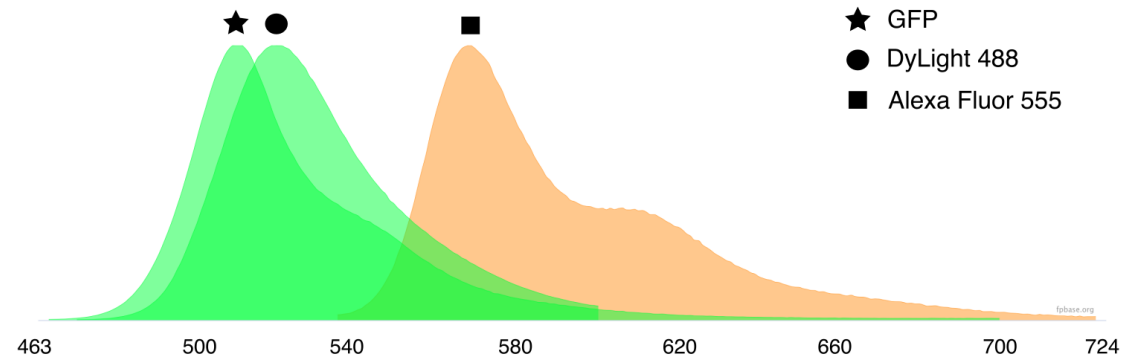

Figure 6 Emission spectra of fluorophores used for fluorescence microscopy. Source: www.fpbase.org, edited.

crossing the look-up section were counted. Nevertheless, to obtain unbiased estimation of autophagosomes in fixed cells the number of particles should be stated per volume (Maynard, 1996).

Therefore, number density (n) of autophagosomes was estimated by:

$$n = \frac{N}{estV(dis)}$$

where N is the number of labelled particles inside the disector and estV(dis) is estimated volume of plant tissue inside the disector. The volume of tissue inside the disector was estimated with Cavalieri's estimator (Gundersen and Jensen, 1987). A systematic fixed set of test points was thrown at the tissue image at random and each point crossing the tissue was counted. Finally, an unbiased volume estimator was counted by:

$$estV(dis) = T.a.\sum_{j=1}^{n} P_j(dis)$$

where T is distance between two sections, a is area unit corresponding to the one unit of test point grid and $P_j(dis)$ is number of test point hitting the j-th tissue section.

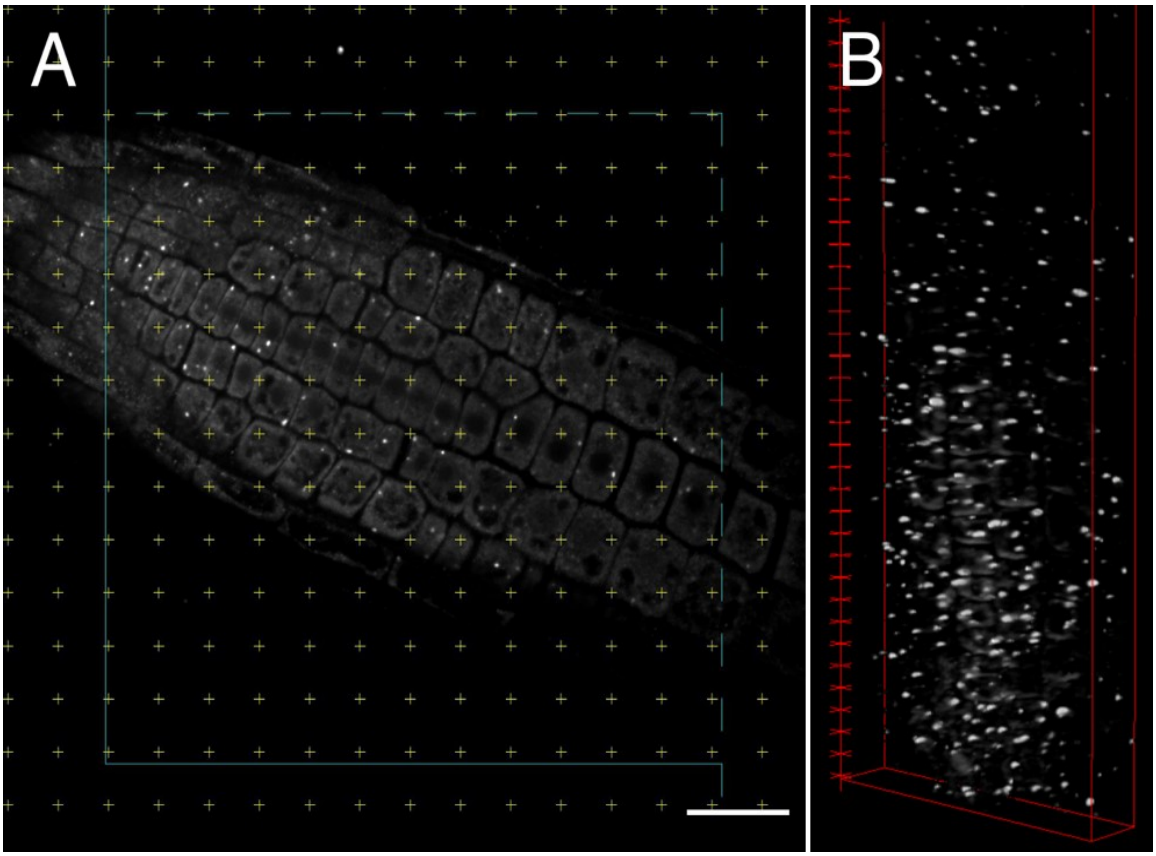

Figure 7 Disector reference section and systematic set of test points scale = 25 μm (A). 3-dimensional view of autophagosomes in root meristematic zone (B).

4 RESULTS

This thesis reports on the role of lipids and lipid-metabolizing enzymes in plant autophagy. As autophagy is a crucial process for plant cells, a number of methods have been developed for studying autophagy, most of them optimized for *Arabidopsis thaliana*. Here, I used various methods for analysing the role of lipids in plant autophagy, including phenotype screening of *A. thaliana* mutants with knocked-out genes for phospholipases and analysis of products of lipid-metabolizing enzymes of *A. thaliana* wild type and mutant plants with knocked-out *ATG10* gene separated by high performance thin layer chromatography (HPTLC). Finally, I have optimized a method for quantification of autophagosomes in the root cells of *A. thaliana*. Emphasis has been placed on unbiased estimation of autophagosome number inside the root cell. For each method, I used a different type of stressor for autophagy induction, typically carbon and nitrogen starvation.

4.1 Phenotype Screening of *A. thaliana* Phospholipases Mutants

Here, I compared the length of primary root increment of *A. thaliana* mutant plants with knocked-out genes for phosphoinositide-specific phospholipases C (PI-PLC), non-specific phospholipases C (NPC), and phospholipases D (PLD) to wild type (WT) after carbon starvation. Five days old plants were transferred to the dark for 6 days, then recovered in control conditions for another 7 days (Tsai *et al.*, 2013). As a positive control, I used the phenotype of *A. thaliana* mutants with knocked out *ATG10* gene (Fig. 8).

After 6 days of carbon starvation and 7 days of recovery, I scanned Petri dishes with the seedlings, and measured the length of primary root increment. *A. thaliana pi-plc2* (Fig.8), *pi-plc3*, *pi-plc5, pldα2* and *pldζ2* knock-out mutants exhibit significantly lower primary root increment, when compared to wild type (Fig. 9, 10) using T-test. Nevertheless, the primary root inhibition was mild compared to *atg10* mutants.

In conclusion, this experiment provided data of various *pi-plc* knock-out mutants in genes coding PI-PLC, NPC and PLD phenotype after 6 days of carbon starvation in the dark. The experiment was repeated by the laboratory of my supervisor and their data did not confirmed the results of this experiment. Based on their unpublished results, knock-out mutants *dgk7*, *pldα3* and *pldβ1* have been selected for further analysis.

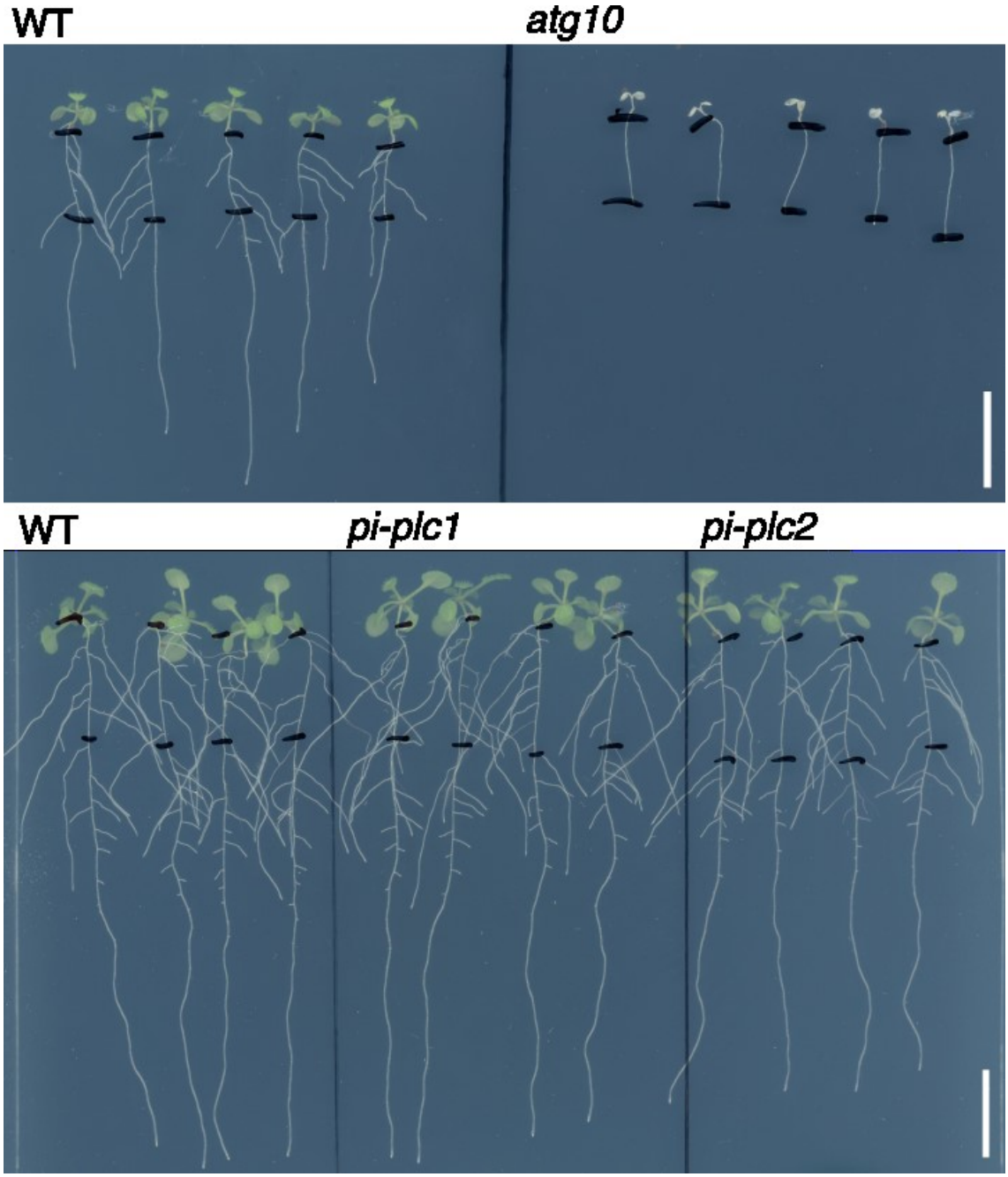

Figure 8: Phenotype of *A. thaliana atg10* mutant seedlings compared to wild type (WT) and *pi-plc1*, *pi-plc2* mutant seedlings compared to WT after 6 days of carbon starvation in the dark. Mutants *pi-plc2* exhibit significantly lower length of primary root increment. Mutant *atg10* with disrupted autophagy is used as a positive control. Scale = 1 cm.

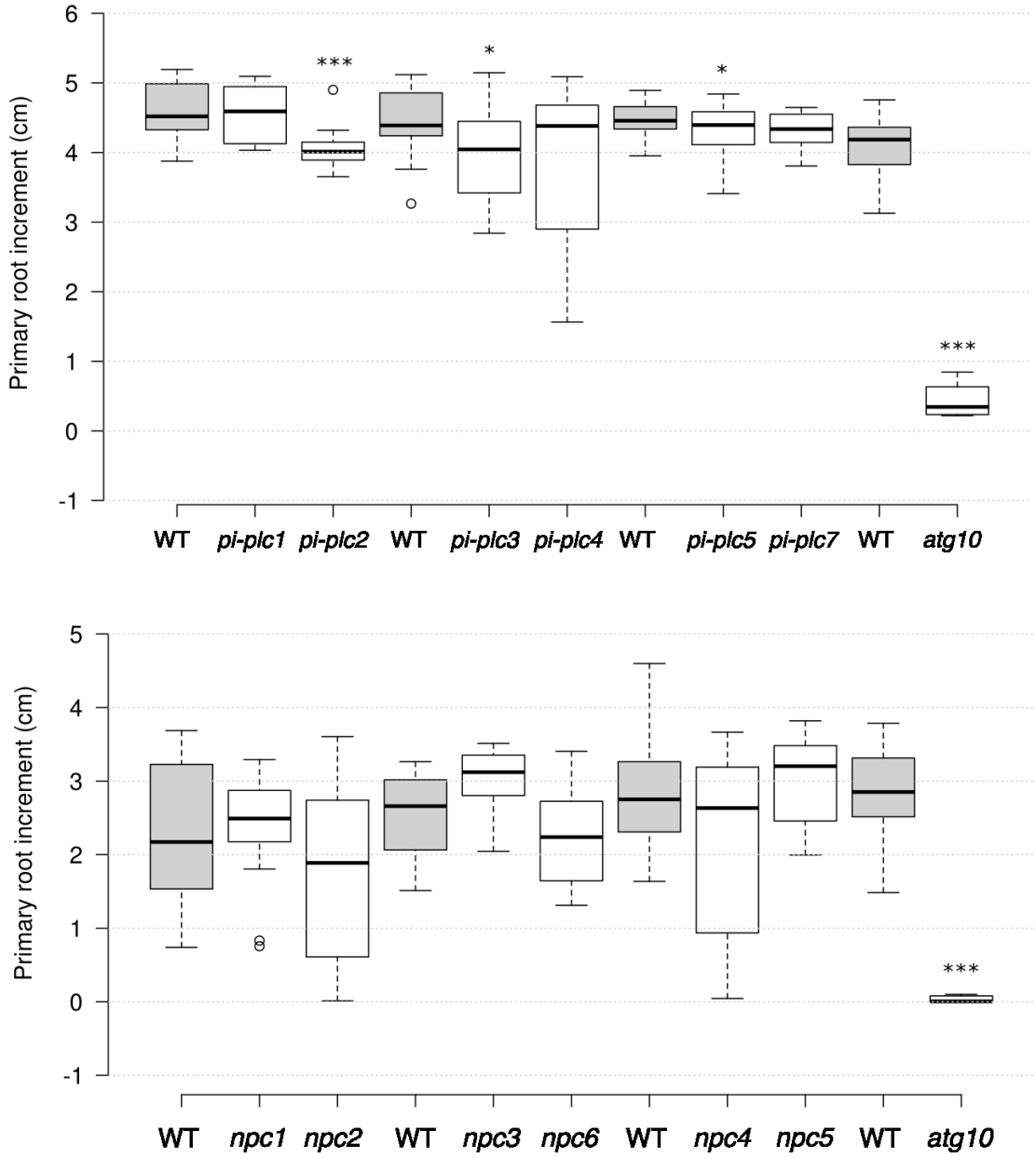

Figure 9 Length of primary root increment of *A. thaliana* wild type (grey) and knock-out mutants in genes coding phospholipases C (white) after 6 days of carbon starvation in the dark. Each wild type seedlings were compared to two following knock-out mutants. Mutants *pi-plc2*, *pi-plc3* and *pi-plc5* exhibit a significant difference in primary root increment length compared to wildtype. Mutant *atg10* was used as a positive control. Asterisks indicate a significant difference compared to wild type. (n = 10-16; T-test, * $P < 0.1$; ** $P < 0.01$; *** $P < 0.001$) Horizontal black line represents median.

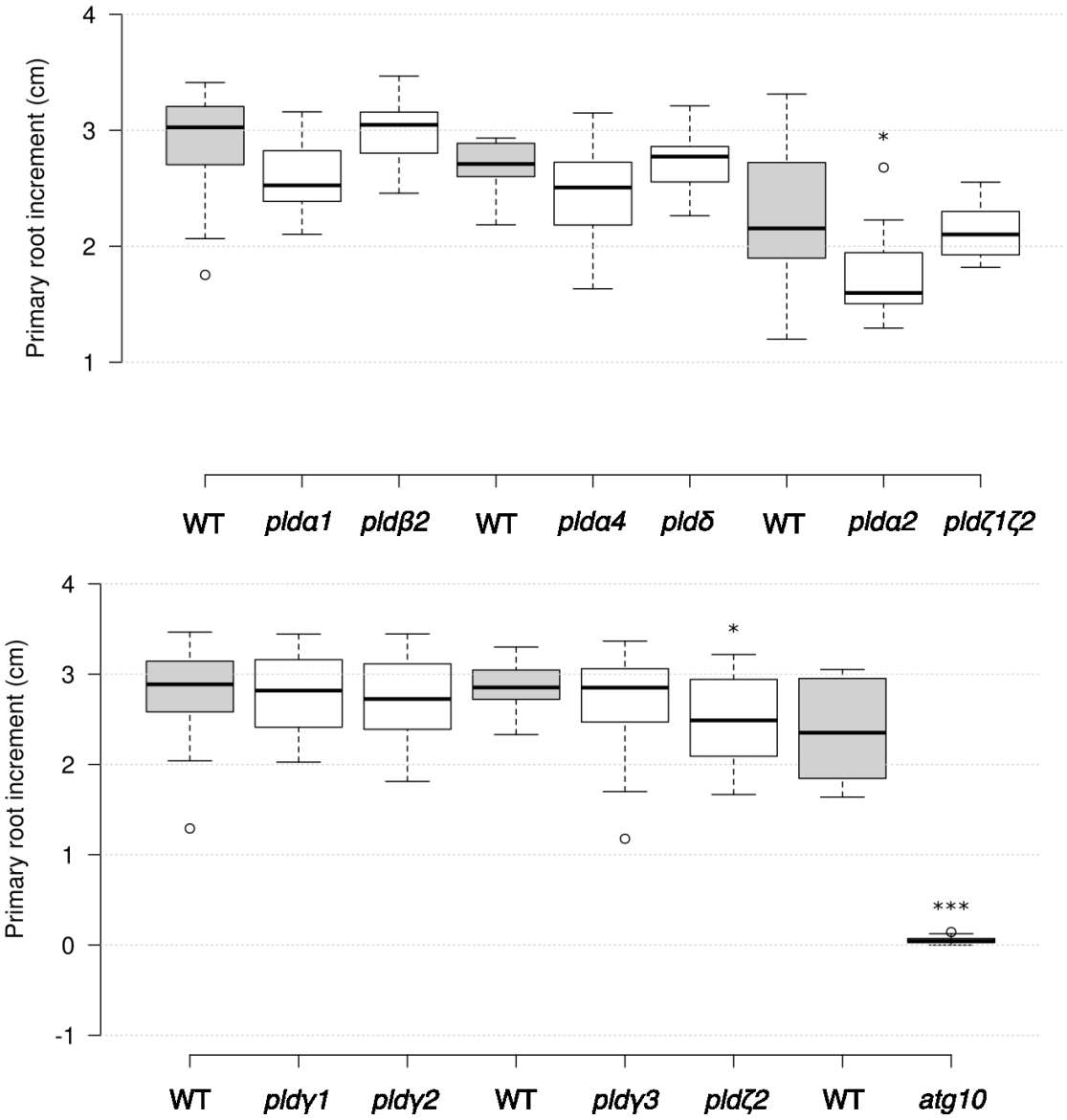

Figure 10 Length of primary root increment of *A. thaliana* wild type (grey) and knock-out mutants in phospholipases D (white) after 6 days of carbon starvation in the dark. Each wild type seedlings were compared to two following knock-out mutants. Mutants *pldα2* and *pldζ2* exhibit a significant difference in primary root increment length compared to wildtype. Mutant *atg10* was used as a positive control. Asterisks indicate a significant difference compared to wild type. (n = 10-16, T-test, * $P < 0.1$; ** $P < 0.01$; *** $P < 0.001$). Horizontal black line represents median.

4.2 Measuring Activity of Lipid Processing Enzymes *in vitro*

Phospholipase D (PLD) catalyses the hydrolysis of membrane phospholipids such as, phosphatidylcholine (PC) or phosphatidylethanolamine (PE) to produce phosphatidic acid (PA). PLD has an exclusive ability to substitute a primary alcohol, e.g., n-butanol, for water in hydrolytic reaction.

Here, I have used PC fluorescently labelled by β-BODIPY (4,4-difluoro-4-bora-3a,4a-diaza-s-indacene) to measure fluorescently labelled products of phospholipases

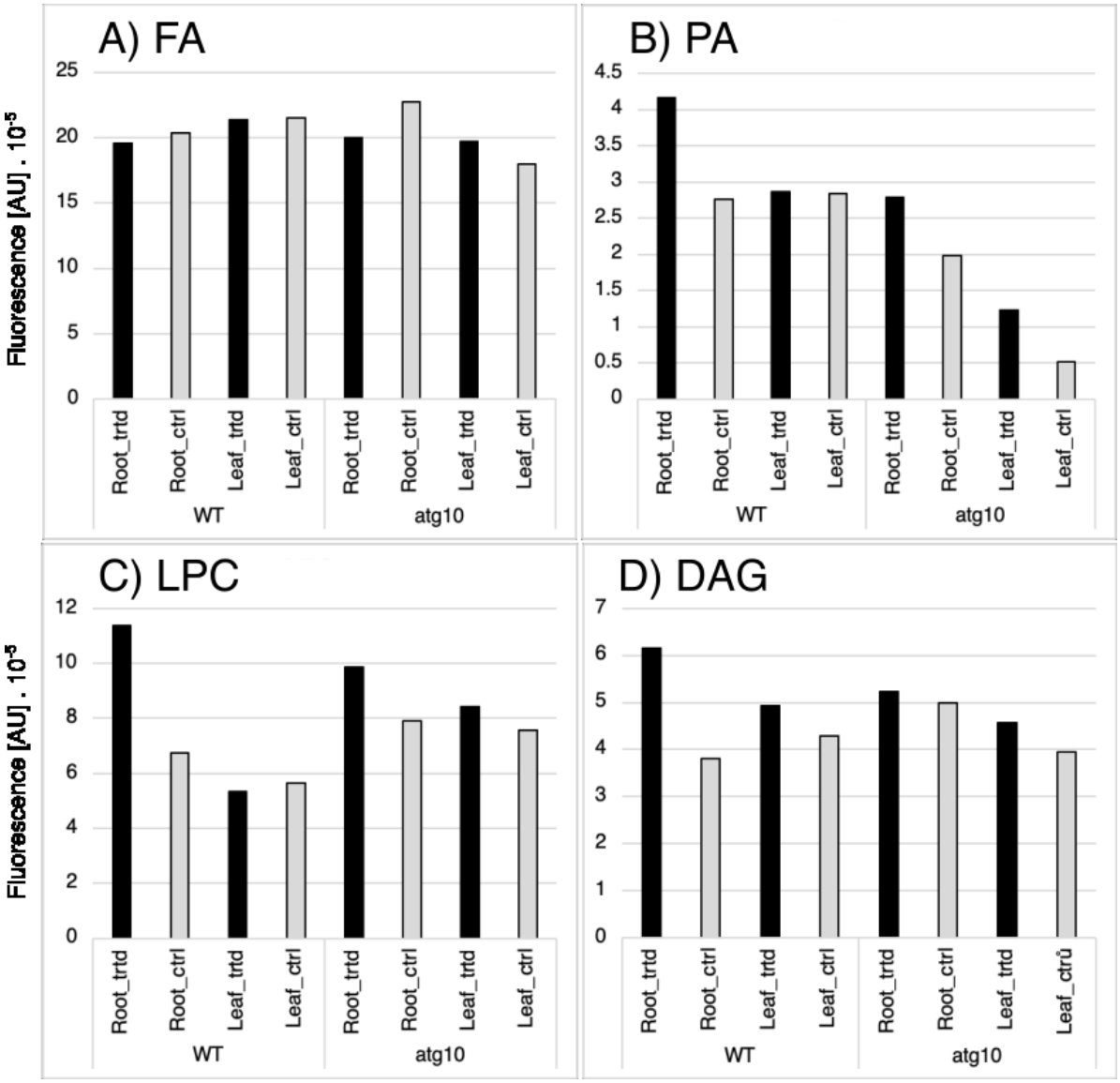

Figure 11 Measurement of fluorescently labelled products of plant phospholipases in cytosolic fraction of *A. thaliana* 28-day-old wild type (WT) and *atg10* knock-out mutant. Autophagy was induced by extended dark (3 days). Trtd – plants with induced autophagy, Ctrl – plants in control conditions. FA = fatty acids (A), PA = phosphatidic (B) acid, LPC = lysophosphatidylcholine (C), DAG = diacylglycerol (D). Fluorescence is stated in arbitrary units (AU). Chromatographic plate is shown in Section 9 (Appx. A).

in cytosolic fraction of leaves and roots of *Arabidopsis thaliana* wild type (WT) and *atg10* mutant. Plants were grown hydroponically, and autophagy was induced on 28-day-old plants by extended dark (3 days). As β-BODIPY is bound to the fatty acid residue of PC in position *sn2*, activity of phospholipase A1 (PLA1) produces fluorescently labelled lysophosphatidylcholine (LPC), phospholipase A2 (PLA2) fatty acids (FA), non-specific phospholipase C (NPC) diacylglycerol (DAG) and finally, diacylglycerol kinase (DGK) phosphatidic acid (PA). Nevertheless, PA can be produced either by PLD or DGK. Here, n-butanol was used to inhibit PLD activity, hence the level of PA corresponds to DGK activity.

In wild type roots cytosolic fraction, there was a remarkable increase of DAG (38%; Fig.11D), LPC (40.7%; Fig.11C) and PA (50.7%; Fig.11B) level plants in extended dark compared to plants in control conditions. On the contrary, in *atg10* knock-out mutants with disrupted autophagy, there was no considerable change of diacylglycerol level and 19% increase of lysophosphatidylcholine in treated plants. Mutants *atg10* show similar increase in PA level in root cytosolic fraction (40.3%) as wild type plants in extended dark. On the other hand, in leaf cytosolic fraction of *atg10* level of PA increased by 58.2%, while there was no change in wild type (Fig11). Chromatographic plate with annotation is shown in Section 9 (Appx.A).

Overall, using HPTLC I have analysed the level of fluorescently labelled products of PLA1, PLA2, NPC and PLD in cytosolic fraction from roots and leaves of *A. thaliana* WT and *atg10* mutant. Presented analysis revealed considerably increased level of DAG and LPC in WT plants with induced autophagy compared to plants in control conditions. On the contrary, analysis of root cytosolic fractions from *atg10* mutants did not indicate significant change in DAG and LPC level.

4.3 Estimation of Autophagosome Number *In Vivo*

Located on both sides of autophagosome membrane, protein ATG8 fused with fluorescent protein is very often used as a marker of autophagic structures. Here, I used GFP-ATG8e transgenic lines for visualisation of autophagosomes labelled by GFP-ATG8e fluorescent protein in root elongation zone of 6-day-old seedlings. Autophagy was induced by 2 hours of carbon and nitrogen starvation in the dark (Merkulova *et al.*, 2014). GFP-ATG8e fluorescent protein was visualised using Spinning Disk Microscope (Nikon, Eclipse Ti-E, inverted). Visualised particles were counted using the disector counting technique (Sterio, 1984).

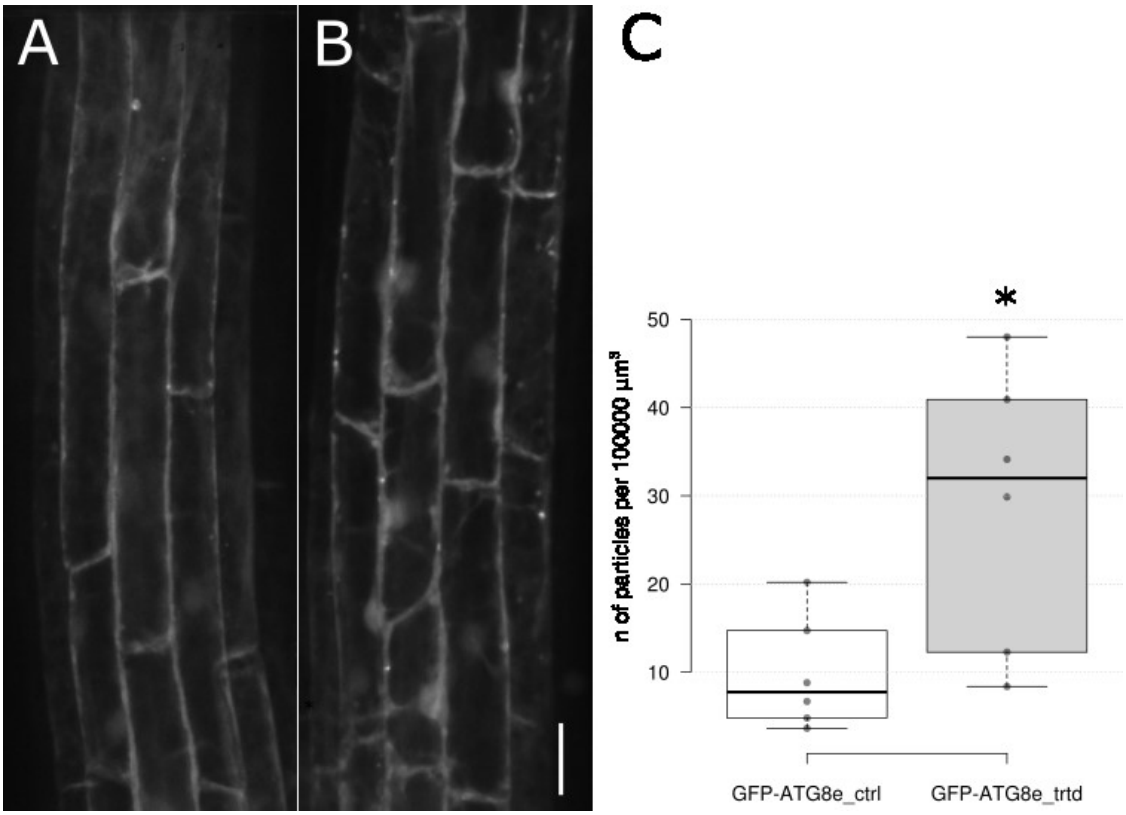

Figure 12 Root elongation zone of *A. thaliana* GFP-ATG8e transgenic seedlings in control conditions (A) and after 2 hours of carbon and nitrogen starvation in the dark (B). Treated plants create significantly higher number of autophagosomes compared to plants under control conditions. Scale = 25 µm. Number density (n) of autophagosomes in *A. thaliana* transgenic line GFP-ATG8e root elongation zone (C) in control conditions (white) and after 2 hours of nitrogen and carbon starvation (light grey). T-test, * $P < 0.1$; n=8. Horizontal black line represents median.

Root elongation zone cells of transgenic GFP-ATG8e seedlings with induced autophagy show significantly higher number of particles labelled by GFP-ATG8e fluorescent protein than seedlings in control conditions (Fig.12).

4.4 Estimation of Autophagosome Number Labelled Using Immunolabelling

Another possible way how to visualise autophagic structures in plant cells is using fluorescence immunolabelling. Here, I have used indirect immunolabelling assay to visualise autophagosomes in 6-day-old *Arabidopsis thaliana* wild type (WT, Fig. 15,16) and *dgk7, pldα3*, *pldβ1* mutant seedlings with induced autophagy and in control conditions (Fig. 16-19, 21-24). Autophagy was induced by 2 hours of carbon and nitrogen starvation in the dark (Merkulova *et al.*, 2014). Seedlings were labelled by primary antibody against ATG8 protein and secondary antibody conjugated to fluorescent dye DyLight 488. Also, seedlings were stained calcofluor-white for cell

wall visualisation. Labelled structures were visualised separately in root elongation and meristematic zone using Nikon Spinning Disk microscope and counted using the disector counting technique (Sterio, 1984). A large area of root elongation and meristematic zone is shown, as the disector covered a significant part of each root developmental zone.

Immunolabelling of long cells in root elongation zone brings the risk of cell shrinking and staining artefacts. Nevertheless, the disector counting technique is independent on cell volume (Maynard, 1996). On the other hand, shape of cells stained by immunolabelling in root meristematic zone corresponds to the cell wall stained by calcofluor white. Strong signal in the cytoplasm of meristematic zone cells could correspond to ATG8 protein diluted in the cytoplasm. However, the signal is weaker in root elongation zone (Fig. 15-19). Mutant a*tg10* with completely disabled autophagy (Soto-Burgos *et al.*, 2018a) does not create autophagosomes and here is used as a positive control. Data was not statistically analysed due to low number of samples.

Surprisingly, no analysed knock-out mutant seedling showed significantly different number density of labelled particles than wild type. However, *pldα3* knock-out mutant seems to exhibit higher number density of labelled particles in root elongation zone cells (Fig. 13). On the contrary, mutant *pldβ1* show lower number density of labelled particles then wild type in root elongation zone. This finding can be explained by low number of used samples and high variability in values from root elongation zone cells.

Furthermore, root elongation and meristematic zone cells considerably differ in number density of labelled particles. Root meristematic zone shows higher number of labelled particles (Fig. 13 and 14) and remarkably lower variability of values (Appx. B).

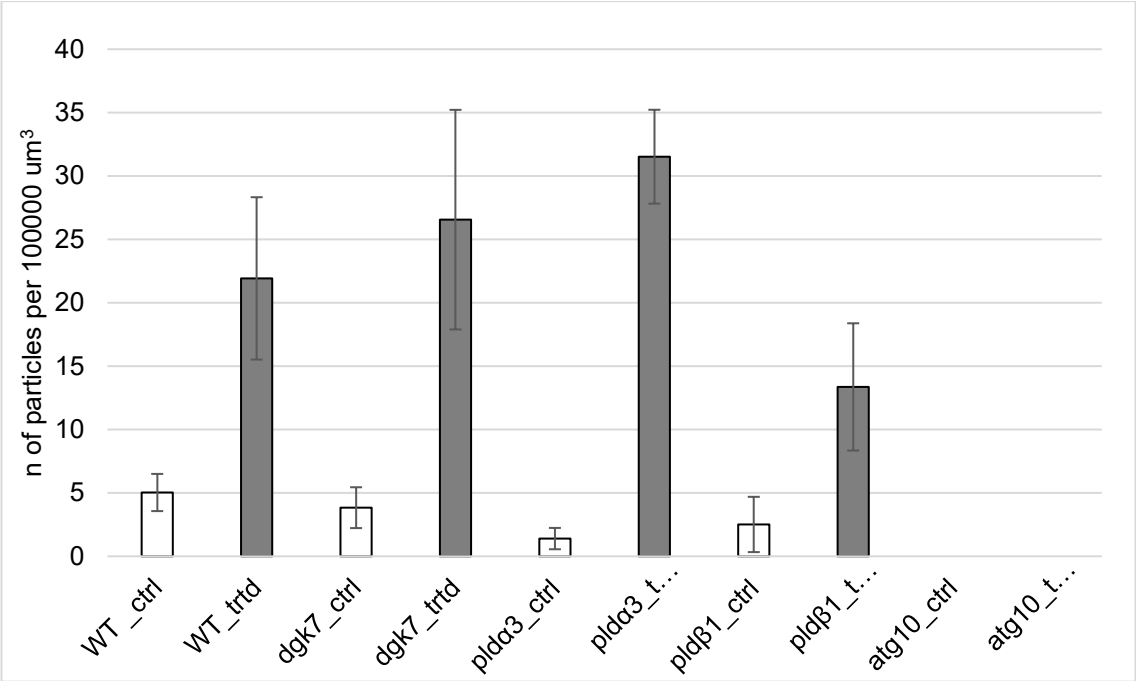

Figure 13 Number density (n) of autophagosomes in root elongation zone of selected *A. thaliana* mutants in lipid-metabolizing enzymes under control conditions (white) and after 2 hours of carbon and nitrogen starvation in the dark (grey). Treated plants form considerably higher number density of autophagosomes, than control plants. n=3-5. Error bars represent standard deviation.

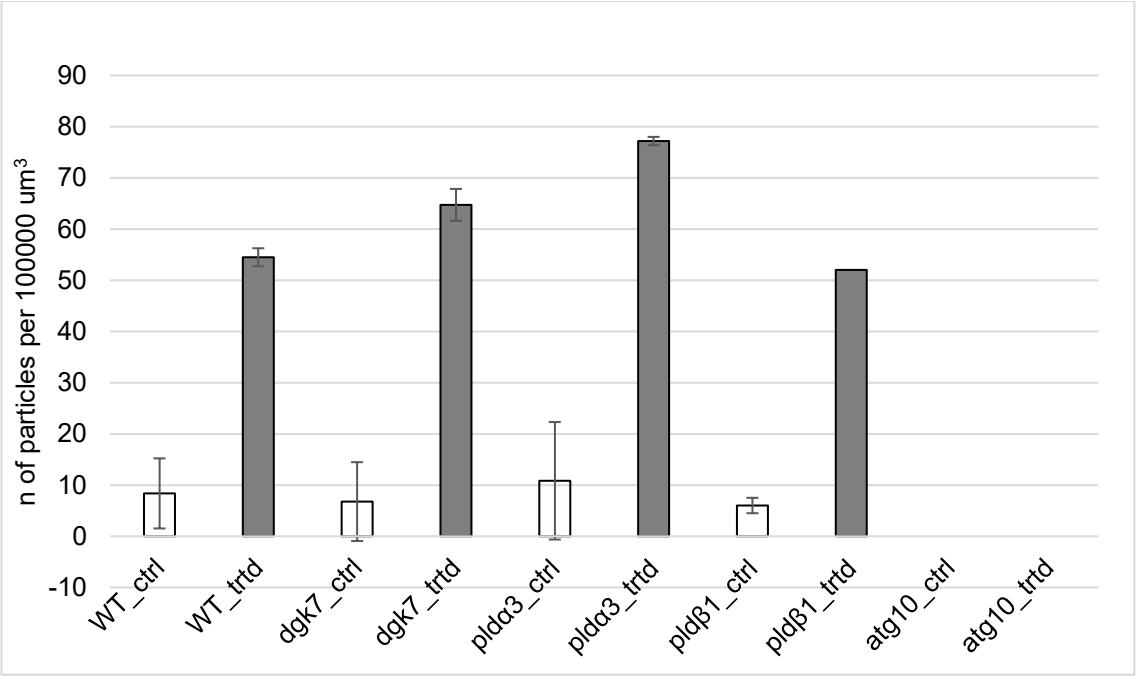

Figure 14 Number density (n) of autophagosomes in root meristematic zone of selected *A. thaliana* mutants in lipid-metabolizing enzymes under control conditions (white) and after 2 hours of carbon and nitrogen starvation in the dark (grey). Treated plants form considerably higher number density of autophagosomes, than control plants. n=3-5. Error bars represent standard deviation.

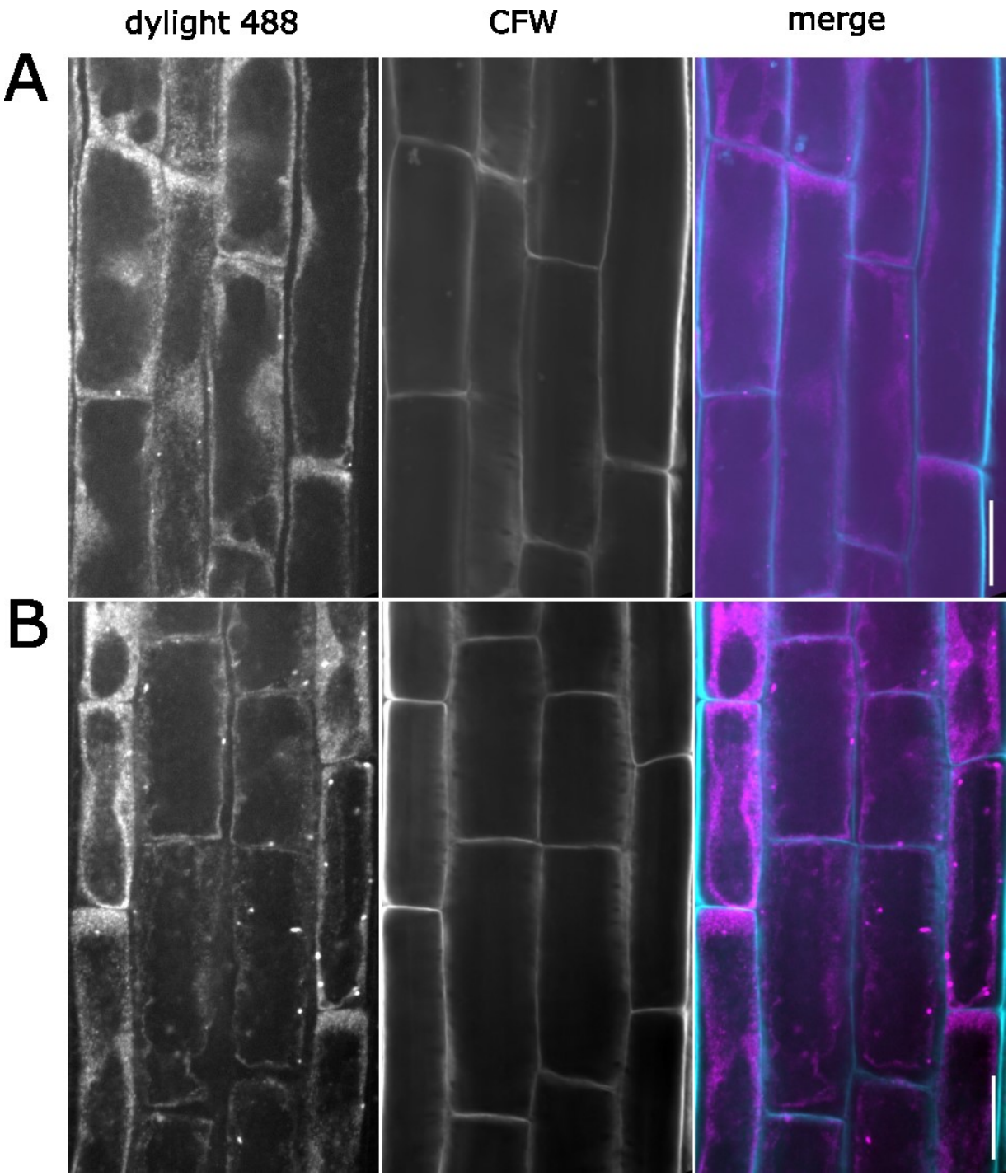

Figure 15 Root elongation zone of *A. thaliana* wild type under control conditions (A) and after 2 hours of carbon and nitrogen starvation (B). Plants were stained by ATG8 primary antibody and dylight488 secondary antibody (dylight488) for autophagosome visualisation and by calcofluor-white (CFW) for cell wall visualisation. Treated plants create remarkably higher number of autophagosomes (B) compared to plants under control conditions (A). Artificial colour magenta corresponds to DyLight 488, cyan to CFW. Scale = 25 μm.

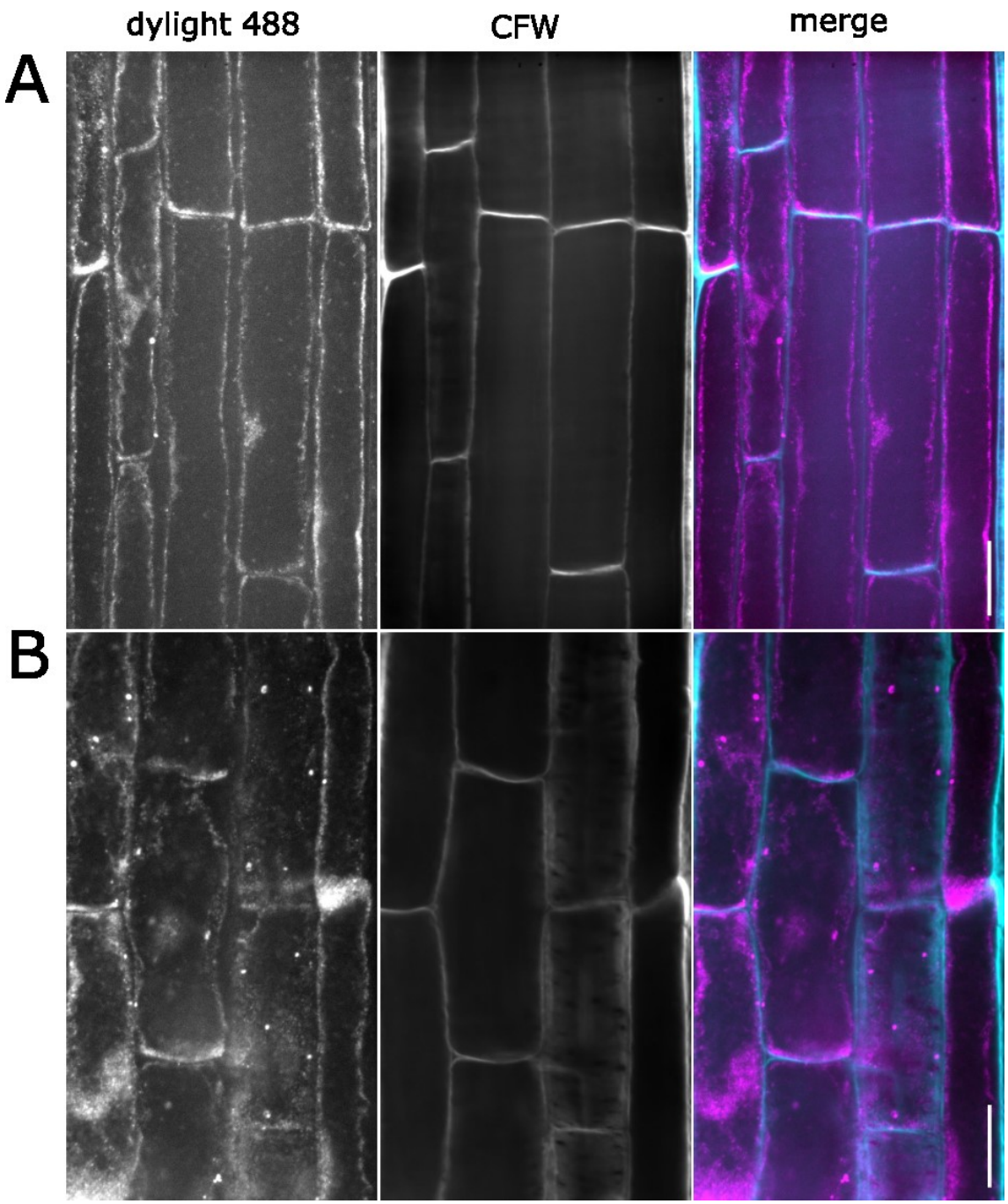

Figure 16 Root elongation zone of *A. thaliana dgk7* mutant in control conditions (A) and after 2 hours of carbon and nitrogen starvation (B). Plants were stained by ATG8 primary antibody and DyLight488 secondary antibody (dylight 488) for autophagosome visualisation and by calcofluor-white (CFW) for cell wall visualisation. Treated plants form remarkably higher number of autophagosomes (B) compared to plants under control conditions (A). Artificial colour magenta corresponds to DyLight 488, cyan to CFW. Scale = 25 μm.

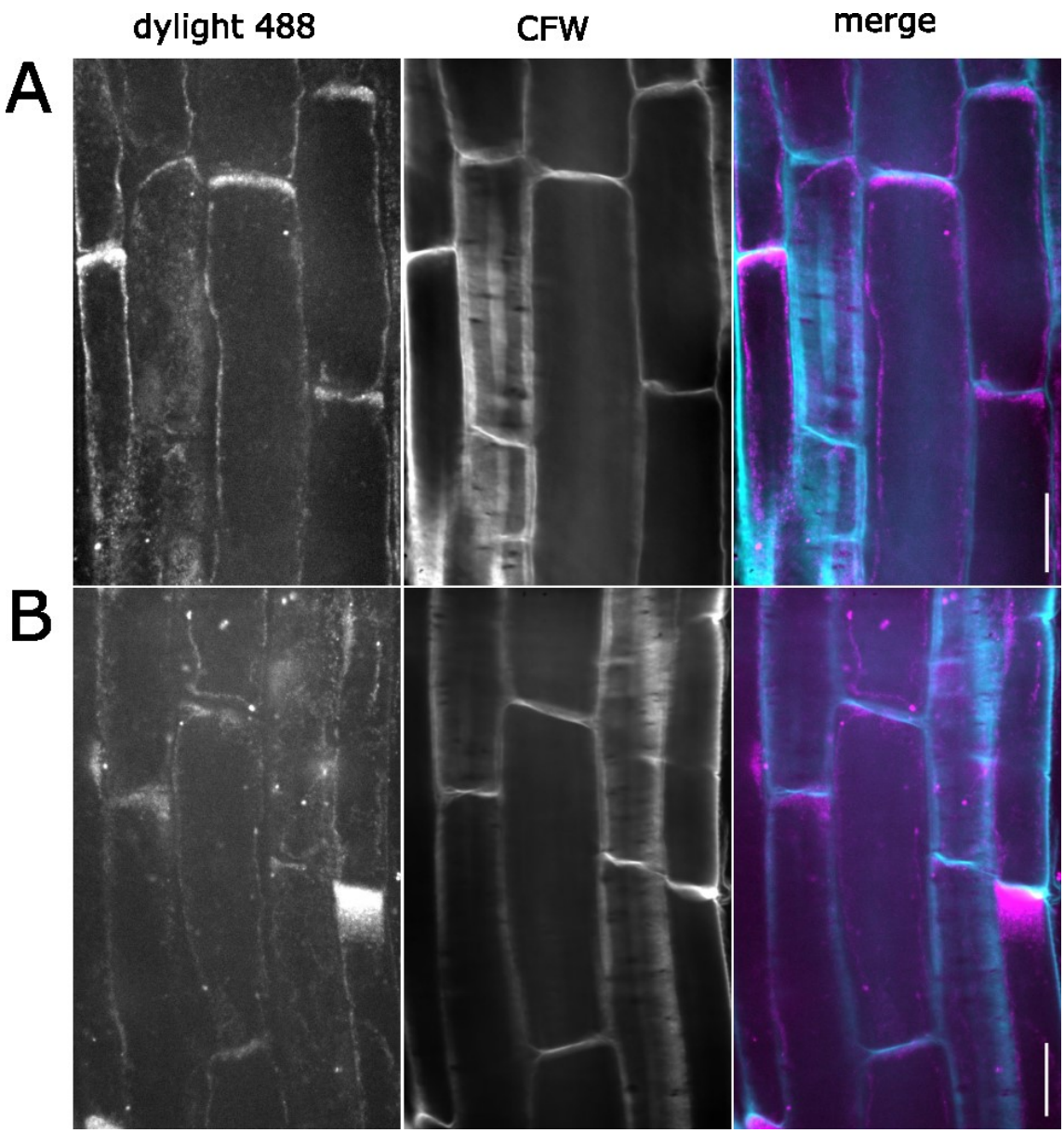

Figure 17 Root elongation zone of *A. thaliana pldα3* mutant in control conditions (A) and after 2 hours of carbon and nitrogen starvation (B). Plants were stained by ATG8 primary antibody and DyLight488 secondary antibody (dylight 488) for autophagosome visualisation and by calcofluor-white (CFW) for cell wall visualisation. Treated plants form remarkably higher number of autophagosomes (B) compared to plants under control conditions (A). Artificial colour magenta corresponds to DyLight488, cyan to CFW. Scale = 25 μm.

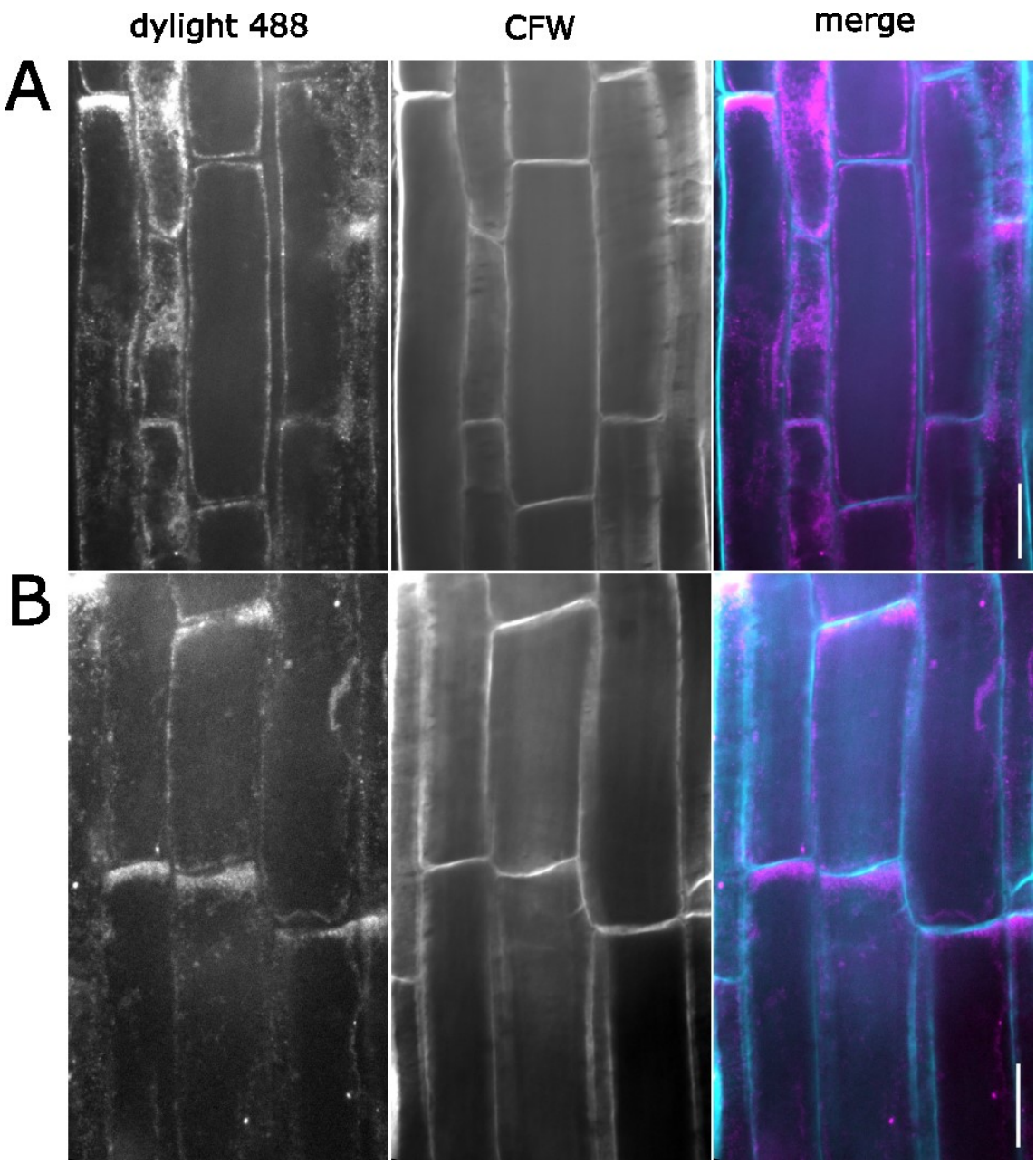

Figure 18 Root elongation zone of *A. thaliana pldβ1*mutant in control conditions (A) and after 2 hours of carbon and nitrogen starvation (B). Plants were stained by ATG8 primary antibody and DyLight488 secondary antibody (dylight 488) for autophagosome visualisation and by calcofluor-white (CFW) for cell wall visualisation. Treated plants form remarkably higher number of autophagosomes (B) compared to plants under control conditions (A). Artificial colour magenta corresponds to DyLight488, cyan to CFW. Scale = 25 μm.

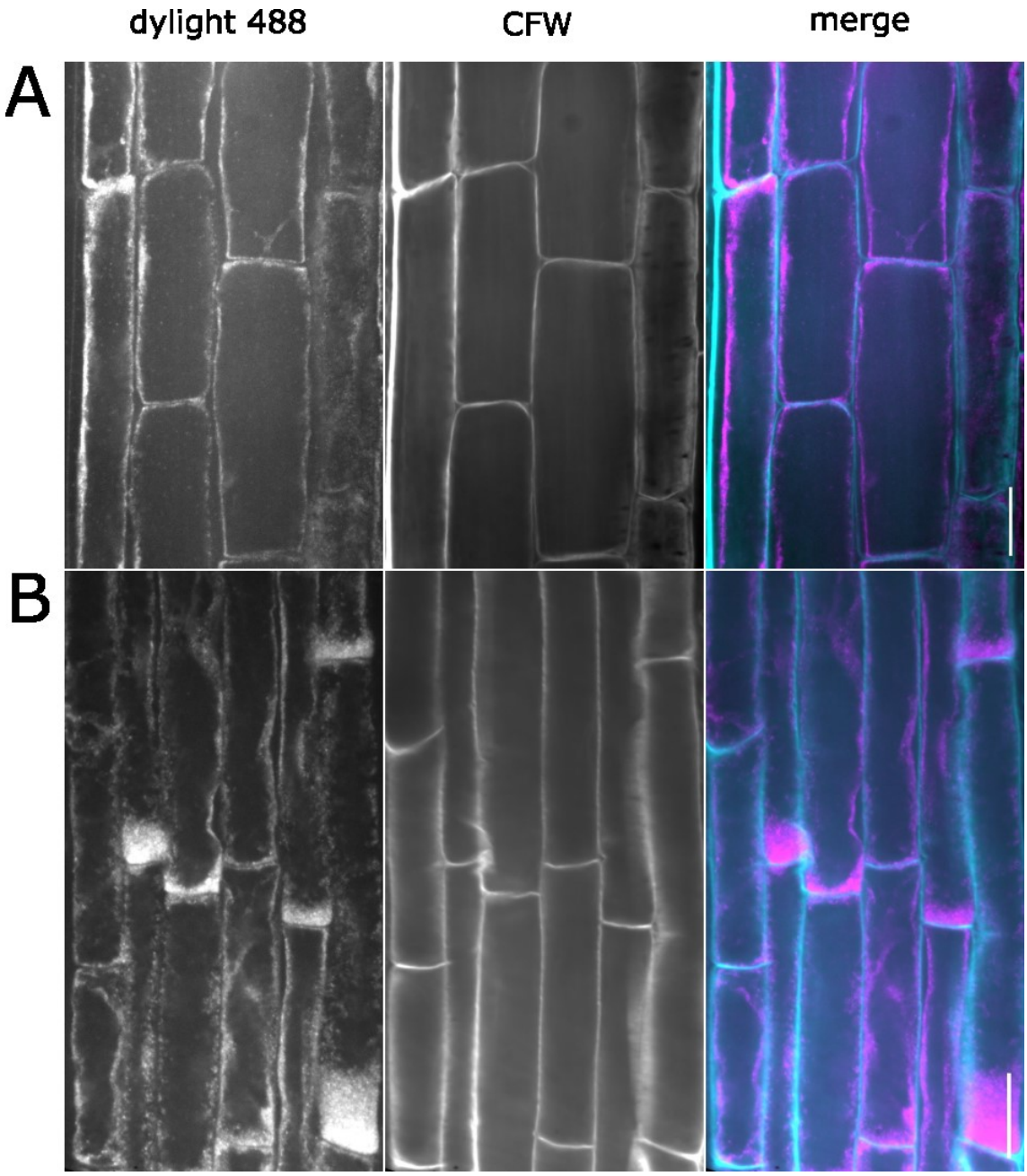

Figure 19 Root elongation zone of *A. thaliana atg10* in control conditions (A) and after 2 hours of carbon and nitrogen starvation (B). Plants were stained by ATG8 primary antibody and DyLight488 secondary antibody (dylight 488) for autophagosome visualisation and by calcofluor-white (CFW) for cell wall visualisation. Mutants *atg10* form no autophagosomes Artificial colour magenta corresponds to DyLight 488, cyan to CFW. Scale = 25 μm.

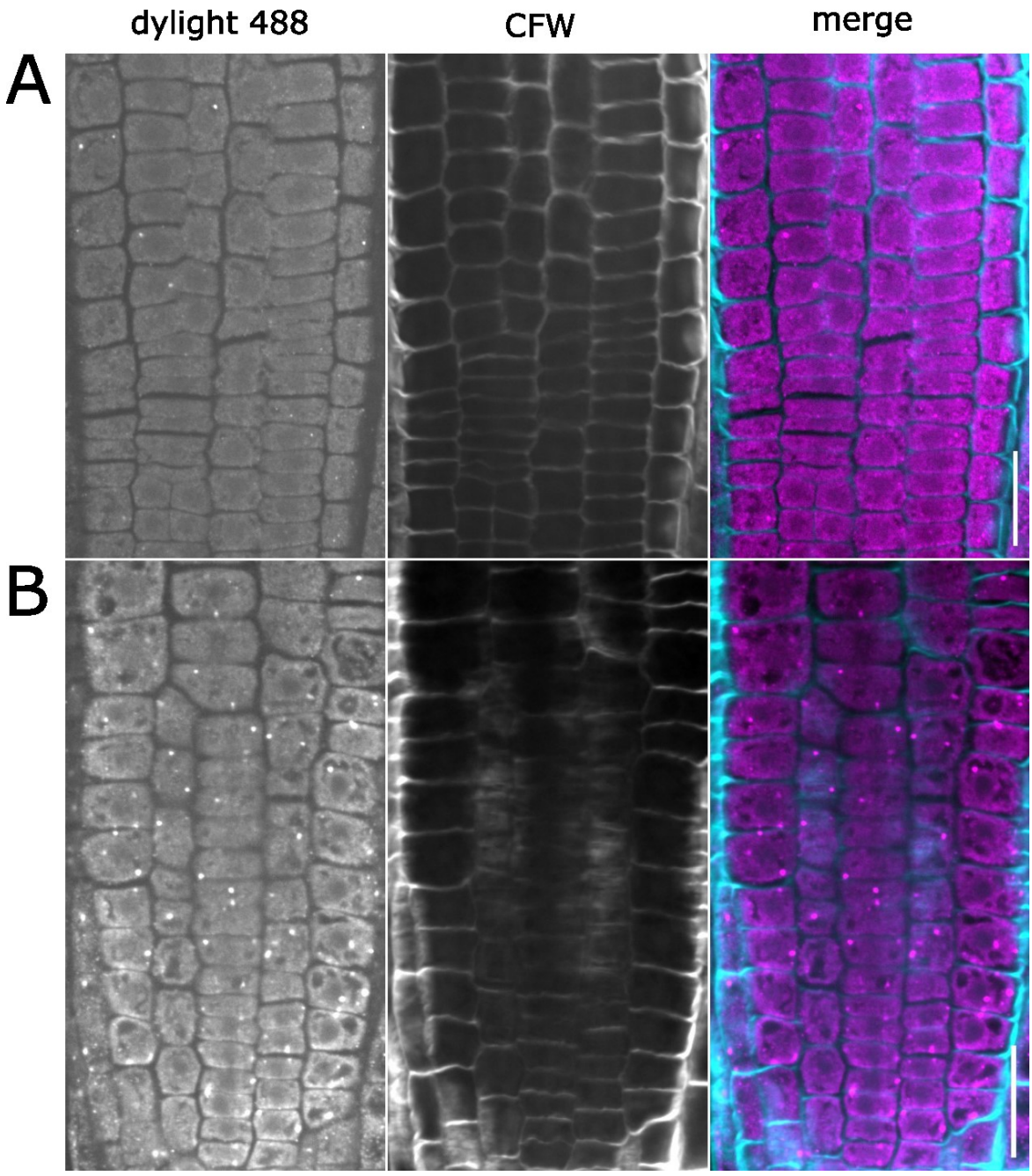

Figure 20 Root meristematic zone of *A. thaliana* wild type under control conditions (A) and after 2 hours of carbon and nitrogen starvation (B). Plants were stained by ATG8 primary antibody and DyLight488 secondary antibody (dylight 488) for autophagosome visualisation and by calcofluor-white (CFW) for cell wall visualisation. Treated plants form remarkably higher number of autophagosomes (B) compared to plants under control conditions (A). Artificial colour magenta corresponds to DyLight488, cyan to CFW. Scale = 25 μm.

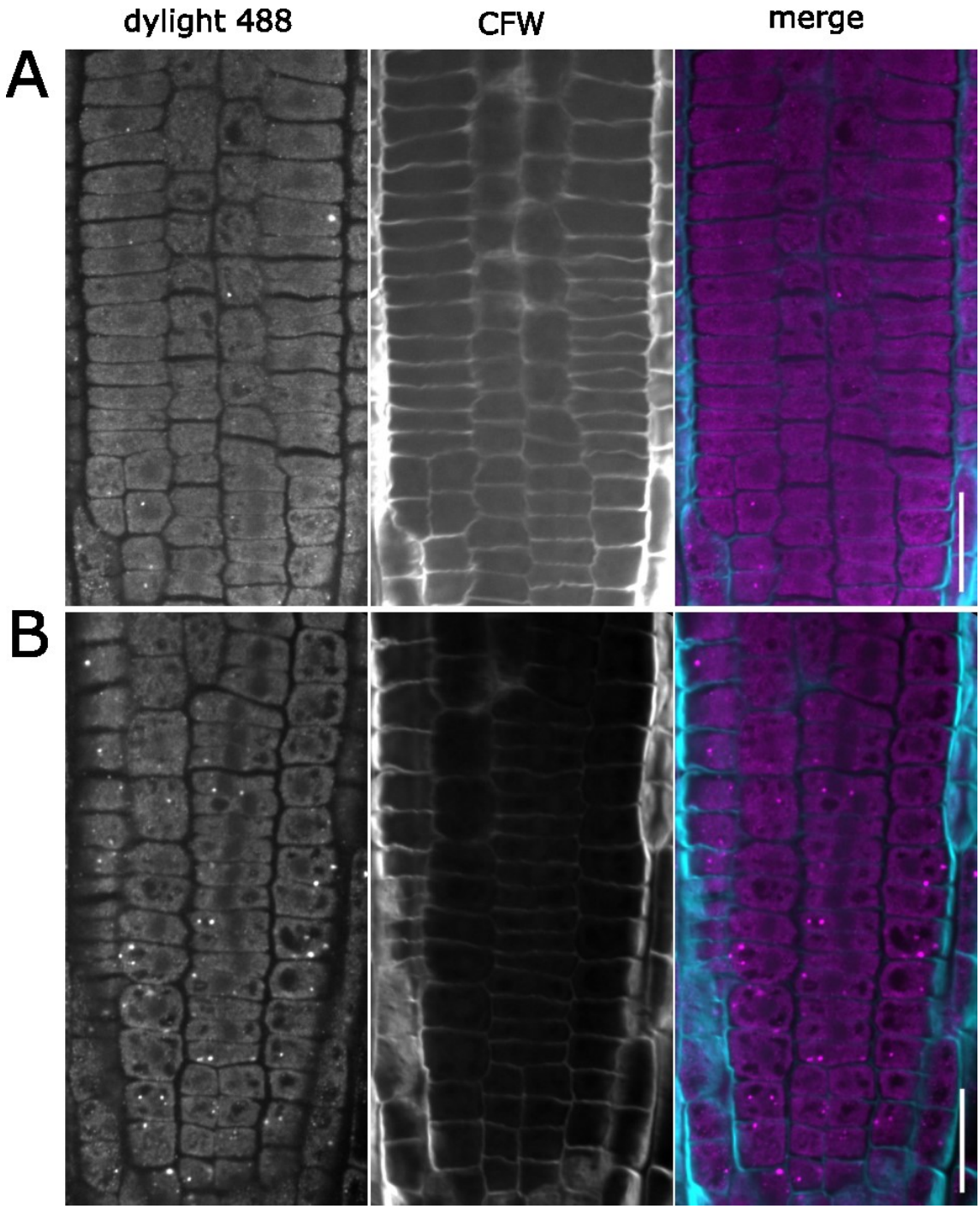

Figure 21 Root meristematic zone of *A. thaliana dgk7* under control conditions (A) and after 2 hours of carbon and nitrogen starvation (B). Plants were stained by ATG8 primary antibody and DyLight488 secondary antibody (dylight 488) for autophagosome visualisation and by calcofluor-white (CFW) for cell wall visualisation. Treated plants form remarkably higher number of autophagosomes (B) compared to plants under control conditions (A). Artificial colour magenta corresponds to DyLight488, cyan to CFW. Scale = 25 μm.

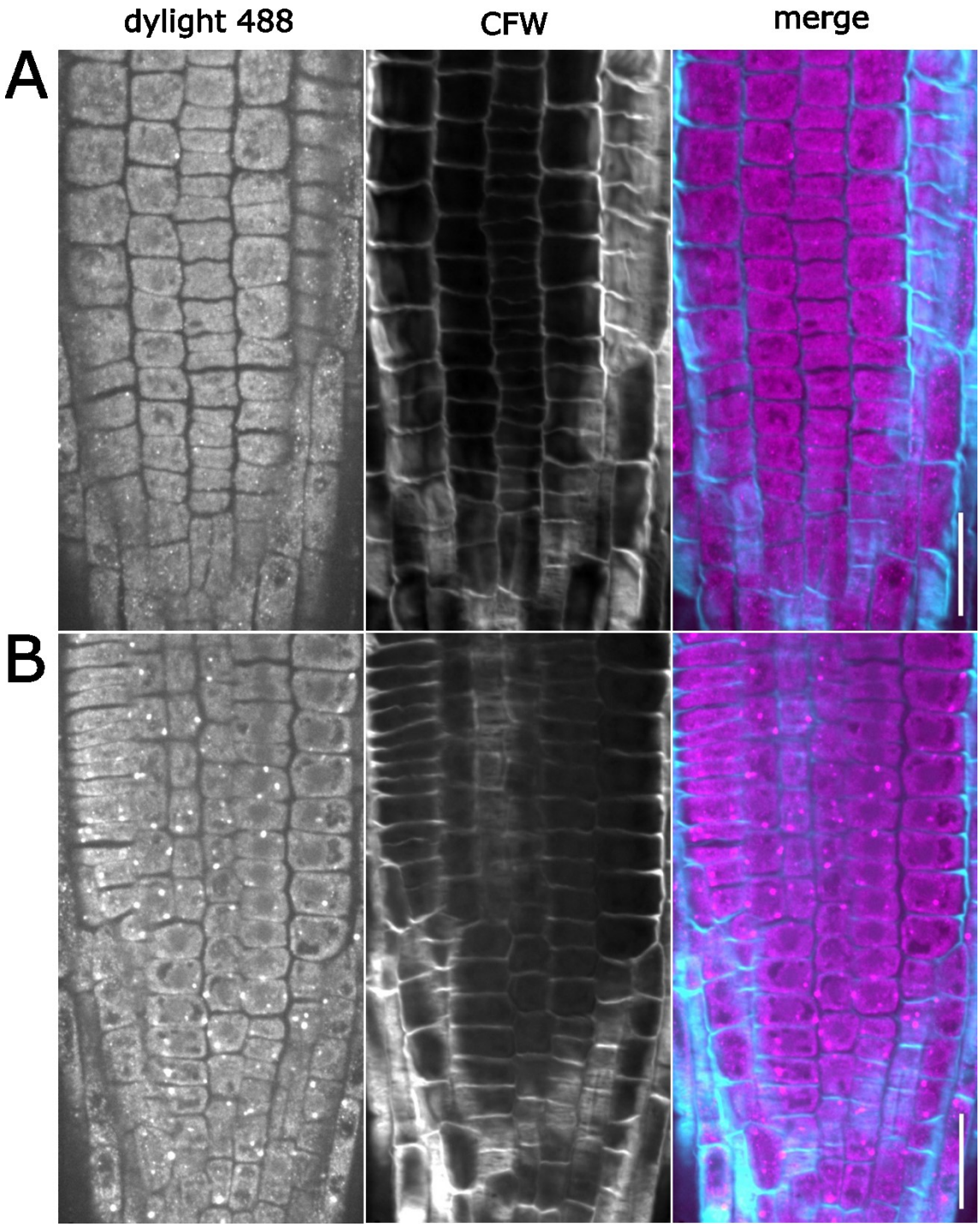

Figure 22 Root meristematic zone of *A. thaliana pldα3* under control conditions (A) and after 2 hours of carbon and nitrogen starvation (B). Plants were stained by ATG8 primary antibody and DyLight488 secondary antibody (dylight 488) for autophagosome visualisation and by calcofluor-white (CFW) for cell wall visualisation. Treated plants form remarkably higher number of autophagosomes (B) compared to plants under control conditions (A). Artificial colour magenta corresponds to DyLight488, cyan to CFW. Scale = 25 μm.

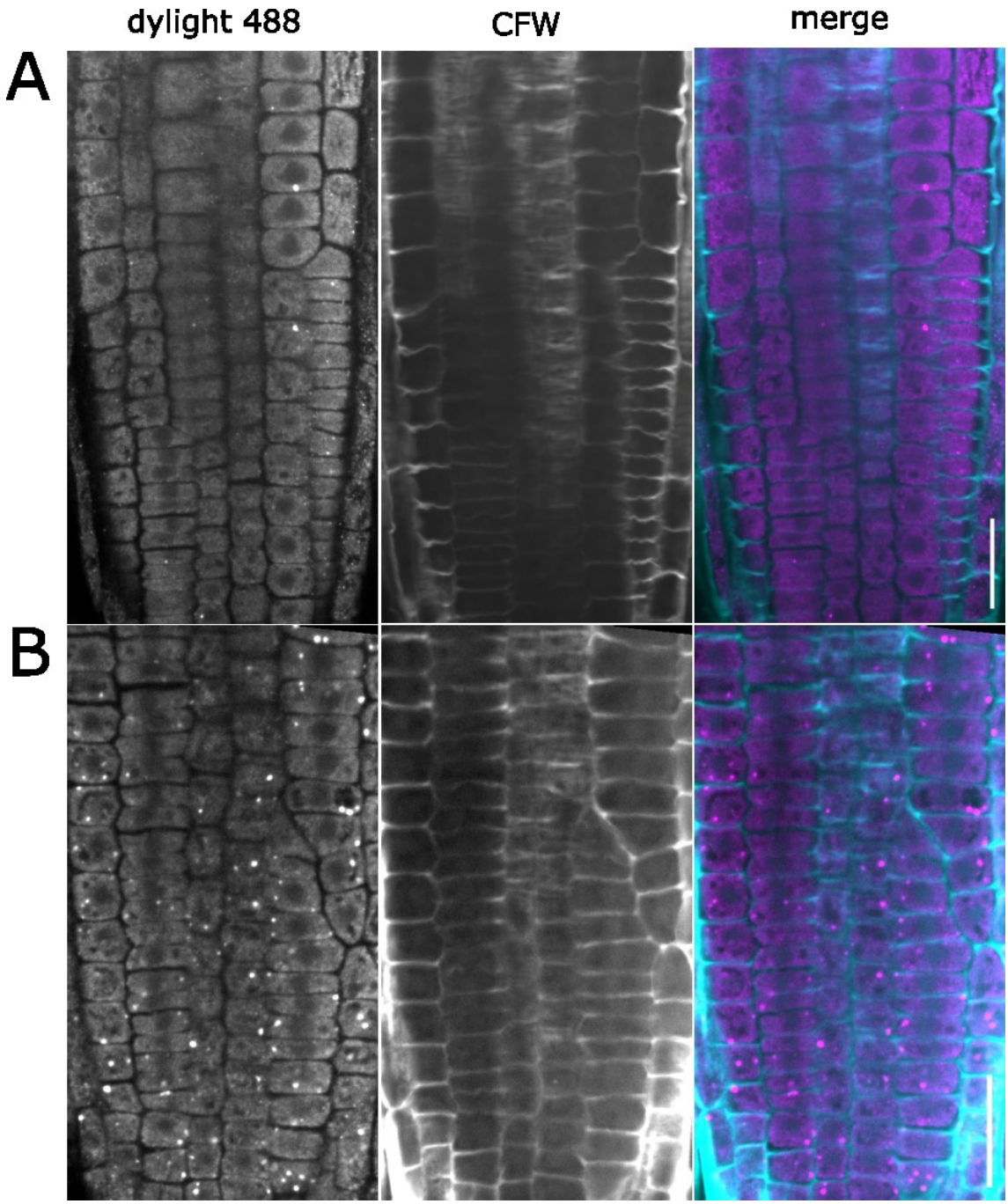

Figure 23 Root meristematic zone of *A. thaliana pldβ1*mutant under control conditions (A) and after 2 hours of carbon and nitrogen starvation (B). Plants were stained by ATG8 primary antibody and DyLight488 secondary antibody (dylight 488) for autophagosome visualisation and by calcofluor-white (CFW) for cell wall visualisation. Treated plants form remarkably higher number of autophagosomes (B) compared to plants under control conditions (A). Artificial colour magenta corresponds to DyLight488, cyan to CFW. Scale = 25 μm.

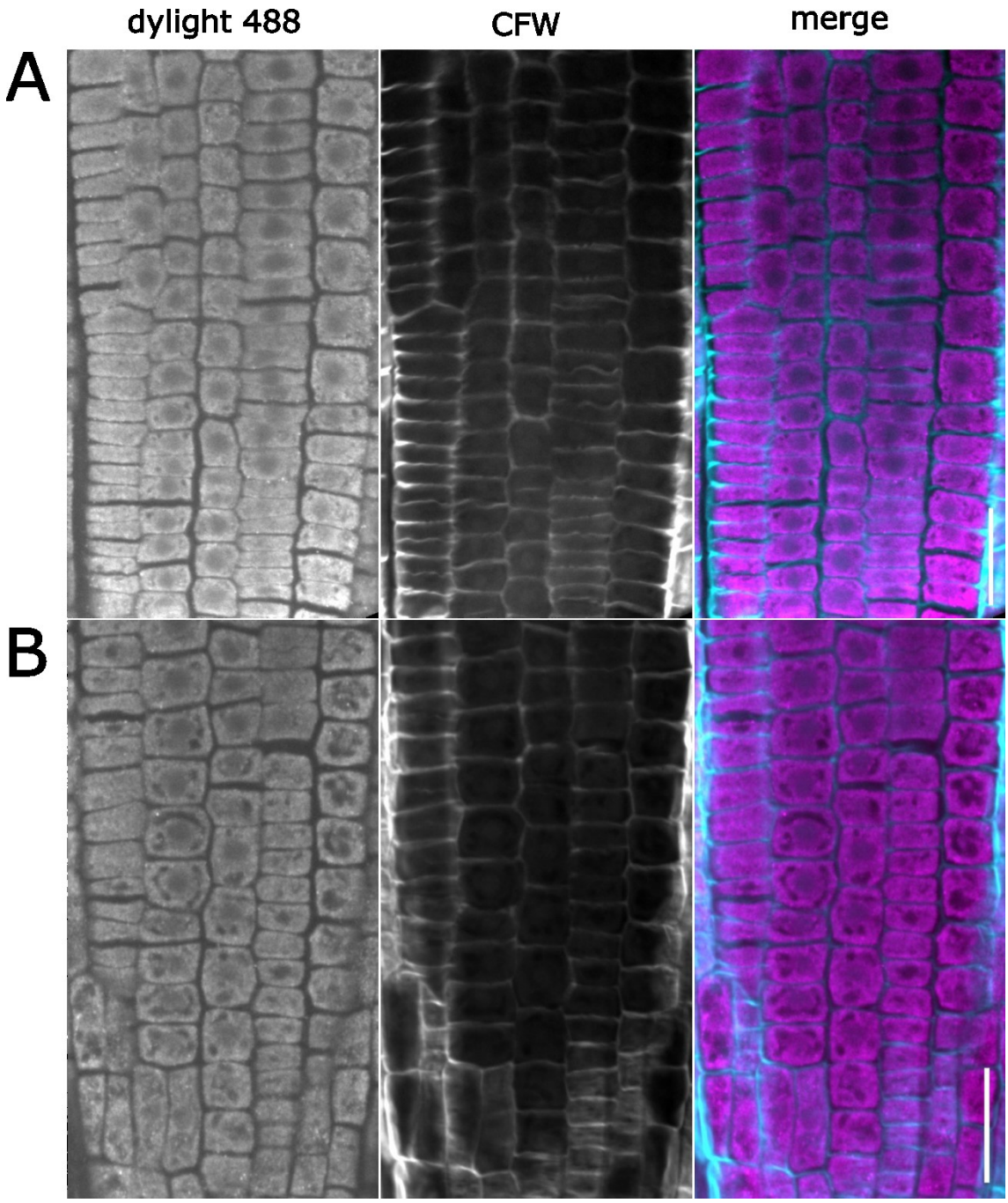

Figure 24 Root meristematic zone of *A. thaliana atg10* under control conditions (A) and after 2 hours of carbon and nitrogen starvation (B). Plants were stained by ATG8 primary antibody and DyLight488 secondary antibody (dylight 488) for autophagosome visualisation and by calcofluor-white (CFW) for cell wall visualisation. Mutants *atg10* form no autophagosomes. Artificial colour magenta corresponds to DyLight488, cyan to CFW. Scale = 25 μm.

4.5 Colocalization of Particles Labelled by Different Fluorophores

Measurement of colocalization provides information of co-occurrence of signal from different fluorophores and corelation of their intensity. Transgenic 6-day-old GFP-ATG8e seedlings with induced autophagy were labelled by rabbit anti-ATG8 primary antibody (Agrisera) and Alexa Fluor 555 goat anti-rabbit secondary antibody (Thermo Fisher Scientific). For autophagosome quantification, I used secondary antibody conjugated to fluorescent dye DyLight488. However, the emission spectrum of DyLight488 overlaps emission spectrum of GFP (Fig. 6) used for live cell imaging. Therefore, secondary antibody conjugated to Alexa Fluor 555 was used for colocalization, instead. Autophagy was induced by 2 hours of carbon and nitrogen starvation in the dark (Merkulova *et al.*, 2014). Root meristematic zone of labelled seedlings was observed using Nikon Spinning Disk microscope.

Here, I showed co-occurrence of signal from GFP-ATG8e protein and secondary antibody conjugated to Alexa Fluor 555 florescent dye in *A. thaliana* wild type root meristematic zone. Most of GFP labelled particles colocalize to Alexa Fluor 555 labelled particles (Fig. 25). Nevertheless, co-occurrence and corelation quantification would be necessary for detailed colocalization analysis.

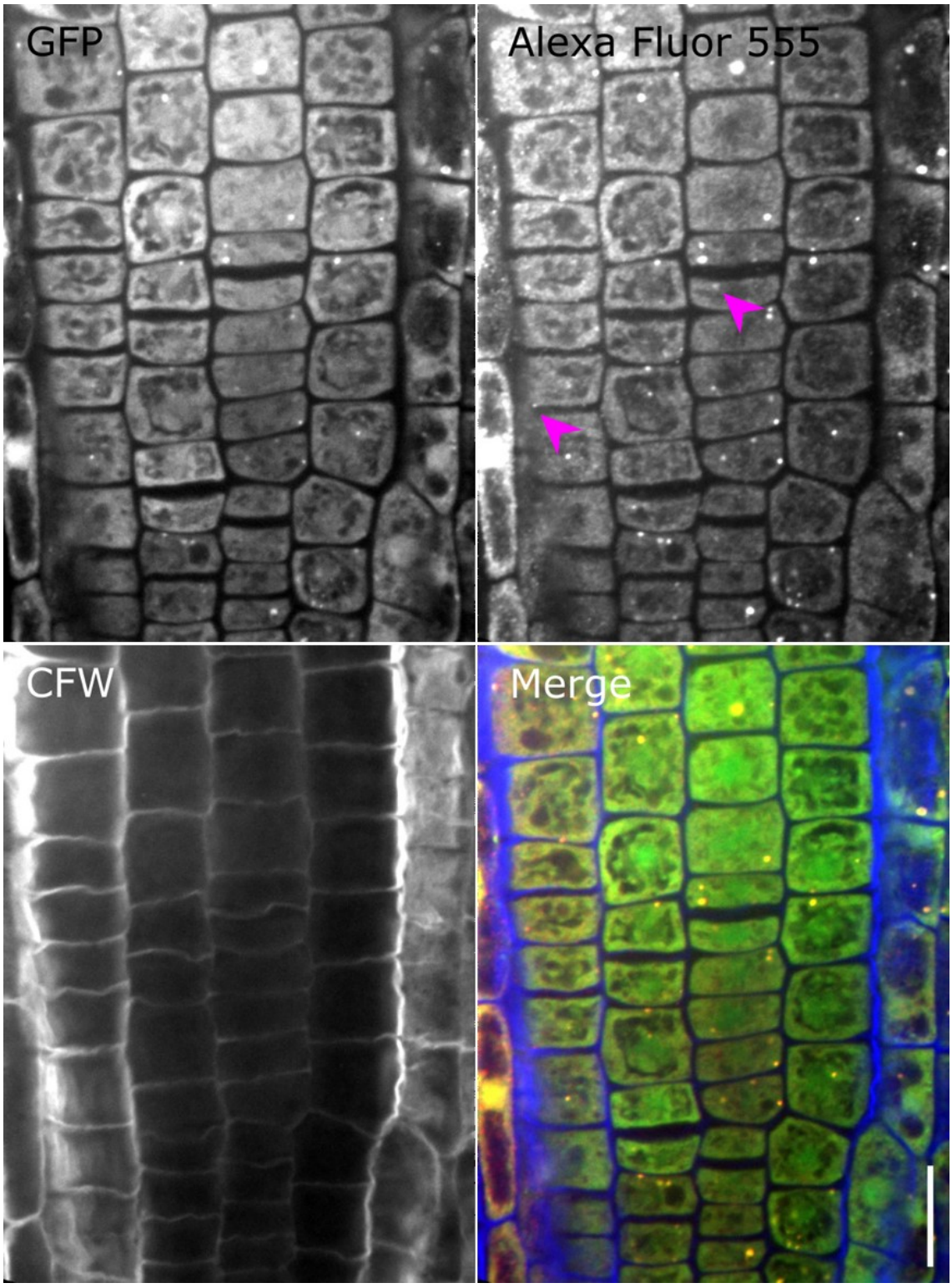

Figure 25 Colocalization of structures labelled by different fluorophores. Most of GFP labelled particles colocalize to Alexa Fluor 555 labelled particles. Arrows show particles that do not colocalize. GFP = Green fluorescent protein, CFW = Calcofluor white. Artificial colour blue corresponds to CFW, green to GFP and red to Alexa Fluor 555. Raw data provided by Michal Daněk, unpublished. Scale = 15 μm.

5 DISCUSSION

Most of contemporary studies reporting on the connection of plant autophagy and lipid metabolism attempt to explain the function of autophagy in degradation of lipid droplets making storage lipids available for plant metabolism (Fan *et al.*, 2017, 2019; Kokabi *et al.*, 2020). However, the major question of how lipid signalling affects the process of plant autophagy, remains unanswered. Plant autophagy is inhibited by TOR kinase (Kim *et al.*, 2011; Li and Vierstra, 2012). In plants, TOR kinase is responsible for a myriad of downstream effectors regulating numerous cellular processes. Could this versatile kinase serve as a crossroad connecting pathways regulating lipid metabolism and autophagy?

In mammalian cells, PA generated by PLD1 activity dissociates DEPTOR, a negative regulator of mTOR, thus regulates mTOR activity (Yoon *et al.*, 2015). However, mammals have only two genes encoding PLDs (Exton, 2002), while there are twelve PLD genes in *A.thaliana* (Qin and Wang, 2002). I have analysed the primary root inhibition of various mutants with knocked-out genes for phospholipase D isoforms in conditions of induced autophagy. From 10 tested knock-out mutants, *pldα2* and *pldζ2* exhibit significantly lower length of primary root increment after 6 days of carbon starvation in the dark. A very recent study demonstrated the role of PLDα2 in heat stress memory in *A. thaliana* (Urrea Castellanos *et al.*, 2020). Sedaghatmehr *et al.*, 2019 showed, that autophagy is needed for specific degradation of heat shock proteins (HSPs) at late stage of the thermorecovery phase. Mutants with disrupted autophagy retained HSPs longer compared to WT, suggesting a vital role of autophagy in heat stress memory. Previous studies have also demonstrated the involvement of PLDζ2 in response to phosphate starvation (Cruz-Ramírez *et al.*, 2006; Li, Welti and Wang, 2006). Although, the function of autophagy is well documented in conditions of macronutrient starvation (C, N, S), the role of autophagy in phosphate deficiency remains to be elucidated. A comparative study of Naumann *et al.*, (2019) demonstrated, that ER stress-dependent autophagy is rapidly induced as part of a developmental response to phosphate limitation.

In addition, analysis of the length of primary root increment revealed a significant inhibition of primary root growth of *pi-plc2*, *pi-plc3*, *pi-plc5.* PI-PLCs are activated by extracellular receptors and produce inositol 1,4,5-triphosphate ($InsP_3$) and DAG. The activity of plant PI-PLCs also affects the level and distribution of PI4P and polyphosphoinositides (PPIs). As PI4P is involved in plant phosphoinositide metabolism

(Fig. 5), it may be converted to PI3P, which is needed for phagophore initiation. The hypothesis about the role of PI-PLCs in plant autophagy is supported by the data from measurement of lipid metabolising enzymes activity. My preliminary data show a remarkable increase of DAG in wild type plants in extended dark compared to no increase in *atg10* knock-out mutants. The finding, that there was no change in LPC and DAG level in root cytosolic fraction of *atg10* mutant plants with induced autophagy could suggests the role of autophagy in phospholipid metabolism. Measuring activity of phospholipases is a valuable approach typically used for studying PLD activity *in vivo* (Munnik and Laxalt, 2013) as well as *in vitro* (Pappan and Wang, 2013). Moreover, using labelled phosphatidylcholine (PC), a wide spectrum of lipids can be separated by high performance thin layer chromatography (HPTLC) and used for studying activity of lipid-metabolising enzymes. Observed increased level of lysophosphatidylcholine (LPC) and diacylglycerol (DAG) in root cytosolic fraction of *A. thaliana* wild type plants with induced autophagy is in accordance with Šídlová, 2020. Nevertheless, this analysis shows data only from the cytosolic fraction and a single biological and technical replicate. To provide the evidence of PI-PLCs, PLA1 and NPC involvement in autophagy, supplementary data would be necessary.

A. thaliana knock-out mutant *atg10* does not form autophagic bodies, hence the process of autophagy is completely disrupted in this mutant. Besides, *atg10* mutants are hypersensitive to carbon and nitrogen starvation and initiate senescence and programmed cell death faster than wild type plants (Soto-Burgos *et al.*, 2018a). Analysis of *atg10* phenotype revealed, that after autophagy was induced by carbon starvation, growth of primary root was strongly inhibited. If phospholipases were involved in plant autophagy regulation, would the growth of primary root of phospholipases knock-out mutants be inhibited in the same manner? Measurement of primary root increment length of phospholipase mutants show milder primary root inhibition than *atg10* mutants, but statistically significant when compared to wild type plants. In addition to primary root growth inhibition, another typical phenotypic expression of *atg10* mutants is faster initiation of senescence. Senescence is connected to major structural changes in plants cells, such as degradation of macromolecules, including chlorophyll (Smart, 1994). Therefore, measurement of leaf chlorophyll concentration would provide complementary information about the phenotype of mutants with knocked-out genes coding phospholipases.

A quantitative estimate of autophagy activity can be obtained by counting the number of autophagosomes. However, the number of particles is given by the rate of the autophagosome degradation, as well as formation. Therefore, the results of such analysis must be treated with caution (Bassham, 2015). Autophagosomes can be visualised by fusion of ATG8 protein with fluorescent proteins (FP). There are 9 genes coding ATG8 proteins, while specific function of each gene product is unknown. Nevertheless, all of ATG8 protein isoforms localise to autophagosome membrane and may be used as autophagosome marker (Yoshimoto *et al.*, 2004; Sláviková *et al.*, 2005; Woo *et al.*, 2014). Using transgenic plants overexpressing ATG8 for the estimation of autophagy activity brings a risk of undesirable autophagy stimulation caused by *ATG8* overexpression (Chen *et al.*, 2019). Disadvantages of observing autophagy in transgenic lines may be overcome by using indirect immunolabelling of ATG8 in wild type plants. Here, I have shown the cooccurrence of most structures labelled by GFP and secondary antibody conjugated to Alexa Fluor 555 fluorophore. It is hardly surprising, that more structures were labelled by indirect immunostaining than fluorescent protein, as GFP was conjugated only to ATG8e isoform. On the contrary, immunolabelling by primary antibody against ATG8 recognizes all ATG isoforms.

Autophagosomes labelled by indirect fluorescence immunolabelling were observed in *A. thaliana* meristematic and elongation zone of wild type and *dgk7, pldα3*, *pldβ1*. Root meristematic zone showed higher number density of autophagosomes than elongation zone. This finding is in strong contradiction with Yano et al. (2007), who reported higher number of autophagosomes in root elongation and differentiation zone than root meristem. Nevertheless, observed high variability of autophagosomes in different root developmental zones is in accordance with Le Bars *et al.*, (2014). Furthermore, there is higher number density of autophagosomes in *pldα3* mutant and lower number density in *pldβ1* mutant.

A common technique for autophagosome number estimation is counting and averaging the number of autophagosomes from 2-dimensional (2D) sectional images (Pu, Luo and Bassham, 2017) or maximum intensity projections (Le Bars *et al.*, 2014) acquired using confocal scanning microscopy. Nevertheless, the plant cells are 3-dimensional (3D) objects and counting autophagosomes spread in the space using 2D sections may give inaccurate and biased results. For example, Kubínová *et al.*, 2014 compared commonly used method for counting chloroplasts in plant cells from 2D sections with the unbiased disector technique in 3D. Their analysis revealed that

the number of chloroplasts counted from 2D sections was 10 times underestimated compared to values obtained by the disector counting technique in 3D. Here, I used the disector counting technique (Sterio, 1984) for obtaining unbiased estimation of autophagosome number in plant cells. This stereological approach is also suitable for estimation number of particles in fixed samples, because the reference volume of the section can be obtained using Cavalieri's principle (Gundersen and Jensen, 1987) and the estimation of particle number is not biased by shrinkage (Maynard, 1996).

6 CONCLUSION

By measuring the length of primary root increment, I have identified *Arabidopsis thaliana* mutants in phospholipases C and phospholipase D with inhibited primary root growth after autophagy induction. Knock-out mutants *pi-plc2*, *pi-plc3*, *pi-plc5, pldα2* and *pldζ2* show significantly lower primary root increment compared to wild type after 6 days of carbon starvation in the dark.

Also, I measured the level of fluorescently labelled products of plant phospholipases in cytosolic fraction of *A. thaliana* wild type plants and *atg10* mutants. After extended dark, the level of DAG (38%), LPC (40,7%) and PA (50,7%) in root cytosolic fraction of treated plants remarkably increased, compared to plants in control conditions. On the other hand, there was no significant change in DAG level in root cytosolic fraction of *atg10* mutants and only 19% increase of LPC level. Therefore, this change in lipids level may be related to plant autophagy.

Using live cell imaging, I observed autophagosomes in root elongation zone of *A. thaliana* GFP-ATG8e transgenic line. An unbiased estimation of autophagosome number was made using the disector counting technique. After two hours of carbon and nitrogen starvation in the dark, plant cells formed significantly higher number of autophagosomes per volume compared to seedlings in control conditions.

Moreover, autophagosomes were labelled by indirect fluorescence immunolabelling in root elongation and meristematic zone of *A. thaliana dgk7, pldα3*, *pldβ1, atg10* mutants and wild type. Compared to wild type, mutant *pldα3* show higher number density of autophagosomes in both elongation and meristematic zone, while *pldβ1* exhibits lower number density of autophagosomes only in elongation zone. Given that my findings are based on a limited number of samples, the results from this analysis should be treated with considerable caution.

Finally, a method for unbiased estimation of autophagosome number from 2-dimensional sections using stereological methods was introduced.

7 LITERATURE

Alonso J.M., Stepanova A.N., Leisse T.J., Kim C.J., Chen H., Shinn P., *et al.* (2003): Genome-wide insertional mutagenesis of Arabidopsis thaliana. *Science* **301**, 653–657

Anderson G.H., Veit B. & Hanson M.R. (2005): The Arabidopsis AtRaptor genes are essential for post-embryonic plant growth. *BMC Biology* **3**, 1201

Arisz S.A. & Munnik T. (2013): Distinguishing Phosphatidic Acid Pools from De Novo Synthesis, PLD, and DGK. pp. 55–62.

Arisz S.A., Testerink C. & Munnik T. (2009): Plant PA signaling via diacylglycerol kinase. *Biochimica et Biophysica Acta (BBA) - Molecular and Cell Biology of Lipids* **1791**, 869–875

Axe E.L., Walker S.A., Manifava M., Chandra P., Roderick H.L., Habermann A., *et al.* (2008): Autophagosome formation from membrane compartments enriched in phosphatidylinositol 3-phosphate and dynamically connected to the endoplasmic reticulum. *Journal of Cell Biology* **182**, 685–701

Bahn S.C., Lee H.Y., Kim H.J., Ryu S.B. & Shin J.S. (2003): Characterization of Arabidopsis secretory phospholipase A 2 -γ cDNA and its enzymatic properties 1. *FEBS Letters* **553**, 113–118

Le Bars R., Marion J., Le Borgne R., Satiat-Jeunemaitre B. & Bianchi M.W. (2014): ATG5 defines a phagophore domain connected to the endoplasmic reticulum during autophagosome formation in plants. *Nature Communications* **5**, 4121

Bassham D.C. (2015): Methods for analysis of autophagy in plants. *Methods* **75**, 181–188

Bassham D.C. (2007): Plant autophagy—more than a starvation response. *Current Opinion in Plant Biology* **10**, 587–593

Benning C. (2009): Mechanisms of Lipid Transport Involved in Organelle Biogenesis in Plant Cells. *Annual Review of Cell and Developmental Biology* **25**, 71–91

Bradford M.M. (1976): A rapid and sensitive method for the quantitation of microgram quantities of protein utilizing the principle of protein-dye binding. *Analytical Biochemistry* **72**, 248–254

Caldana C., Li Y., Leisse A., Zhang Y., Bartholomaeus L., Fernie A.R., *et al.* (2013): Systemic analysis of inducible target of rapamycin mutants reveal a general metabolic switch controlling growth in Arabidopsis thaliana. *The Plant Journal* **73**, 897–909

Chapman K.D. & Ohlrogge J.B. (2012): Compartmentation of Triacylglycerol Accumulation in Plants. *Journal of Biological Chemistry* **287**, 2288–2294

Chen G., Greer M.S. & Weselake R.J. (2013): Plant phospholipase A: advances in molecular biology, biochemistry, and cellular function. *BioMolecular Concepts* **4**, 527–532

Chen L., Su Z.Z., Huang L., Xia F.N., Qi H., Xie L.J., *et al.* (2017): The AMP-activated protein kinase kin10 is involved in the regulation of autophagy in arabidopsis. *Frontiers in Plant Science*

Chen Q., Soulay F., Saudemont B., Elmayan T., Marmagne A. & Masclaux-Daubresse C. (2019): Overexpression of ATG8 in Arabidopsis Stimulates Autophagic Activity and Increases Nitrogen Remobilization Efficiency and Grain Filling. *Plant and Cell Physiology* **60**, 343–352

Cheong J.-J. & Choi Y. Do (2003): Methyl jasmonate as a vital substance in plants. *Trends in Genetics* **19**, 409–413

Chung T. (2019): How phosphoinositides shape autophagy in plant cells. *Plant Science* **281**, 146–158

Contento A.L., Xiong Y. & Bassham D.C. (2005): Visualization of autophagy in Arabidopsis using the fluorescent dye monodansylcadaverine and a GFP-AtATG8e fusion protein. *Plant Journal* **42**,598–608

Cruz-Ramírez A., Oropeza-Aburto A., Razo-Hernández F., Ramírez-Chávez E. & Herrera-Estrella L. (2006): Phospholipase DZ2 plays an important role in extraplastidic galactolipid biosynthesis and phosphate recycling in Arabidopsis roots. *Proceedings of the National Academy of Sciences of the United States of America* **103**, 6765–6770

Dall'Armi C., Hurtado-Lorenzo A., Tian H., Morel E., Nezu A., Chan R.B., *et al.* (2010): The phospholipase D1 pathway modulates macroautophagy. *Nature Communications* **1**, 1–11

Deprost D., Truong H.N., Robaglia C. & Meyer C. (2005): An Arabidopsis homolog of RAPTOR/KOG1 is essential for early embryo development. *Biochemical and Biophysical Research Communications* **326**, 844–850

Dettmer J., Hong-Hermesdorf A., Stierhof Y.D. & Schumacher K. (2006): Vacuolar H+-ATPase activity is required for endocytic and secretory trafficking in Arabidopsis. *Plant Cell* **18**, 715–730

Dhonukshe P., Laxalt A.M., Goedhart J., Gadella T.W.J. & Munnik T. (2003): Phospholipase D Activation Correlates with Microtubule Reorganization in Living Plant Cells[W]. *The Plant Cell* **15**, 2666–2679

Díaz-Troya S., Pérez-Pérez M.E., Florencio F.J. & Crespo J.L. (2008): The role of TOR in autophagy regulation from yeast to plants and mammals. *Autophagy* **4**, 851–865

Van Doorn W.G. & Papini A. (2013): Ultrastructure of autophagy in plant cells: A review. *Autophagy* **9**, 1922–1936

Dowd P.E., Coursol S., Skirpan A.L., Kao T. & Gilroy S. (2006): Petunia Phospholipase C1 Is Involved in Pollen Tube Growth. *The Plant Cell* **18**, 1438–1453

Eastmond P.J. (2006): SUGAR-DEPENDENT1 Encodes a Patatin Domain Triacylglycerol Lipase That Initiates Storage Oil Breakdown in Germinating Arabidopsis Seeds. *The Plant Cell* **18**, 665–675

Eskelinen E.-L. (2005): Maturation of Autophagic Vacuoles in Mammalian Cells. *Autophagy* **1**, 1–10

Exton J.H. (2002): Regulation of phospholipase D. *FEBS Letters* **531**, 58–61

Fan J., Yu L. & Xu C. (2017): A Central Role for Triacylglycerol in Membrane Lipid Breakdown, Fatty Acid β -Oxidation, and Plant Survival under Extended Darkness. *Plant Physiology* **174**, 1517–1530

Fan J., Yu L. & Xu C. (2019): Dual Role for Autophagy in Lipid Metabolism in Arabidopsis. *The Plant Cell* **31**, 1598–1613

Fan L., Zheng S., Cui D. & Wang X. (1999): Subcellular Distribution and Tissue Expression of Phospholipase Dα, Dβ, and Dγ in Arabidopsis. *Plant Physiology* **119**, 1371–1378

Fang Y., Vilella-Bach M., Bachmann R., Flanigan A. & Chen J. (2001): Phosphatidic acid-mediated mitogenic activation of mTOR signaling. *Science* **294**, 1942–1945

Farmer E.E., Alméras E. & Krishnamurthy V. (2003): Jasmonates and related oxylipins in plant responses to pathogenesis and herbivory. *Current Opinion in Plant Biology* **6**, 372–378

Di Fino L.M., D'Ambrosio J.M., Tejos R., van Wijk R., Lamattina L., Munnik T., *et al.* (2017): Arabidopsis phosphatidylinositol-phospholipase C2 (PLC2) is required for female gametogenesis and embryo development. *Planta* **245**, 717–728

Fujiki Y., Yoshimoto K. & Ohsumi Y. (2007): An Arabidopsis homolog of yeast ATG6/VPS30 is essential for pollen germination. *Plant Physiology* **143**, 1132–1139

Gao K., Liu Y.L., Li B., Zhou R.G., Sun D.Y. & Zheng S.Z. (2014): Arabidopsis thaliana phosphoinositide-specific phospholipase C isoform 3 (AtPLC3) and AtPLC9 have an additive effect on thermotolerance. *Plant and Cell Physiology* **55**, 1873–1883

Gardiner J. (2003): The Effects of the Phospholipase D-Antagonist 1-Butanol on Seedling Development and Microtubule Organisation in Arabidopsis. *Plant and Cell Physiology* **44**, 687–696

Gardiner J.C., Harper J.D.I., Weerakoon N.D., Collings D.A., Ritchie S., Gilroy S., *et al.* (2001): A 90-kD Phospholipase D from Tobacco Binds to Microtubules and the Plasma Membrane. *The Plant Cell* **13**, 2143–2158

Gaude N., Nakamura Y., Scheible W.-R., Ohta H. & Dörmann P. (2008): Phospholipase C5 (NPC5) is involved in galactolipid accumulation during phosphate limitation in leaves of Arabidopsis. *The Plant Journal* **56**, 28–39

Ge L., Melville D., Zhang M. & Schekman R. (2013): The ER–Golgi intermediate compartment is a key membrane source for the LC3 lipidation step of autophagosome biogenesis. *eLife* **2**, e00947

Geng J. & Klionsky D.J. (2008): The Atg8 and Atg12 ubiquitin-like conjugation systems in macroautophagy. "Protein Modifications: Beyond the Usual Suspects" Review Series. *EMBO Reports*, 859–864

Gorelova O., Baulina O., Solovchenko A., Selyakh I., Chivkunova O., Semenova L., *et al.* (2015): Coordinated rearrangements of assimilatory and storage cell compartments in a nitrogen-starving symbiotic chlorophyte cultivated under high light. *Archives of Microbiology* **197**, 181–195

Gundersen H.J.G. & Jensen E.B. (1987): The efficiency of systematic sampling in stereology and its prediction. *Journal of Microscopy* **147**, 229–263

Guo L., Mishra G., Markham J.E., Li M., Tawfall A., Welti R., *et al.* (2012): Connections between Sphingosine Kinase and Phospholipase D in the Abscisic Acid Signaling Pathway in Arabidopsis. *Journal of Biological Chemistry* **287**, 8286–8296

Hailey D.W., Rambold A.S., Satpute-Krishnan P., Mitra K., Sougrat R., Kim P.K., *et al.* (2010): Mitochondria Supply Membranes for Autophagosome Biogenesis during Starvation. *Cell* **141**, 656–667

Hamasaki M., Furuta N., Matsuda A., Nezu A., Yamamoto A., Fujita N., *et al.* (2013): Autophagosomes form at ER-mitochondria contact sites. *Nature* **495**, 389–393

Hanaoka H., Noda T., Shirano Y., Kato T., Hayashi H., Shibata D., *et al.* (2002): Leaf Senescence and Starvation-Induced Chlorosis Are Accelerated by the Disruption of an Arabidopsis Autophagy Gene. *Plant Physiology* **129**, 1181–1193

Hara K., Maruki Y., Long X., Yoshino K. ichi, Oshiro N., Hidayat S., *et al.* (2002): Raptor, a binding partner of target of rapamycin (TOR), mediates TOR action. *Cell* **110**, 177–189

Harrison-Lowe N.J. & Olsen L.J. (2008): Autophagy protein 6 (ATG6) is required for pollen germination in Arabidopsis thaliana. *Autophagy* **4**, 339–348

Heilmann I. (2016): Phosphoinositide signaling in plant development. *Development* **143**, 2044–2055

Helling D., Possart A., Cottier S., Klahre U. & Kost B. (2007): Pollen Tube Tip Growth Depends on Plasma Membrane Polarization Mediated by Tobacco PLC3 Activity and Endocytic Membrane Recycling. *The Plant Cell* **18**, 3519–3534

Hendrix K.W., Assefa H. & Boss W.F. (1989): The polyphosphoinositides, phosphatidylinositol monophosphate and phosphatidylinositol bisphosphate, are present in nuclei isolated from carrot protoplast. *Protoplasma* **151**, 62–72

Hoagland, D. R.; Arnon D.I. (1950): The water-culture method for growing plants without soil. *Circular* **347**, 1–32

Hong Y., Devaiah S.P., Bahn S.C., Thamasandra B.N., Li M., Welti R., *et al.* (2009): Phospholipase Dε and phosphatidic acid enhance Arabidopsis nitrogen signaling and growth. *The Plant Journal* **58**, 376–387

Hong Y., Zhao J., Guo L., Kim S.-C., Deng X., Wang G., *et al.* (2016): Plant phospholipases D and C and their diverse functions in stress responses. *Progress in Lipid Research* **62**, 55–74

Hu Q., Sommerfeld M., Jarvis E., Ghirardi M., Posewitz M., Seibert M., *et al.* (2008): Microalgal triacylglycerols as feedstocks for biofuel production: perspectives and advances. *The Plant Journal* **54**, 621–639

Huang S., Gao L., Blanchoin L. & Staiger C.J. (2006): Heterodimeric Capping Protein from Arabidopsis Is Regulated by Phosphatidic Acid. *Molecular Biology of the Cell* **17**, 1946–1958

Imamura S., Kawase Y., Kobayashi I., Sone T., Era A., Miyagishima S., *et al.* (2015): Target of rapamycin (TOR) plays a critical role in triacylglycerol accumulation in microalgae. *Plant Molecular Biology* **89**, 309–318

Inoue Y., Suzuki T., Hattori M., Yoshimoto K., Ohsumi Y. & Moriyasu Y. (2006): AtATG genes, homologs of yeast autophagy genes, are involved in constitutive autophagy in Arabidopsis root tip cells. *Plant and Cell Physiology* **47**, 1641–1652

Izumi M., Hidema J., Makino A. & Ishida H. (2013): Autophagy contributes to nighttime energy availability for growth in Arabidopsis. *Plant Physiology* **161**, 1682–1693

Janáček J. (2012): Disector

Jang Y.H., Choi K.Y. & Min D.S. (2014): Phospholipase D-mediated autophagic regulation is a potential target for cancer therapy. *Cell Death and Differentiation* **21**, 533–546

Jones D., Morgan C. & Cockcroft S. (1999): Phospholipase D and membrane traffic. *Biochimica et Biophysica Acta (BBA) - Molecular and Cell Biology of Lipids* **1439**, 229–244

Kajikawa M. & Fukuzawa H. (2020): Algal Autophagy Is Necessary for the Regulation of Carbon Metabolism Under Nutrient Deficiency. *Frontiers in Plant Science* **11**, 36

Kajikawa M., Yamauchi M., Shinkawa H., Tanaka M., Hatano K., Nishimura Y., *et al.* (2019): Isolation and Characterization of Chlamydomonas Autophagy-Related Mutants in Nutrient-Deficient Conditions. *Plant and Cell Physiology* **60**, 126–138

Kamada Y. & Muto S. (1991): Ca2+ regulation of phosphatidylinositol turnover in the plasma membrane of tobacco suspension culture cells. *Biochimica et Biophysica Acta (BBA) - Molecular Cell Research* **1093**, 72–79

Kanehara K., Yu C.-Y., Cho Y., Cheong W.-F., Torta F., Shui G., *et al.* (2015): Arabidopsis AtPLC2 Is a Primary Phosphoinositide-Specific Phospholipase C in Phosphoinositide Metabolism and the Endoplasmic Reticulum Stress Response. *PLoS genetics* **11**, e1005511

Karanasios E., Walker S.A., Okkenhaug H., Manifava M., Hummel E., Zimmermann H., *et al.* (2016): Autophagy initiation by ULK complex assembly on ER tubulovesicular regions marked by ATG9 vesicles. *Nature Communications* **7**, 12420

Kast D.J. & Dominguez R. (2017): The Cytoskeleton–Autophagy Connection. *Current Biology* **27**, R318–R326

Kato T., Morita M.T., Fukaki H., Yamauchi Y., Uehara M., Niihama M., *et al.* (2002): SGR2, a Phospholipase-Like Protein, and ZIG/SGR4, a SNARE, Are Involved in the Shoot Gravitropism of Arabidopsis. *The Plant Cell* **14**, 33–46

Ketelaar T., Voss C., Dimmock S.A., Thumm M. & Hussey P.J. (2004): Arabidopsis homologues of the autophagy protein Atg8 are a novel family of microtubule binding proteins. *FEBS Letters* **567**, 302–306

Kim J., Kundu M., Viollet B. & Guan K.-L. (2011): AMPK and mTOR regulate autophagy through direct phosphorylation of Ulk1. *Nature Cell Biology* **13**, 132–141

Kim S.-C., Guo L. & Wang X. (2013): Phosphatidic Acid Binds to Cytosolic Glyceraldehyde-3-phosphate Dehydrogenase and Promotes Its Cleavage in Arabidopsis*. *Journal of Biological Chemistry* **288**, 11834–11844

Kleinboelting N., Huep G., Kloetgen A., Viehoever P. & Weisshaar B. (2012): GABI-Kat SimpleSearch: New features of the Arabidopsis thaliana T-DNA mutant database. *Nucleic Acids Research* **40**

Kokabi K., Gorelova O., Zorin B., Didi-Cohen S., Itkin M., Malitsky S., *et al.* (2020): Lipidome Remodeling and Autophagic Respose in the Arachidonic-Acid-Rich Microalga Lobosphaera incisa Under Nitrogen and Phosphorous Deprivation. *Frontiers in Plant Science* **11**

Komatsu M., Waguri S., Ueno T., Iwata J., Murata S., Tanida I., *et al.* (2005): Impairment of starvation-induced and constitutive autophagy in Atg7-deficient mice. *Journal of Cell Biology* **169**, 425–434

Komis G., Galatis B., Quader H., Galanopoulou D. & Apostolakos P. (2008): Phospholipase C signaling involvement in macrotubule assembly and activation of the mechanism regulating protoplast volume in plasmolyzed root cells of Triticum turgidum. *New Phytologist* **178**, 267–282

Kooijman E.E., Tieleman D.P., Testerink C., Munnik T., Rijkers D.T.S., Burger K.N.J., *et al.* (2007): An Electrostatic/Hydrogen Bond Switch as the Basis for the Specific Interaction of Phosphatidic Acid with Proteins. *Journal of Biological Chemistry* **282**, 11356–11364

Krčková Z., Brouzdová J., Daněk M., Kocourková D., Rainteau D., Ruelland E., *et al.* (2015): Arabidopsis non-specific phospholipase C1: characterization and its involvement in response to heat stress. *Frontiers in Plant Science* **6**, 928

Krčková Z., Kocourková D., Daněk M., Brouzdová J., Pejchar P., Janda M., *et al.* (2018): The Arabidopsis thaliana non-specific phospholipase C2 is involved in the response to Pseudomonas syringae attack. *Annals of Botany* **121**, 297–310

Kubínová Z., Janáček J., Lhotáková Z., Kubínová L. & Albrechtová J. (2014): Unbiased estimation of chloroplast number in mesophyll cells: Advantage of a genuine three-dimensional approach. *Journal of Experimental Botany* **65**

Kulich I., Pečenková T., Sekereš J., Smetana O., Fendrych M., Foissner I., *et al.* (2013): Arabidopsis exocyst subcomplex containing subunit EXO70B1 is involved in autophagy-related transport to the vacuole. *Traffic (Copenhagen, Denmark)* **14**, 1155–65

Kusner D.J., Barton J.A., Qin C., Wang X. & Iyer S.S. (2003): Evolutionary conservation of physical and functional interactions between phospholipase D and actin. *Archives of Biochemistry and Biophysics* **412**, 231–241

Lamb C.A., Yoshimori T. & Tooze S.A. (2013): The autophagosome: origins unknown, biogenesis complex. *Nature Reviews Molecular Cell Biology* **14**, 759–774

Lee H.N., Zarza X., Kim J.H., Yoon M.J., Kim S.H., Lee J.H., *et al.* (2018): Vacuolar trafficking protein VPS38 is dispensable for autophagy. *Plant Physiology* **176**, 1559–1572

Levine B., Liu R., Dong X. & Zhong Q. (2015): Beclin orthologs: Integrative hubs of cell signaling, membrane trafficking, and physiology. *Trends in Cell Biology* **25**, 533–544

Li F., Chung T. & Vierstra R.D. (2014): AUTOPHAGY-RELATED11 plays a critical role in general autophagy- and senescence-induced mitophagy in Arabidopsis. *Plant Cell* **26**, 788–807

Li F. & Vierstra R.D. (2012): Autophagy: a multifaceted intracellular system for bulk and selective recycling. *Trends in Plant Science* **17**, 526–537

Li F., Zhang C., Li Y., Wu G., Hou X., Zhou X., *et al.* (2018): Beclin1 restricts RNA virus infection in plants through suppression and degradation of the viral polymerase. *Nature Communications* **9**

Li J. (2003): Brassinosteroids signal through two receptor-like kinases. *Current Opinion in Plant Biology* **6**, 494–499

Li J., Henty-Ridilla J.L., Huang S., Wang X., Blanchoin L. & Staiger C.J. (2012): Capping Protein Modulates the Dynamic Behavior of Actin Filaments in Response to Phosphatidic Acid in Arabidopsis. *The Plant Cell* **24**, 3742–3754

Li M., Welti R. & Wang X. (2006): Quantitative profiling of Arabidopsis polar glycerolipids in response to phosphorus starvation. Roles of phospholipases Dζ1 and Dζ2 in phosphatidylcholine hydrolysis and digalactosyldiacylglycerol accumulation in phosphorus-starved plants. *Plant Physiology* **142**, 750–761

Lindsey K., Pullen M.L. & Topping J.F. (2003): Importance of plant sterols in pattern formation and hormone signalling. *Trends in Plant Science* **8**, 521–525

Liu F., Hu W. & Vierstra R.D. (2018): The vacuolar protein sorting-38 subunit of the arabidopsis phosphatidylinositol-3-kinase complex plays critical roles in autophagy, endosome sorting, and gravitropism. *Frontiers in Plant Science* **9**

Liu Y. & Bassham D.C. (2012): Autophagy: Pathways for Self-Eating in Plant Cells. *Annual Review of Plant Biology* **63**, 215–237

Liu Y. & Bassham D.C. (2010): TOR is a negative regulator of autophagy in Arabidopsis thaliana. *PLoS ONE* **5**, e11883

Liu Y., Schiff M., Czymmek K., Tallóczy Z., Levine B. & Dinesh-Kumar S.P. (2005): Autophagy regulates programmed cell death during the plant innate immune response. *Cell* **121**, 567–577

Liu Y., Su Y. & Wang X. (2013): Phosphatidic Acid-Mediated Signaling. In: *Advances in Experimental Medicine and Biology*. pp. 159–176.

Lundberg G.A. & Sommarin M. (1992): Diacylglycerol kinase in plasma membranes from wheat. *Biochimica et Biophysica Acta (BBA) - Lipids and Lipid Metabolism* **1123**, 177–183

Martin S. & Parton R.G. (2006): Lipid droplets: a unified view of a dynamic organelle. *Nature Reviews Molecular Cell Biology* **7**, 373–378

Matsuoka K., Higuchi T., Maeshima M. & Nakamura K. (1997): A vacuolar-type H+-ATPase in a nonvacuolar organelle is required for the sorting of soluble vacuolar protein precursors in tobacco cells. *Plant Cell* **9**, 533–546

Maynard R.L. (1996): Don't dissect use the disector! "If you assume, you can make an ass out of u and me": a decade of the disector for sterological counting of particles in 3D space. *Human & experimental toxicology* **15**, 862–863

Mehrpour M., Esclatine A., Beau I. & Codogno P. (2010): Overview of macroautophagy regulation in mammalian cells. *Cell Research* **20**, 748–762

Meijer H.J.G. & Munnik T. (2003): P <scp>HOSPHOLIPID</scp> -B <scp>ASED</scp> S <scp>IGNALING IN</scp> P <scp>LANTS</scp>. *Annual Review of Plant Biology* **54**, 265–306

Menand B., Desnos T., Nussaume L., Berger F., Bouchez D., Meyer C., *et al.* (2002): Expression and disruption of the Arabidopsis TOR (target of rapamycin) gene. *Proceedings of the National Academy of Sciences* **99**, 6422–6427

Merkulova E.A., Guiboileau A., Naya L., Masclaux-Daubresse C. & Yoshimoto K. (2014): Assessment and Optimization of Autophagy Monitoring Methods in Arabidopsis Roots Indicate Direct Fusion of Autophagosomes with Vacuoles. *Plant and Cell Physiology* **55**, 715–726

Mishra G., Zhang W., Deng F., Zhao J. & Wang X. (2006): A bifurcating pathway directs abscisic acid effects on stomatal closure and opening in Arabidopsis. *Science* **312**, 264–266

Mizushima N. (2010): The role of the Atg1/ULK1 complex in autophagy regulation. *Current Opinion in Cell Biology* **22**, 132–139

Mizushima N., Levine B., Cuervo A.M. & Klionsky D.J. (2008): Autophagy fights disease through cellular self-digestion. *Nature* **451**, 1069–1075

Morita M.T., Kato T., Nagafusa K., Saito C., Ueda T., Nakano A., *et al.* (2002): Involvement of the Vacuoles of the Endodermis in the Early Process of Shoot Gravitropism in Arabidopsis. *The Plant Cell* **14**, 47–56

Moriyasu Y. & Ohsumi Y. (1996): Autophagy in tobacco suspension-cultured cells in response to sucrose starvation. *Plant Physiology* **111**, 1233–1241

Müller M.-O., Meylan-Bettex M., Eckstein F., Martinoia E., Siegenthaler P.-A. & Bovet L. (2000): Lipid Phosphorylation in Chloroplast Envelopes. *Journal of Biological Chemistry* **275**, 19475–19481

Munafó D.B. & Colombo M.I. (2001): A novel assay to study autophagy: Regulation of autophagosome vacuole size by amino acid deprivation. *Journal of Cell Science* **114**, 3619–3629

Munnik T. & Laxalt A.M. (2013): Measuring PLD activity in vivo. *Methods in Molecular Biology* **1009**, 219–231

Murashige T. & Skoog F. (1962): A Revised Medium for Rapid Growth and Bio Assays with Tobacco Tissue Cultures. *Physiologia Plantarum* **15**, 473–497

Nakamura Y., Awai K., Masuda T., Yoshioka Y., Takamiya K. & Ohta H. (2005): A Novel Phosphatidylcholine-hydrolyzing Phospholipase C Induced by Phosphate Starvation in Arabidopsis. *Journal of Biological Chemistry* **280**, 7469–7476

Nakatogawa H., Ichimura Y. & Ohsumi Y. (2007): Atg8, a Ubiquitin-like Protein Required for Autophagosome Formation, Mediates Membrane Tethering and Hemifusion. *Cell* **130**, 165–178

Naumann C., Müller J., Sakhonwasee S., Wieghaus A., Hause G., Heisters M., *et al.* (2019): The local phosphate deficiency response activates endoplasmic reticulum stress-dependent autophagy1[OPEN]. *Plant Physiology* **179**

Ngo A.H., Lin Y.-C., Liu Y., Gutbrod K., Peisker H., Dörmann P., *et al.* (2018): A pair of nonspecific phospholipases C, NPC2 and NPC6, are involved in gametophyte development and glycerolipid metabolism in Arabidopsis. *New Phytologist* **219**, 163–175

Noack L.C. & Jaillais Y. (2017): Precision targeting by phosphoinositides: how PIs direct endomembrane trafficking in plants. *Current Opinion in Plant Biology* **40**, 22–33

Nobel Media AB (2016): Press Release

Novák D., Vadovič P., Ovečka M., Šamajová O., Komis G., Colcombet J., *et al.* (2018): Gene Expression Pattern and Protein Localization of Arabidopsis Phospholipase D Alpha 1 Revealed by Advanced Light-Sheet and Super-Resolution Microscopy. *Frontiers in Plant Science* **9**

Pappan K., Zheng S. & Wang X. (1997): Identification and Characterization of a Novel Plant Phospholipase D That Requires Polyphosphoinositides and Submicromolar Calcium for Activity in Arabidopsis. *Journal of Biological Chemistry* **272**, 7048–7054

Pappan K.L. & Wang X. (2013): Assaying different types of plant phospholipase D activities in vitro. *Methods in Molecular Biology* **1009**, 205–217

Pasternak T., Tietz O., Rapp K., Begheldo M., Nitschke R., Ruperti B., *et al.* (2015): Protocol: An improved and universal procedure for whole-mount immunolocalization in plants. *Plant Methods* **11**

Patel S. & Dinesh-Kumar S.P. (2008): Arabidopsis ATG6 is required to limit the pathogen-associated cell death response. *Autophagy* **4**, 20–27

Peters C., Kim S.-C., Devaiah S., Maoyin L. & Wang X. (2014): Non-specific phospholipase C5 and diacylglycerol promote lateral root development under mild salt stress in Arabidopsis. *Plant, Cell & Environment* **37**, 2002–2013

Peterson T.R., Sengupta S.S., Harris T.E., Carmack A.E., Kang S.A., Balderas E., *et al.* (2011): mTOR Complex 1 Regulates Lipin 1 Localization to Control the SREBP Pathway. *Cell* **146**, 408–420

Pinosa F., Buhot N., Kwaaitaal M., Fahlberg P., Thordal-Christensen H., Ellerstrom M., *et al.* (2013): Arabidopsis Phospholipase D Is Involved in Basal Defense and Nonhost Resistance to Powdery Mildew Fungi. *PLANT PHYSIOLOGY* **163**, 896–906

Pleskot R., Li J., Žárský V., Potocký M. & Staiger C.J. (2013): Regulation of cytoskeletal dynamics by phospholipase D and phosphatidic acid. *Trends in Plant Science* **18**, 496–504

Pleskot R., Potocký M., Pejchar Př., Linek J., Bezvoda R., Martinec J., *et al.* (2010): Mutual regulation of plant phospholipase D and the actin cytoskeleton. *Plant Journal* **62**, 494–507

Pokotylo I., Pejchar P., Potocký M., Kocourková D., Krčková Z., Ruelland E., *et al.* (2013): The plant non-specific phospholipase C gene family. Novel competitors in lipid signalling. *Progress in Lipid Research* **52**, 62–79

Pol A., Gross S.P. & Parton R.G. (2014): Biogenesis of the multifunctional lipid droplet: Lipids, proteins, and sites. *Journal of Cell Biology* **204**, 635–646

Pool M., Thiemann J., Bar-Or A. & Fournier A.E. (2008): NeuriteTracer: A novel ImageJ plugin for automated quantification of neurite outgrowth. *Journal of Neuroscience Methods* **168**, 134–139

Pu Y., Luo X. & Bassham D.C. (2017): Tor-dependent and -independent pathways regulate autophagy in arabidopsis thaliana. *Frontiers in Plant Science* **8**

Qin C. & Wang X. (2002): The Arabidopsis Phospholipase D Family. Characterization of a Calcium-Independent and Phosphatidylcholine-Selective PLDzeta 1 with Distinct Regulatory Domains. *PLANT PHYSIOLOGY* **128**, 1057–1068

Qin G., Ma Z., Zhang L., Xing S., Hou X., Deng J., *et al.* (2007): Arabidopsis AtBECLIN 1/AtAtg6/AtVps30 is essential for pollen germination and plant development. *Cell Research* **17**, 249–263

Rainteau D., Humbert L., Delage E., Vergnolle C., Cantrel C., Maubert M.-A., *et al.* (2012): Acyl Chains of Phospholipase D Transphosphatidylation Products in Arabidopsis Cells: A Study Using Multiple Reaction Monitoring Mass Spectrometry. *PLoS ONE* **7**, e41985

Rao Y., Perna M.G., Hofmann B., Beier V. & Wollert T. (2016): The Atg1-kinase complex tethers Atg9-vesicles to initiate autophagy. *Nature communications* **7**, 10338

Ren M., Qiu S., Venglat P., Xiang D., Feng L., Selvaraj G., *et al.* (2011): Target of Rapamycin Regulates Development and Ribosomal RNA Expression through Kinase Domain in Arabidopsis. *Plant Physiology* **155**, 1367–1382

Ren M., Venglat P., Qiu S., Feng L., Cao Y., Wang E., *et al.* (2013): Target of Rapamycin Signaling Regulates Metabolism, Growth, and Life Span in Arabidopsis. *The Plant Cell* **24**, 4850–4874

Ricoult S.J.H. & Manning B.D. (2013): The multifaceted role of mTORC1 in the control of lipid metabolism. *EMBO reports* **14**, 242–251

Roy Choudhury S. & Pandey S. (2016): The role of PLDα1 in providing specificity to signal-response coupling by heterotrimeric G-protein components in Arabidopsis. *The Plant Journal* **86**, 50–61

Ruelland E., Kravets V., Derevyanchuk M., Martinec J., Zachowski A. & Pokotylo I. (2015): Role of phospholipid signalling in plant environmental responses. *Environmental and Experimental Botany* **114**, 129–143

Ryu S.B. (2004): Phospholipid-derived signaling mediated by phospholipase A in plants. *Trends in Plant Science* **9**, 229–235

Ryu S.B. & Wang X. (1996): Activation of phospholipase D and the possible mechanism of activation in wound-induced lipid hydrolysis in castor bean leaves. *Biochimica et Biophysica Acta (BBA) - Lipids and Lipid Metabolism* **1303**, 243–250

Scherer G.F.E. (2002): Secondary messengers and phospholipase A2 in auxin signal transduction. *Plant molecular biology* **49**, 357–372

Schindelin J., Arganda-Carreras I., Frise E., Kaynig V., Longair M., Pietzsch T., *et al.* (2012): Fiji: An open-source platform for biological-image analysis. *Nature Methods* **9**, 676–682

Schmid K.M. & Ohlrogge J.B. (2002): Chapter 4 Lipid metabolism in plants. In: *New Comprehensive Biochemistry*. pp. 93–126.

Sedaghatmehr M., Thirumalaikumar V.P., Kamranfar I., Marmagne A., Masclaux-Daubresse C. & Balazadeh S. (2019): A regulatory role of autophagy for resetting the memory of heat stress in plants. *Plant Cell and Environment* **42**

Shatz O., Holland P., Elazar Z. & Simonsen A. (2016): Complex Relations Between Phospholipids, Autophagy, and Neutral Lipids. *Trends in Biochemical Sciences* **41**, 907–923

Shin K.D., Lee H.N. & Chung T. (2014): A revised assay for monitoring autophagic flux in Arabidopsis Thaliana reveals involvement of autophagy-related9 in autophagy. *Molecules and Cells* **37**, 399–405

Šídlová D. (2020): *The Role of Lipids in Plant Autophagy*. University of Chemistry and Technology Prague.

Singh R., Kaushik S., Wang Y., Xiang Y., Novak I., Komatsu M., *et al.* (2009): Autophagy regulates lipid metabolism. *Nature* **458**, 1131–1135

Sláviková S., Shy G., Yao Y., Glozman R., Levanony H., Pietrokovski S., *et al.* (2005): The autophagy-associated Atg8 gene family operates both under favourable growth conditions and under starvation stresses in Arabidopsis plants. *Journal of Experimental Botany* **56**, 2839–2849

Smart C.M. (1994): Gene expression during leaf senescence. *New Phytologist* **126**, 419–448

Snedden W.A. & Blumwald E. (2000): Alternative splicing of a novel diacylglycerol kinase in tomato leads to a calmodulin-binding isoform. *The Plant Journal* **24**, 317–326

Soto-Burgos J., Zhuang X., Jiang L. & Bassham D.C. (2018a): Dynamics of Autophagosome Formation. *Plant physiology* **176**, 219–229

Soto-Burgos J., Zhuang X., Jiang L. & Bassham D.C. (2018b): Dynamics of Autophagosome Formation. *Plant Physiology* **176**, 219–229

Sperling P. & Heinz E. (2003): Plant sphingolipids: structural diversity, biosynthesis, first genes and functions. *Biochimica et Biophysica Acta (BBA) - Molecular and Cell Biology of Lipids* **1632**, 1–15

Sterio D.C. (1984): The unbiased estimation of number and sizes of arbitrary particles using the disector. *Journal of Microscopy* **134**, 127–136

Su Y., Li M., Guo L. & Wang X. (2018): Different effects of phospholipase Dζ2 and non-specific phospholipase C4 on lipid remodeling and root hair growth in Arabidopsis response to phosphate deficiency. *The Plant Journal* **94**, 315–326

Suttangkakul A., Li F., Chung T. & Vierstra R.D. (2011): The ATG1/ATG13 protein kinase complex is both a regulator and a target of autophagic recycling in Arabidopsis. *Plant Cell*

Synek L., Sekereš J. & Žárský V. (2014): The exocyst at the interface between cytoskeleton and membranes in eukaryotic cells. *Frontiers in Plant Science* **4**

Takatsuka C., Inoue Y., Matsuoka K. & Moriyasu Y. (2004): 3-Methyladenine Inhibits Autophagy in Tobacco Culture Cells under Sucrose Starvation Conditions. *Plant and Cell Physiology* **45**, 265–274

Tan Z. & Boss W.F. (1992): Association of Phosphatidylinositol Kinase, Phosphatidylinositol Monophosphate Kinase, and Diacylglycerol Kinase with the Cytoskeleton and F-Actin Fractions of Carrot (Daucus carota L.) Cells Grown in Suspension Culture. *Plant Physiology* **100**, 2116–2120

Tasma I.M., Brendel V., Whitham S.A. & Bhattacharyya M.K. (2008): Expression and evolution of the phosphoinositide-specific phospholipase C gene family in Arabidopsis thaliana. *Plant Physiology and Biochemistry* **46**, 627–637

Testerink C. & Munnik T. (2011): Molecular, cellular, and physiological responses to phosphatidic acid formation in plants. *Journal of Experimental Botany* **62**, 2349–2361

Thompson A.R., Doelling J.H., Suttangkakul A. & Vierstra R.D. (2005): Autophagic nutrient recycling in Arabidopsis directed by the ATG8 and ATG12 conjugation pathways. *Plant Physiology* **138**, 2097–2110

Tsai C.-H., Uygun S., Roston R., Shiu S.-H. & Benning C. (2018): Recovery from N Deprivation Is a Transcriptionally and Functionally Distinct State in Chlamydomonas. *Plant Physiology* **176**, 2007–2023

Tsai Y.-C., Koo Y., Delk N.A., Gehl B. & Braam J. (2013): Calmodulin-related CML24 interacts with ATG4b and affects autophagy progression in Arabidopsis. *The Plant Journal* **73**, 325–335

Ufer G., Gertzmann A., Gasulla F., Röhrig H. & Bartels D. (2017): Identification and characterization of the phosphatidic acid-binding A. thaliana phosphoprotein PLDrp1 that is regulated by PLDα1 in a stress-dependent manner. *The Plant Journal* **92**, 276–290

Urrea Castellanos R., Friedrich T., Petrovic N., Altmann S., Brzezinka K., Gorka M., *et al.* (2020): FORGETTER2 protein phosphatase and phospholipase D modulate heat stress memory in Arabidopsis. *Plant Journal* **104**, 7–17

Vadovič P., Takáč T., Šamaj J., Novák D., Šamajová O., Colcombet J., *et al.* (2019): Biochemical and Genetic Interactions of Phospholipase D Alpha 1 and Mitogen-Activated Protein Kinase 3 Affect Arabidopsis Stress Response. *Frontiers in Plant Science* **10**

Vaultier M.-N., Cantrel C., Guerbette F., Boutté Y., Vergnolle C., Çiçek D., *et al.* (2008): The hydrophobic segment of Arabidopsis thaliana cluster I diacylglycerol kinases is sufficient to target the proteins to cell membranes. *FEBS Letters* **582**, 1743–1748

Walther T.C. & Farese R. V. (2012): Lipid droplets and cellular lipid metabolism. *Annual Review of Biochemistry* **81**, 687–714

Wang X. (2004): Lipid signaling. *Current Opinion in Plant Biology* **7**, 329–336

Wang X. (2002): Phospholipase D in hormonal and stress signaling. *Current Opinion in Plant Biology* **5**, 408–414

Wang X., Devaiah S., Zhang W. & Welti R. (2006): Signaling functions of phosphatidic acid. *Progress in Lipid Research* **45**, 250–278

Wang X., Wang C., Sang Y., Qin C. & Welti R. (2002): Networking of phospholipases in plant signal transduction. *Physiologia Plantarum* **115**, 331–335

Wasternack C. & Song S. (2017): Jasmonates: biosynthesis, metabolism, and signaling by proteins activating and repressing transcription. *Journal of experimental botany* **68**, 1303–1321

Weidberg H., Shpilka T., Shvets E., Abada A., Shimron F. & Elazar Z. (2011): LC3 and GATE-16 N Termini Mediate Membrane Fusion Processes Required for Autophagosome Biogenesis. *Developmental Cell* **20**, 444–454

Wissing J.B., Grabowski L., Drewitz E., Hanenberg A., Wylegalla C. & Wagner K.G. (1992): Plasma membrane preparations from suspension cultured plant cells contain the enzymes for the recycling of phosphatidic acid and diacylglycerol. *Plant Science* **87**, 29–37

Wissing J.B., Riedel B. & Behrbohm H. (1995): Diacylglycerol- and phosphatidic acid-kinase studies in plant cell suspension cultures. *Biochemical Society Transactions* **23**, 867–871

Wissing J.B. & Wagner K.G. (1992): Diacylglycerol Kinase from Suspension Cultured Plant Cells. *Plant Physiology* **98**, 1148–1153

Woo J., Park E. & Dinesh-Kumar S.P. (2014): Differential processing of Arabidopsis ubiquitin-like Atg8 autophagy proteins by Atg4 cysteine proteases. *Proceedings of the National Academy of Sciences of the United States of America* **111**, 863–868

Worrall D. (2003): Sphingolipids, new players in plant signaling. *Trends in Plant Science* **8**, 317–320

Xiong Y., Contento A.L. & Bassham D.C. (2007a): Disruption ol autophagy results in constitutive oxidative stress in Arabidopsis. *Autophagy* **3**, 257–258

Xiong Y., Contento A.L., Nguyen P.Q. & Bassham D.C. (2007b): Degradation of oxidized proteins by autophagy during oxidative stress in arabidopsis. *Plant Physiology* **143**, 291–299

Xiong Y., McCormack M., Li L., Hall Q., Xiang C. & Sheen J. (2013): Glucose–TOR signalling reprograms the transcriptome and activates meristems. *Nature* **496**, 181–186

Xiong Y. & Sheen J. (2015): Novel links in the plant TOR kinase signaling network. *Current Opinion in Plant Biology* **28**, 83–91

Xiong Y. & Sheen J. (2014): The Role of Target of Rapamycin Signaling Networks in Plant Growth and Metabolism. *Plant Physiology* **164**, 499–512

Yamamoto H., Kakuta S., Watanabe T.M., Kitamura A., Sekito T., Kondo-Kakuta C., *et al.* (2012): Atg9 vesicles are an important membrane source during early steps of autophagosome formation. *Journal of Cell Biology*

Yang Z. & Klionsky D.J. (2009a): An overview of the molecular mechanism of autophagy. *Current topics in microbiology and immunology* **335**, 1–32

Yang Z. & Klionsky D.J. (2009b): An Overview of the Molecular Mechanism of Autophagy. pp. 1–32.

Yano K., Matsui S., Tsuchiya T., Maeshima M., Kutsuna N., Hasezawa S., *et al.* (2004): Contribution of the plasma membrane and central vacuole in the formation of autolysosomes in cultured tobacco cells. *Plant and Cell Physiology* **45**, 951–957

Yano K., Suzuki T. & Moriyasu Y. (2007): Constitutive autophagy in plant root cells. *Autophagy* **3**, 360–362

Yoon M.S., Rosenberger C.L., Wu C., Truong N., Sweedler J. V. & Chen J. (2015): Rapid mitogenic regulation of the mTORC1 Inhibitor, DEPTOR, by phosphatidic acid. *Molecular Cell* **58**, 549–556

Yoshimoto K., Hanaoka H., Sato S., Kato T., Tabata S., Noda T., *et al.* (2004): Processing of ATG8s, ubiquitin-like proteins, and their deconjugation by ATG4s are essential for plant autophagy. *Plant Cell* **16**, 2967–2983

Yu L., Nie J., Cao C., Jin Y., Yan M., Wang F., *et al.* (2010): Phosphatidic acid mediates salt stress response by regulation of MPK6 in Arabidopsis thaliana. *New Phytologist* **188**, 762–773

Zhang M., Fan J., Taylor D.C. & Ohlrogge J.B. (2010): DGAT1 and PDAT1 Acyltransferases Have Overlapping Functions in Arabidopsis Triacylglycerol Biosynthesis and Are Essential for Normal Pollen and Seed Development. *The Plant Cell* **21**, 3885–3901

Zhang Q., Lin F., Mao T., Nie J., Yan M., Yuan M., *et al.* (2012): Phosphatidic Acid Regulates Microtubule Organization by Interacting with MAP65-1 in Response to Salt Stress in Arabidopsis. *The Plant Cell* **24**, 4555–4576

Zhang Q., van Wijk R., Shahbaz M., Roels W., Schooten B. van, Vermeer J.E.M., *et al.* (2018): Arabidopsis Phospholipase C3 is Involved in Lateral Root Initiation and ABA Responses in Seed Germination and Stomatal Closure. *Plant and Cell Physiology* **59**, 469–486

Zhao J. (2015): Phospholipase D and phosphatidic acid in plant defence response: from protein–protein and lipid–protein interactions to hormone signalling. *Journal of Experimental Botany* **66**, 1721–1736

Zheng S.-Z., Liu Y.-L., Li B., lin Shang Z.-, Zhou R.-G. & Sun D.-Y. (2012a): Phosphoinositide-specific phospholipase C9 is involved in the thermotolerance of Arabidopsis. *The Plant Journal* **69**, 689–700

Zheng S.-Z., Liu Y.-L., Li B., Shang Z.L., Zhou R.-G. & Sun D.-Y. (2012b): Phosphoinositide-specific phospholipase C9 is involved in the thermotolerance of Arabidopsis. *The Plant Journal* **69**, 689–700

Zhuang X., Wang H., Lam S.K., Gao C., Wang X., Cai Y., *et al.* (2013): A BAR-domain protein SH3P2, which binds to phosphatidylinositol 3-phosphate and ATG8, regulates autophagosome formation in Arabidopsis. *Plant Cell* **25**, 4596–4615

Zienkiewicz A., Zienkiewicz K., Poliner E., Pulman J.A., Du Z.-Y., Stefano G., *et al.* (2020): The Microalga Nannochloropsis during Transition from Quiescence to Autotrophy in Response to Nitrogen Availability. *Plant Physiology* **182**, 819–839

Zientara-Rytter K. & Sirko A. (2014): Selective autophagy receptor Joka2 co-localizes with cytoskeleton in plant cells. *Plant Signaling & Behavior* **9**, e28523

8 LIST OF ABBREVIATIONS

ARA	Arachidonic Acid
ATG	Autophagy Related Gene
BSA	Bovine Serum Albumin
CFW	Calcofluor-White
CBD	Calmodulin Binding Domain
CP	Capping Protein
ConcA	Concanamycin A
DEPTOR	DEP Domain-Containing mTOR-Interacting Protein
DAG	Diacylglycerol
DGK	Diacylglycerolkinase
DGPP	Diacylglycerolpyrophosphate
DMSO	Dimethyl Sulphoxide
DPPC	Dipalmitoylphosphatidylcholine
ER	Endoplasmic Reticulum
ERGIC	ER-Golgi Intermediate Compartment
FA	Fatty Acid
FP	Fluorescent Protein
FFA	Free Fatty Acids
GFP	Green Fluorescent Protein
HPTLC	High Performance Thin Layer Chromatography
HSPs	Heat Shock Proteins
$InsP_3$	Inositol 1,4,5-triphosphate
Ipx	Inositol Polyphosphate
JA	Jasmonic Acid
LD	Lipid Droplets
LPP	Lipid Phosphate Phosphatase
LysoPA	Lysophosphatidic Acid
LPC	Lysophosphatidylcholine
mTORC1	Mammalian Target of Rapamycin Complex 1
MAP65-1	Microtubule-Associated Protein 65-1
LC3	Microtubule-Associtated Protein 1 Light Chain 3
MTSB	Microtubule-Stabilizing Buffer
mitoPLD	Mitochondrial Phospholipase D
MPK6	Mitogen-Activated Protein Kinase 6
MDC	Monodansylcadaverine
MS	Murashige and Skoog
NPC	Non-Specific Phospholipase C
NASC	Nottingham Arabidopsis Stock Centre
pPLAs	Patatin-Like Phospholipases A

PA	Phosphatidic Acid
PAK	Phosphatidic Acid Kinase
PC	Phosphatidylcholine
PC	Phosphatidylcholine
PE	Phosphatidylethanolamine
PG	Phosphatidylglycerol
PI	Phosphatidylinositol
PIKK	Phosphatidylinositol 3-Kinase-Related Protein Kinase
PI3P	Phosphatidylinositol 3-Phosphate
PI(4,5)P2	Phosphatidylinositol 4,5-bisphosphate
PI3K	Phosphatidylinositol-3-Kinase
PI-PLC	Phosphoinositide-Specific Phospholipase C
PLA	Phospholipase A
PLD	Phospholipase D
PDAT1	Phospholipid Diacylglycerol Acyltransferase 1
PM	Plasmatic Membrane
PCD	Programmed Cell Death
PPIs	Polyphosphoinositides
RAPTOR	Regulatory Associated Protein of TOR
RPM	Revolutions Per Minute
SH3P2	SH3 Domain-Containing Protein 2
SDS	Sodium Dodecyl Sulphate
SDP1	Sugar-Dependent 1
SAC	Supressor of Actin
TOR	Target of Rapamycin
TAG	Triacylglycerol
VPS	Vacuolar Protein Sorting
WT	Wild Type